Politecnico di Torino

Collegio di Ingegneria Informatica, del Cinema e Meccatronica

Master Degree

in

Mechatronics Engineering

Cart-inverted pendulum with pneumatic actuation: simulations and experiments

Supervisor:
Prof. Luigi Mazza
Company Tutor:
Mr. Ronald Kett

Author:
Shailesh S Hegde

April 2018

Acknowledgment

With due respect, I would like to take opportunity to express my sincere gratitude to Mr. Ronald Kett from Fluidon GmbH and Professor Luigi Mazza, my supervisors, for their continuous support, patient guidance and motivation.

I would firmly like to thank Dr. Heiko Baum, Mr. Benjamin Erzberger, Mr. Enrico Pasquini and Mrs Katja Juschka from Fluidon GmbH for their invaluable technical support to me from time to time.

I am particularly grateful to Mr.Dirk de Ben from Fluidon GmbH for sharing his expertized experimental knowledge and for his help in setting up the experimental set-up.

I also place on record my sincere thanks to my family and my friends here in Politecnico di Torino who had given me full co-operation through this master studies.

Abstract

A Cart-Inverted pendulum, usually mounted on a cart is actuated by an applied force. The inverted Pendulum system is a classical control problem due to it being Highly Unstable, under actuated and highly Nonlinear. The dynamics of the system is comparable to a wide range of real world applications.
In this thesis, we study the behaviour and the stability of a pneumatically actuated inverted pendulum. The double acting pneumatic cylinder is used as an actuator and a simple low cost on-off 2/2ways electro-pneumatic valves modulated by PWM signal is the interfacing element. The control system is composed of two parallel closed-loop, with PID compensators, to control individually the angular position of the pendulum and the position of the cart.
Commissioning of this project began by mathematically modelling the physical system. Modelling and simulations of the system were performed using different simulation environments. The stand alone models were developed in DSHplus® as well as in Matlab/Simulink®(Simscape package). A co-simulation was performed between different simulation environments, ensuring the development of a common platform to indulge the domain experty of the chosen environment.
The efficacies of the developed method are tested by simulation and validated with experimentation. It has been also observed that the Two parallel closed-Loop PID Controller yields good result in terms of stability and robustness.

Contents

List of Figures

List of Tables

Chapter 1

Introduction

Inverted pendulum is a classical academic example. Inverted Pendulum is basically a simple pendulum with pendulum upright. It represents higher order non linear system, dynamic at a given point of time, unstable equilibrium point. It is a suitable example to test and compare the new and existing control strategies as well as the competency of hardware modifications. Inverted pendulum proves to be a challenging study in the control domain. Complexity of the system increases with the increase in number of links of the pendulum. The Fig.1.1[3] shows the application of the inverted pendulum principles.

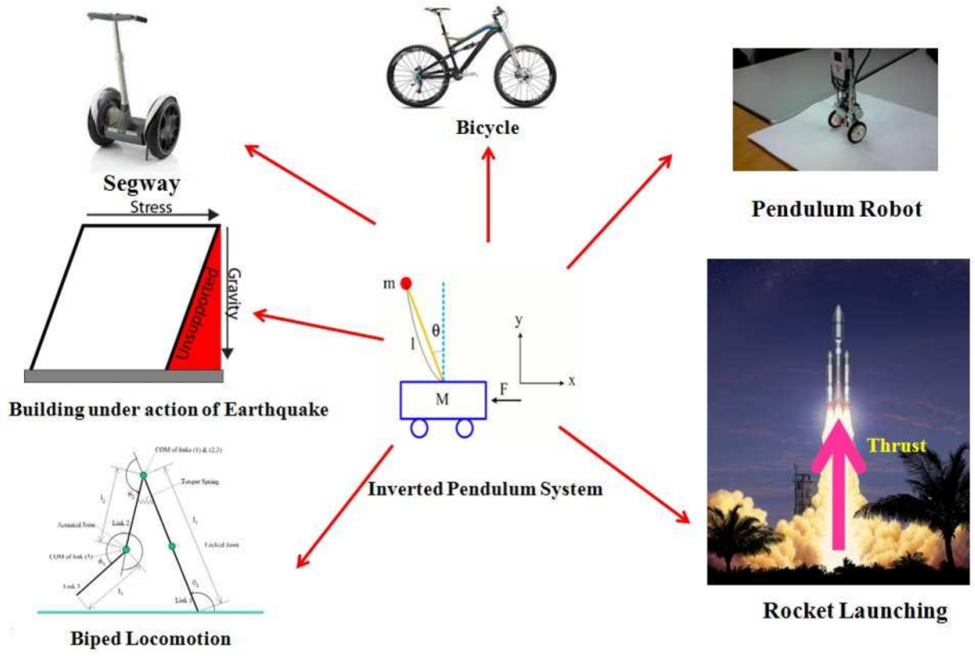

Figure 1.1: Applications of inverted pendulum.

The basic model is the one when the pendulum is made up of one link. Nevertheless it has a wide range of applications:

- In robotics, balancing of the humanoid robots are based on the study of inverted pendulum, some other robots used in domestic as well as industrial[4, 5].
- In Transport machines, where it requires to balance the object,system which helps patient to walk[6, 7, 8].

- Object transporting drones[9].
- Large scale construction building are modelled as inverted pendulum and aslo during earthquake resistant building design[10].
- Rocket launch.
- Most known commercial application of inverted pendulum is Segway[6].

1.1 System Introduction

Cart-inverted pendulum: Cart-inverted pendulum system consist of a mass connected to a cart with a connecting rod. Centre of the mass is in upright position as shown in the Fig.1.2. The connecting rod is pivoted to the cart, which is free to slide. It is very much evident from the Fig.1.2 that when the pendulum mass tilts towards right, the cart must move towards right in order for the pendulum to be in upright position. The primary goal is to determine and define a control law, taking into consideration of the state variables and producing a suitable input, such that the cart stabilizes the rod in the upright vertical position.

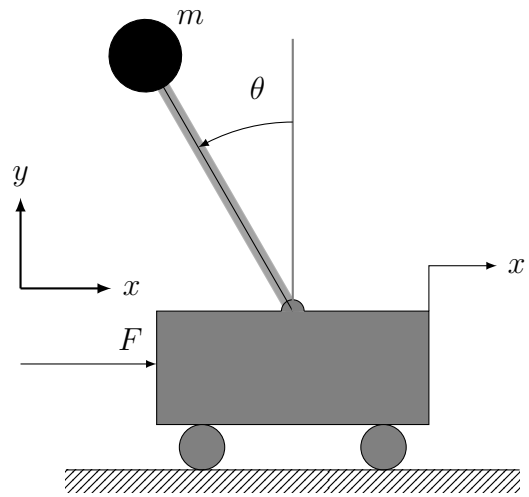

Figure 1.2: Inverted pendulum basic diagram.

The inverted pendulum is a single input multiple output(SIMO) system. The input may be voltage/current, though the actuator may be electric motor or pneumatic cylinder depending on the driver circuit. The outputs are the position of the cart, angle of the pendulum, velocity of the cart, angular velocity of the pendulum. The system seems to be simple in structure but turns out to be challenging when dealing with some of its characteristics:

- Highly Unstable: Inverted pendulum has a unstable equilibrium point,

- Under Actuated: The system has two degree of freedom in motion, but only one actuator is used.
- Highly Nonlinear: Inverted Pendulum is governed with non linear equations and terms

And to make it more complex there are disturbances and limitations in the Hardware implementation, which makes it a good example for control and to test different types of hardware setup and architectures.

1.2 Current Trends

There has been a lot of advances in the control domain of Inverted Pendulum in last two decades. Control strategies like PID, LQR, Fuzzy Logic, Adaptive control, Neural networks etc... have been implemented. In terms of hardware setup, there has been lot of practical experimentations done with the actuators. Varieties in the actuator set-up can be seen in the last couple of decades, which are with different types of electric drives, or with pneumatic systems. And varieties in Microcontroller implementations with NI myrio board, PLC, Arduino boards etc... We will discuss couple of research papers dealing different approaches to stabilize the pendulum.
There are lot of articles on the pole placement and linear quadratic regulator (LQR)[11, 12, 6, 7, 13]. **Control of Inverted Pendulum using pole placement technique** in [14, 15], Pole placement technique is also known as pole-assignment technique . The general idea in pole placement method, all the poles of a closed loop system are placed at desired location. One of the approach would be using Root locus method, finding the poles from characteristic equations and placing these pair of poles far in the left. The linear, time variant, dynamic systems with multiple inputs in the form of differential equations can be represented in the form below:

$$\dot{x} = Ax + Bu \tag{1.1}$$

$$y = Cx + Du \tag{1.2}$$

The state variables are fed back through a constant matrix k, forming a closed loop system.

$$u(t) = -kx(t) \tag{1.3}$$

The article[14] suggests the method to check the controllability and observability of the system. Full order Observer was designed irrespective of whether some state variables are available for direct measurement or not. A full state feedback controller using state variable feedback controller was designed to control Inverted pendulum. The article concluded stating the system to be inherently unstable with non minimum phase zero. The

system desired performance achieved by selecting a pair of poles as a dominant poles. The proposed controller showcased excellent performance, good robustness and additionally it could overcome external disturbances.

Though there are plenty of control algorithm developed, but PID controller is still the most widely adopted Control strategy in industrial application due to its simple architecture. The advantages of PID controller is its simplicity in application and its ability to solve wide practical control problems. When a control system have more than two PID controllers, the tuning of PID parameters is not an easy task. An article on **Simulation studies of inverted pendulum based on PID controllers** in [1], which provides a structure, modelling three types of inverted pendulum, the design procedure of PID controllers and the simulation results of all the three types of the inverted pendulum. The three different types of model are:

- x Inverted Pendulum: the x inverted pendulum on a pivot by horizontal control force. The cart is free to move in one axis that is x axis.
- x-y Inverted Pendulum: the x inverted pendulum on a pivot by two horizontal control forces. The cart is free to move in two horizontal axes that is x and y axes.
- x-z Inverted Pendulum: the x inverted pendulum on a pivot by one horizontal and one vertical control forces. The cart is free to move in one horizontal axis that is x and one vertical axis that is z axis.

The Fig.1.3 shows the PID controller architecture for x and x-z inverted pendulum model, where two PID controllers are used for the x inverted pendulum model and three PID controllers are used for x-z inverted pendulum model. The system control analysis of

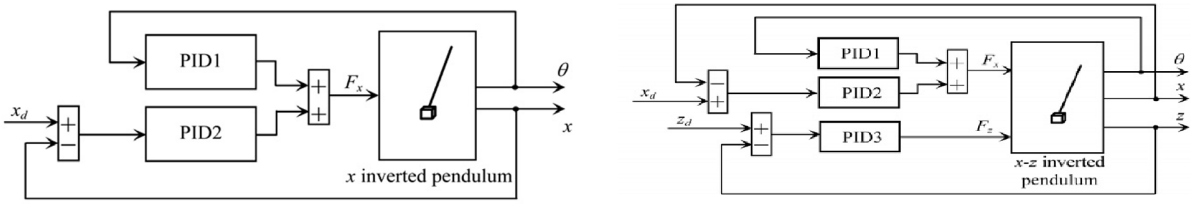

Figure 1.3: Two PID controller architecture[1]

these three types of inverted pendulum suggests that

- PID controllers are powerful enough to control these models.
- One PID is enough for angle control of x inverted pendulum model, while two PID controllers are enough for x-y inverted pendulum model and three PID controllers are enough for x-z inverted pendulum model.

- PID controller design can realize stabilization control and tracking control with good performance as well as shows good robustness.

It is quite interesting to make an comparison between PID controllers and a LQR controller, which takes us to the article on **An Investigation on the Design and Performance Assessment of double-PID and LQR Controllers for the Inverted Pendulum**[16] . In this article, comparison of double PID control method with LQR(linear quadratic regulator) control method is done. The dynamic and steady state performance are assessed and compared based on virtual prototype simulation and experimental setup. In this paper, simulation and experiment are carried out keeping in mind inverted pendulum is driven directly by an ironless permanent magnet linear motor. Article offers an evaluation of system in comparing two methods: Double PID and LQR.
Double-PID: One of the PID controller controls the position of the cart and the other controls the angle of the pendulum. It is quite evident that single PID controller can only control one variable. When only one PID controller is used, the cart position exceeds the limit, the system is stable till cart position is within limits.
LQR: It is an mathematical algorithm to minimize the cost function with weighting factors. The method used to define Q and R was by simulation and trial, where Q and R are input weighting matrices.
Dynamic Performance Assessment on the Designed Controllers: Dynamic performance indices chosen for the response of cart position and pendulum angle were *rise time, transition time, steady state error and maximum overshoot*. LQR has a faster transition time both in cart position and pendulum angle, and with the longer rise time of cart position and pendulum angle, making the process more smooth. Pendulum angle overshoot is bigger in case of double-PID than LQR. In conclusion, LQR controller has shorter settling time, smoother response because of longer rise time, better robustness due to comparatively small overshoot. By now we have understood the performance of PID controller and LQR controller individually. Lets try to understand the behaviour and performance of the system where PID controller is clubbed with the LQR controller. An article on **Optimal Control of Nonlinear Inverted Pendulum System Using PID Controller and LQR: Performance Analysis Without and With Disturbance Input**[17], Linear Quadratic Regulator(LQR) and Proportional-Derivative-Integral(PID) control methodologies are used to control inverted pendulum in this paper. The LQR is one of the optimal control methodologies, uses the states of system and input to produce an optimum control decision. The aim of the paper was to stabilise the pendulum angle while the cart position reaches to a desired position. This paper makes a comparative study and displays the advantage of the LQR and its robustness. The non-linear state space model equations were modelled and linearised with the disturbance input. LQR maximises or minimises a chosen performance criterion. The LQR gain vector K is derived from the minimization of cost function. Three control schemes were developed and

analysed for without and with disturbances:

- Two PIDs i.e., Angle PID and cart PID;
- Two PIDs with LQR.
- One PID with LQR.

As a conclusion it was found that 2PID+LQR is little superior to 1PID+LQR for both with and without disturbances. The control of 2PID+LQR is fast and smooth. The cart position has a smoother response over 1PID+LQR. But 1PID+LQR has structural simplicity, effective and robust technique for optimal control. Both 2PID+LQR and 1PID+LQR is better than 2PID control scheme.
We have already seen the various control strategies such as Pole placement technique based controller, PID controller and LQR. Let us review an article on Fuzzy logic based control strategy in [18, 19], **Stabilization fuzzy control of inverted pendulum systems** in [19] focuses on the introduction and design ideology with the fuzzy logic control. And the conclusions were,

- The dynamic importance degrees are modelled to prioritize the pendulum angle control over the cart position control. The Pendulum angle control and cart position control are implemented in parallel to each other. The switching of the two controls was automatically taken care by the tuning the dynamic importance degrees. This controller has the ability to stabilize the inverted pendulum within 9.0 s for initial angle upto 30.0°.
- Easy implementation in hardware by look-up table, and it requires a small amount of hardware.
- It can take care of systems with more than one input items.

By now we have reviewed the articles dealing software simulation of the inverted pendulum. It will be interesting to review an practical experiment of real time control of the system to understand the practical challenges and its outcome. An article on **The Computer Simulation and Real-Time Control for the Inverted Pendulum System Based on PID** in [2] deals with the single inverted pendulum, it is modelled such that the cart can move backward and forwards in the horizontal direction. The cart is belt driven with the help of an electric motor. The pendulum can rotate in vertical plane and forward or backward in the same plane as the cart. To simplify the system analysis following assumptions were made: The pendulum and the cart are the rigid bodies. There is no comparative movement between the cart and belt. The belt has no extension. The frictional force acting on the cart is proportional to its velocity and the frictional torque acting on the pendulum is proportional to its angular velocity. The equations are

derived with the help of free body diagrams. PID controller is to calculate the control variable actuating the inverted pendulum, according to the error between the desired and the actual output. As shown in Fig.1.4, $r(t)$ is the set reference angle of pendulum, $y(t)$ is the actual angle of the pendulum, $u(t)$ is the resultant force acting on the cart in the horizontal direction.

$$u(t) = kp * e(k) + ki * \sum e(k) + kd * (e(k) - e(k-1))$$

The proportional term P improves response of the system at the cost of big overshoot

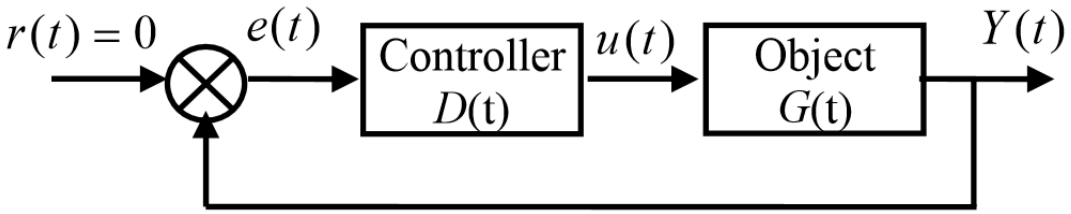

Figure 1.4: Structure of state feedback[2]

causing instability. The integral term I can eliminate the residual steady-state error. Derivative term D has pre-action, it reduces the magnitude of the overshoot and dynamic error, improving the system stability.
The software platform used for the real-time control is Matlab/Simulink. Formation of S function blocks by C Language programming. These blocks can read the values detected by photo electric encoder equipped by servomotor. These encoders are connected to the cart and pendulum.
The following conclusion achieved on the simulation and real time hardware implementation of inverted pendulum:

- The real time control experiment shows that the Conventional PID controller can stabilize the Inverted pendulum .
- The numerical simulation and the real time experiment projects a similar results and system behaviour.
- The PID controller can control the pendulum angle. One PID controller cannot control both the pendulum angle and cart displacement simultaneously. whereas PID control with two input and two output or two separate PID controllers must be used.

In the previous article, the simulation and the real time control was carried out with a electronic drives as an actuator to the cart. In the next article, the actuation of the cart

is done with the help of Pneumatic actuator; **Inverted Pendulum Driven by Pneumatics** [20].
The experimental test-bench setup of an Inverted pendulum system, actuated by a rodless pneumatic cylinder, interfaced by proportional directional valves and use of low cost linear potentiometer position sensor. PID Control method was used to stabilise the system. The PID controller was able to stabilise pendulum angle while the cart position kept moving to infinity. As an alternative control strategy , the state-variable feed controller was designed and developed. The Controller gain matrix K was obtained using LQR optimal design. State-variable feed controller stabilized the system, time required to stabilize is 5 s. Some observations were developed by changing the pendulum length. With doubling the length of pendulum, it was observed that the pendulum couldn't be stabilized completely, though it did not fall. It also could recover angles more than 10° from equilibrium. For very large Pendulum length, strong vibrations were observed.
Another article on pneumatic actuation in [21], **Modeling and control of a pneumatically actuated inverted pendulum** describes model on inverted pendulum actuated by linear pneumatic motor with an use of low cost potentiometer for measuring the positions.Effects of friction and development of a linearised model is derived. This linearised model is used to design the state feedback controller based on Linear quadratic(LQ) and Linear quadratic Gaussian(LQG) optimization procedures. The nonlinear effects of friction were modelled based on the results of identification experiment. These results indicated striebeck effect. Linear state feedback controller was designed with the help of LQ and LQG performance criteria. Since these controller explicitly account for non linear effects(e.g. Stribeck friction); appropriate friction compensator was designed. The mentioned controller design is verified by means of computer simulation as well as on experimental test bench. The Analysis shows that the state feedback controller can stabilise the inverted pendulum with external disturbances. The stribeck friction effect resulted in a pendulum position perturbations. Introduction of friction compensator though reduced the undesired effects but with notably increase of noise levels.

1.3 Our Approach

This section will give a brief introduction of the architecture and approach to be followed henceforth. The aim of this project is the study and control of the Inverted Pendulum being actuated by a Pneumatic cylinder, where the actuator is interfaced by a imple low cost on-off 2/2 ways electro-pneumatic valves modulated by PWM signals. There are several research article on inverted pendulum being stabilised with the help of pneumatic actuator and proportional solenoid valves. Pneumatic actuators are widely used in industry and are generally used for two position controls. When the continuous position control is required, pneumatic servo or proportional valves are used. Pneumatic servo

valves are expensive and proportional valves do not have the fastest response time due to the spool dead band. The alternative would be to use a fast-switching digital valves to achieve linear flow control characteristics with low response time possible. The Fig.1.5 shows the architecture of a fast switching valves in a pneumatic system.

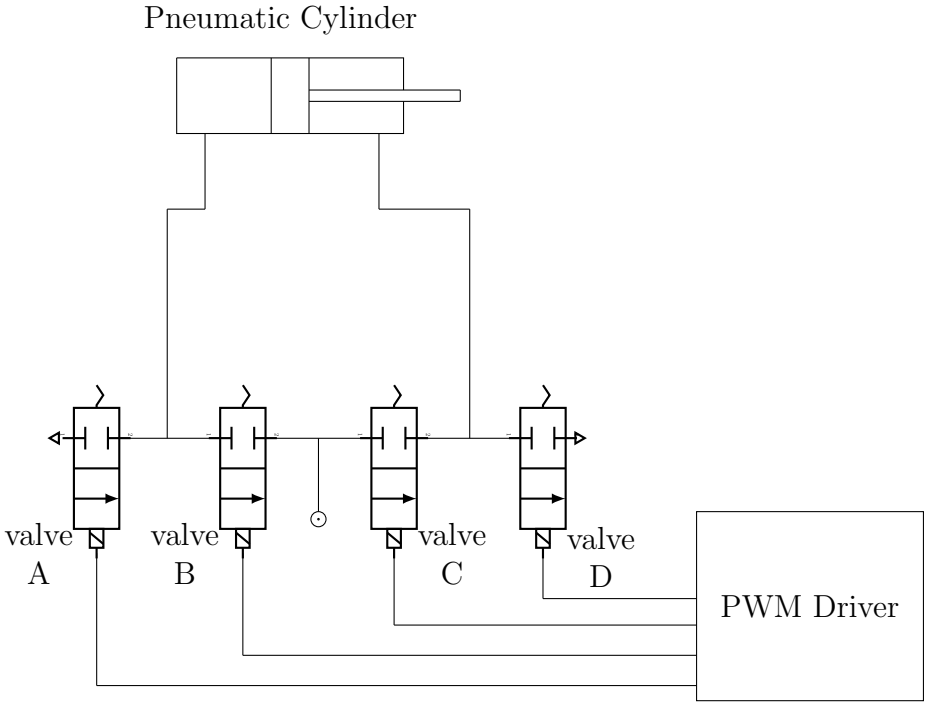

Figure 1.5: General layout of the pneumatic system

Inverted pendulum is chosen for this experiment due to its nature and characteristic as discussed in section 1.1, which makes it a perfect system to understand and evaluate the performance of the monostable directional solenoid valves.
For the sake of modelling and simulation only, it can be broadly said that, this system is a interaction of 3 domains:

- Mechanics: inverted pendulum are governed by the law of mechanics. And it consist of mechanical components.
- Pneumatics: actuators and interface elements being pneumatic elements are studied in pneumatic domain.
- Controls: identification of control law and design of the controller.

The Fig.1.6, shows the general block diagram of the implementation. It is a closed loop system; where control unit generates the signal comparing the reference signal and the measured values from the sensors. Interface elements are the connecting medium between the control unit and actuator, and finally the Inverted pendulum is actuated by pneumatic actuators.

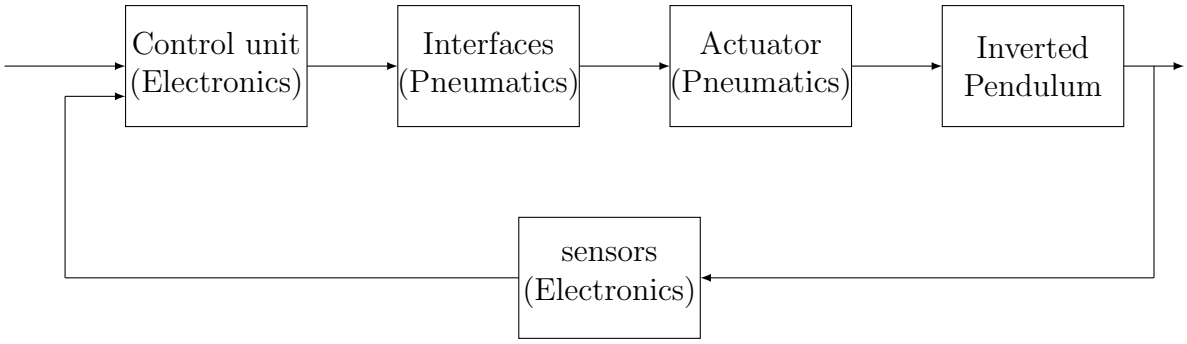

Figure 1.6: Block diagram of the complete system

Actuator: There are variety of pneumatic actuators depending on size, shape and function; such as, Pneumatic cylinders, rotary, Rodless actuators with magnetic linkage. Pneumatic cylinder is chosen as an actuator for this project. There are different types of pneumatic cylinders like single acting cylinder, double acting cylinder, telescopic etc... One we are using for this project will be a double acting single rod pneumatic cylinder.
Characteristics:

- Pneumatic actuator is capable of developing small/medium forces.
- It can perform well with low pressure range.
- It exhibits good ratio of developed power to weight.
- Low cost makes it a good choice.

Interfaces:
Interface elements make it possible to connect between the low power signal of a control elements and the high power signal of actuators and to convert from one technology to another. Solenoid valves are used to convert electrical signals to pneumatic signals. We are using 2/2 on-off Directional Solenoid valves, of-course due to their low cost over proportional valves. In order for 2/2 on-off directional solenoid valves to compete with proportional solenoid valves on the performance basis it is mandatory that the chosen valve has a fast switching property.
Control Units:
There are different types of control units such as Electronic devices, electromechanical relays, pneumatic logic valves. We are using micro-controllers, which will discussed much later in the chapter5.
Sensors: The Double acting single rod pneumatic cylinder is coupled to the cart of the Inverted pendulum system. The Position of the cart and Angle of the Pendulum link are measured by the position sensor and angle sensor respectively.
The Fig.1.7 depicts the layout of the complete system. The Set-point of Cart position

and pendulum angle are compared with their respective actual signals which are fed back from the sensors. The error generated from the comparison is fed to the controller. The output of the controller is a reference signal for the PWM signal generator. The PWM Driver triggers the 2/2 on-off solenoid valves. The valve A and C are connected to the pressure source and the valve B and D are connected to sink. The Valve A and B are connected to the cylinder port 1, while valve C and D are connected to port 2. The pneumatic actuator is coupled with the cart of the inverted pendulum. Henceforth in this report, we will be following this layout in a more detailed manner.

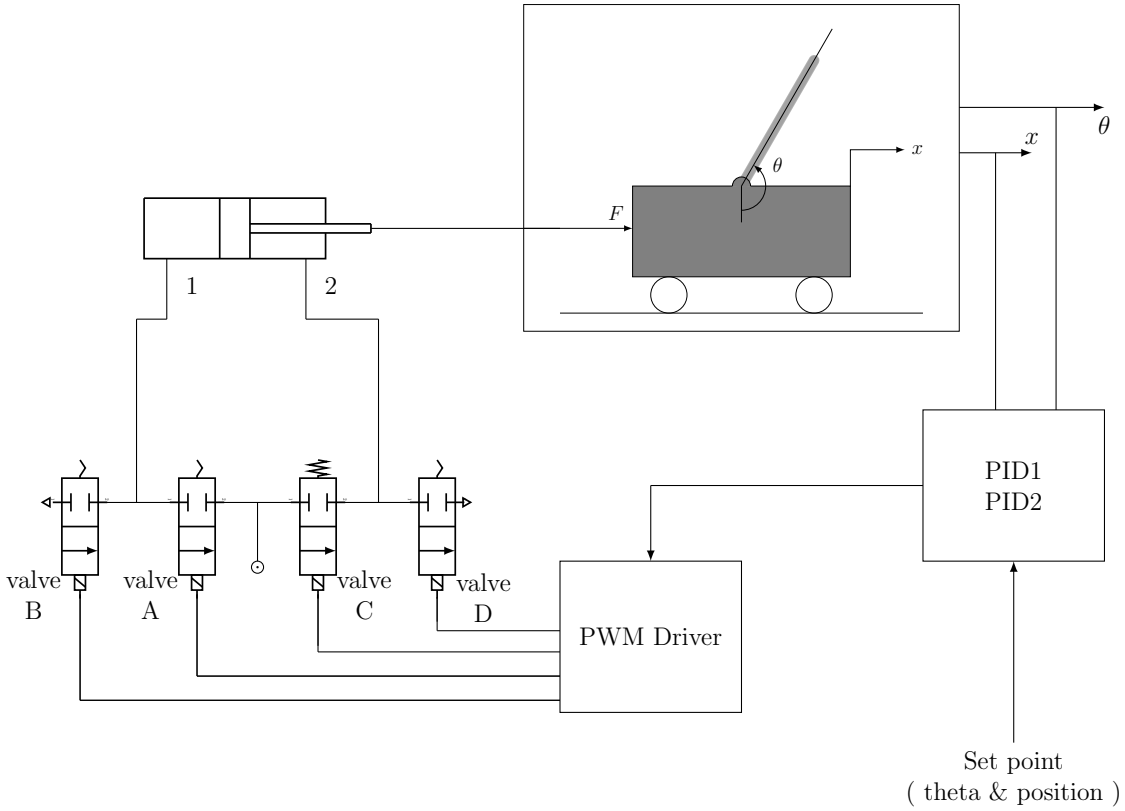

Figure 1.7: General layout of the complete system

Chapter 2

Modelling

The modelling and simulation of the system, fully and partially were designed in various platforms to evaluate and understand the system behaviour with and without control. The aim being to primarily understand the behaviour of the system and second to find an easy implementation of the model in a user friendly environment. The majority of the modelling were done in DSHplus and Matlab and partially in Altair Activate package for co-simulation.
For the ease of presenting the report, we have classified the system in 3 parts:

- Mechanical
- Pneumatic
- Control

We will try to produce a mathematical model of our proposed system to get an understanding and grip on the system.

2.1 Mathematical Model

Mathematical modelling is a representation of the behaviour of real objects in mathematical terms [22]. After developing a conceptual model of a physical system it is natural to develop a mathematical model that will allow one to estimate the quantitative behaviour of the system. Quantitative results from mathematical models can easily be compared with observational data to identify a model's strengths and weaknesses. Gives precision and direction for problem solution, enables a thorough understanding of the system modelled, prepares the way for better design or control of a system and allows the efficient use of modern computing capabilities.

2.1.1 Mechanical:

The dynamics of inverted pendulum is derived with the help of Newton's laws of motion[23]. We will consider a two-dimensional system of inverted pendulum as shown in Fig.2.1 for the ease of mathematical modelling. The pendulum is able to move only in vertical plane, Force moves the cart horizontally and the outputs are the horizontal position of cart and angular position of pendulum.

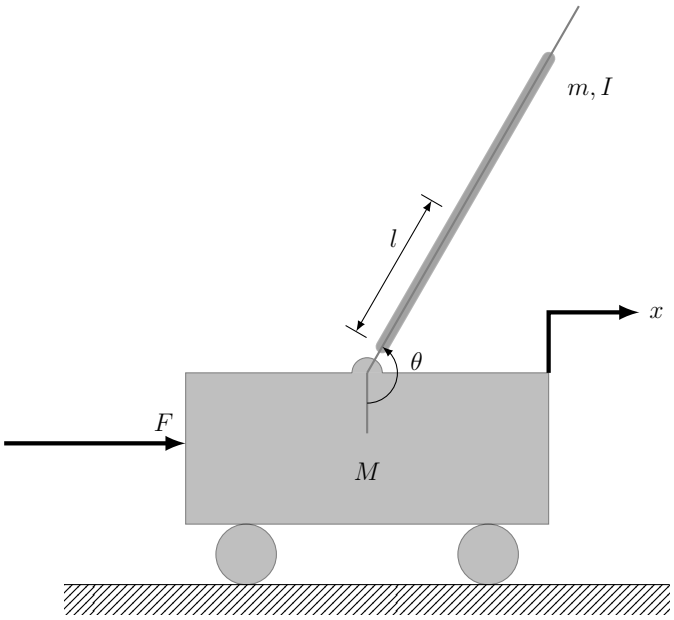

Figure 2.1: Basic diagram of inverted pendulum

where,
M = mass of the cart
m = mass of the pendulum
b = coefficient of friction for cart
l = length to pendulum center of mass
I = mass moment of inertia of the pendulum
F = force applied to the cart
x = cart position coordinate
θ = angular position of pendulum from the vertical (down)
The free body diagram of the two elements of inverted pendulum are shown in Fig.2.2. Summing the forces in free body diagram in horizontal direction for the cart, can be expressed as,

$$M\ddot{x} + b\dot{x} + N = F \tag{2.1}$$

We can sum the forces in vertical direction of the cart, but no useful data can be acquired. Summing forces in the free body diagram in the horizontal direction for the pendulum can be represented as,

$$N = m\ddot{x} + ml\ddot{\theta}\cos\theta - ml\dot{\theta}^2\sin\theta \tag{2.2}$$

Substituting Eq.2.2 into Eq.2.1 we get,

$$(M+m)\ddot{x} + b\dot{x} + ml\ddot{\theta}\cos\theta - ml\dot{\theta}^2\sin\theta = F \tag{2.3}$$

The second equation of motion is obtained by sum of forces perpendicular to the pendulum

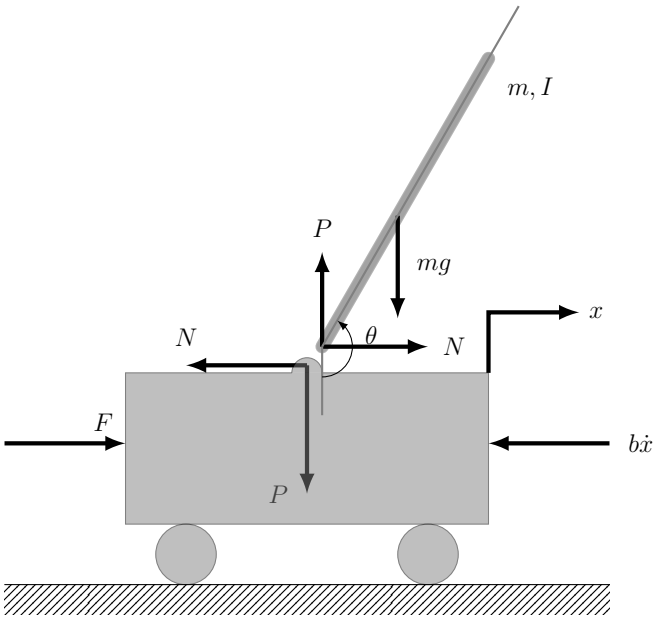

Figure 2.2: Free body diagram of inverted pendulum

and is expressed as,

$$P\sin\theta + Ncos\theta - mg\sin\theta = ml\ddot{\theta} + m\ddot{x}\cos\theta \tag{2.4}$$

Sum of moments about the centroid of the pendulum gives,

$$-Pl\sin\theta - Nl\cos\theta = I\ddot{\theta} \tag{2.5}$$

Combining Eq.2.4 and Eq.2.5 we get,

$$(I + ml^2)\ddot{\theta} + mgl\sin\theta = -ml\ddot{x}\cos\theta \tag{2.6}$$

Analysis and control design techniques works well for a linearised systems, the equation mentioned earlier have to be linearised. We will linearise the equations about vertically upward equilibrium position; $\theta = \pi$. And we assume that the system stays within a small neighbourhood of the selected equilibrium point.
Let's assume that ϕ is the deviation of pendulum's position from the equilibrium point, that is,

$$\theta = \pi + \phi \tag{2.7}$$

Assuming the deviation ϕ about the equilibrium to be small, we try to make an approximation of the non linear system as following,

$$cos\theta = \cos(\pi + \phi) \approx -1 \tag{2.8}$$

$$\sin\theta = \sin(\pi + \phi) \approx -\phi \tag{2.9}$$

$$\dot{\theta}^2 = \dot{\phi}^2 = 0 \tag{2.10}$$

Substituting Eqs.2.8,2.9 and 2.10 into Eq.2.3 and Eq.2.6, we get the following two linearised equations of motion,

$$(I + ml^2)\ddot{\phi} - mgl\phi = ml\ddot{x} \tag{2.11}$$

$$(M + m)\ddot{x} + b\dot{x} - ml\ddot{\phi} = u \tag{2.12}$$

We can obtain the transfer function from the linearised system equation. First we must take the Laplace transform of the system equation which assumes zero initial conditions. The Laplace transform of the system equations are,

$$(I + ml^2)\phi(s)s^2 - mgl\phi(s) = mlX(s)S^2 \tag{2.13}$$

$$(M + m)X(s)S^2 + bX(s)s - ml\phi(s)s^2 = U(s) \tag{2.14}$$

The transfer function represents the relationship between a single input to the single output at a time. So we need to find the relationship between output $\phi(s)$ and input $U(s)$. To do that, solve for $X(s)$ from Eq.2.13.
we get,

$$X(s) = \left[\frac{I + ml^2}{ml} - \frac{g}{s^2}\right]\phi(s) \tag{2.15}$$

Then substitute Eq.2.15 into Eq.2.14

$$(M + m)\left[\frac{I + ml^2}{ml} - \frac{g}{s^2}\right]\phi(s)s^2 + b\left[\frac{I + ml^2}{ml} - \frac{g}{s^2}\right]\phi(s)s - ml\phi(s)s^2 = U(s) \tag{2.16}$$

Rearranging and we get the transfer equation as,

$$\frac{\phi(s)}{U(s)} = \frac{\frac{ml}{q}s^2}{s^4 + \frac{b(I+ml^2)}{q}s^3 - \frac{(M+m)mgl}{q}s^2 - \frac{bmgl}{q}s} \tag{2.17}$$

where,

$$q = [(M + m)(I + ml^2) - (ml)^2] \tag{2.18}$$

From the transfer function 2.15, it can be seen that there is a pole and a zero at the origin. These can be cancelled and the transfer function obtained for pendulum angle $\theta(s)$ as an output and $U(s)$ as an input is,

$$P_{Pend}(s) = \frac{\phi(s)}{U(s)} = \frac{\frac{ml}{q}(s)}{s^3 + \frac{b(I+ml^2)}{q}s^2 - \frac{(M+m)mgl}{q}s - \frac{bmgl}{q}} \qquad [\frac{rad}{N}] \tag{2.19}$$

Also the transfer function with the cart position $X(s)$ as an output and $U(s)$ as an input can be derived in a similar manner. The transfer function obtained is the following,

$$P_{cart}(s) = \frac{X(s)}{U(s)} = \frac{\frac{(I+ml^2)s^2 - gml}{q}}{s^4 + \frac{b(I+ml^2)}{q}s^3 - \frac{(M+m)mgl}{q}s^2 - \frac{bmgl}{q}s} \qquad [\frac{m}{N}] \tag{2.20}$$

The linearised equations of motion can be represented in state-space form if they are arranged in first order differential equations. They can be put into a matrix form as shown below,

$$\dot{x} = Ax + Bu \tag{2.21}$$

$$y = Cx + Du \tag{2.22}$$

The state-space representation of system is,

$$\begin{bmatrix} \dot{x} \\ \ddot{x} \\ \dot{\phi} \\ \ddot{\phi} \end{bmatrix} = \begin{bmatrix} 0 & 1 & 0 & 0 \\ 0 & \frac{-(I+ml^2)b}{I(M+m)+Mml^2} & \frac{m^2gl^2}{I(M+m)+Mml^2} & 0 \\ 0 & 0 & 0 & 1 \\ 0 & \frac{-mlb}{I(M+m)+Mml^2} & \frac{mgl(M+m)}{I(M+m)+Mml^2} & 0 \end{bmatrix} \begin{bmatrix} x \\ \dot{x} \\ \phi \\ \dot{\phi} \end{bmatrix} + \begin{bmatrix} 0 \\ \frac{I+ml^2}{I(M+m)+Mml^2} \\ 0 \\ \frac{ml}{I(M+m)+Mml^2} \end{bmatrix} u \tag{2.23}$$

$$y = \begin{bmatrix} 1 & 0 & 0 & 0 \\ 0 & 0 & 1 & 0 \end{bmatrix} \begin{bmatrix} x \\ \dot{x} \\ \phi \\ \dot{\phi} \end{bmatrix} + \begin{bmatrix} 0 \\ 0 \end{bmatrix} u \tag{2.24}$$

2.1.2 Pnuematic:

A typical pneumatic system consist of force element (pneumatic cylinder), interfacing elements (valves), connecting tubes and sensors[24, 25].

2.1.2.1 Pneumatic Cylinder

The equation of motion for the piston-rod-load assembly depicted in Fig.2.3 can be expressed as,

$$(M_L + M_p)\ddot{x} + \beta\dot{x} + F_f + F_L = P_1A_1 - P_2A_2 - P_aA_r \tag{2.25}$$

where,
M_L = External load mass
M_p = piston and rod assembly mass
x = piston position
F_f = Coulumb friction coefficient
β = Viscous friction coefficient

F_L = external force
P_1, P_2 = pressures of chamber 1,2
A_1, A_2 = Areas of chamber 1,2
A_r = rod cross-sectional area.

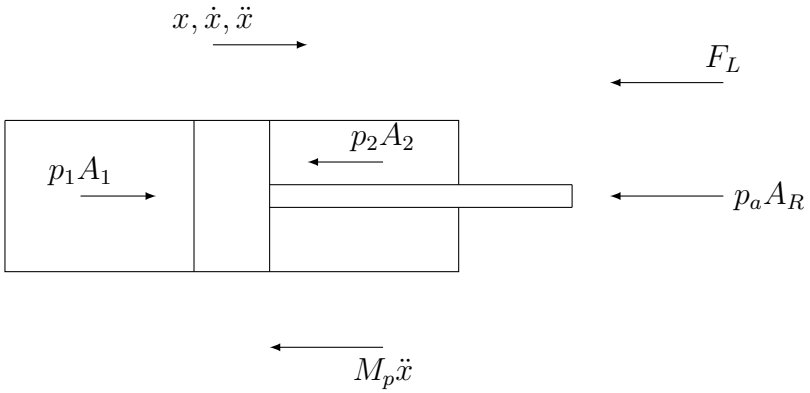

Figure 2.3: Pneumatic cylinder model

The right hand side of the Eq.2.25 represents the actuator active force produced by the actuator chambers. In order to control the force output of the actuator it is necessary to control the pressure in these chambers. The control of the pressure in the chamber are done through the valves.

The most general volume of gas model consist of three equations: an equation of state (ideal gas law), conservation of mass (continuity) equation and the energy equation. Assuming that: (i) the gas is perfect, (ii) Homogeneous pressure and temperature in the chambers, (iii) Kinetic and Potential energy terms are negligible.
The ideal gas law can be written as

$$P = \rho RT \tag{2.26}$$

where,
R = ideal gas constant
ρ = density
T = temperature of gas.
Applying the continuity equation, the mass flow rate,

$$\dot{m} = \frac{d}{dt}(\rho V) \tag{2.27}$$

where,
m = mass
V = volume.

Simplifying further,

$$\dot{m}_{in} - \dot{m}_{out} = \dot{\rho}V + \rho\dot{V} \tag{2.28}$$

where $\dot{m}_{in}$ and $\dot{m}_{out}$ are the mass flow entering and exiting the cylinder chamber. The energy equation can be represented as:

$$q_{in} - q_{out} + kC_v(\dot{m}_{in}T_{in} - \dot{m}_{out}T) - \dot{W} = \dot{U} \tag{2.29}$$

where,
q_{in}, q_{out} = heat transfer terms
k = specific heat ratio
T_{in} = temperature of incoming gas flow
W = rate of change in work
$\dot{U}$ = change of internal energy.
The total change of internal energy is,

$$\dot{U} = \frac{d}{dt}(C_v mT) = \frac{1}{k-1}\frac{d}{dt}(PV) = \frac{1}{k-1}(V\dot{P} + P\dot{V}) \tag{2.30}$$

where we used the ideal gas relation $C_v = \frac{R}{k-1}$.
Now, substituting $\dot{W} = P\dot{V}$ and Eq.2.30 into Eq.2.29,we get,

$$q_{in} - q_{out} + \frac{k}{k-1}\frac{P}{\rho T}(\dot{m}_{in}T_{in} - \dot{m}_{out}T) - \frac{k}{k-1}P\dot{V} = \frac{1}{k-1}V\dot{P} \tag{2.31}$$

Assuming incoming flow gas temperature is same as the temperature of the gas in the chamber.The Equation becomes,

$$\frac{k-1}{k}(q_{in} - q_{out}) + \frac{1}{\rho}(\dot{m}_{in} - \dot{m}_{out}) - \dot{V} = \frac{V}{kP}\dot{P} \tag{2.32}$$

For further simplification the process is assumed to be adiabatic i.e. $q_{in} - q_{out} = 0$ the time derivative of pressure in chamber is,

$$\dot{P} = k\frac{P}{\rho V}(\dot{m}_{in} - \dot{m}_{out}) - k\frac{P}{V}\dot{V} \tag{2.33}$$

substituting ρ from Eq. 2.26,

$$\dot{P} = k\frac{RT}{V}(\dot{m}_{in} - \dot{m}_{out}) - k\frac{P}{V}\dot{V} \tag{2.34}$$

Above equation can be written more specifically,

$$\dot{P} = \frac{RT}{V}(\alpha_{in}\dot{m}_{in} - \alpha_{out}\dot{m}_{out}) - \alpha\frac{P}{V}\dot{V} \tag{2.35}$$

For inflow; α_{in} is close to k, for outflow; α_{out} is close to 1 and the thermal characteristic of compression/expansion process due to movement of piston is given by $\alpha = 1.2$ Keeping the origin of the piston displacement at the centre of the stroke, the volume of each chamber can be expressed as,

$$V_i = V_{0i} + A_i(\frac{1}{2}L \pm x) \tag{2.36}$$

where,
i = 1,2
V_{0i} = dead volume of the cylinder at the end of the stroke
A_i = piston effective area
L = piston stroke
x = piston position.
The difference in the area of chamber 1 and 2 is due to the area of the piston rod. Substituting Eq.2.36 into Eq.2.35, the time derivative of pressure in the pneumatic cylinder chamber is,

$$\dot{P} = \frac{RT}{V_{0i} + A_i(\frac{1}{2}L \pm x)}(\alpha_{in}\dot{m}_{in} - \alpha_{out}\dot{m}_{out}) - \alpha\frac{PA_i}{V_{0i} + A_i(\frac{1}{2}L \pm x)}\dot{x} \tag{2.37}$$

With this form, the pressure dynamics equation accounts for:

- heat transfer characteristics of charging and discharging equation
- air compression and expansion due to piston movement
- differnce in the effective area of the piston in the chambers

The first term of the right hand side of the Eq.2.37 represent the change in pressure due to mass flow in and out, while the second term represent the change in pressure due to piston movement.

2.1.2.2 2/2 on-off valves:

The directional valve[26] is an important component which contributes the overall performance of the actuator, as it influences both in steady state and in transient conditions. Directional Valves assisted with PWM technique i.e. digital valves have high dynamic performance and good flow capacity, where flow is a function of duty cycle. Generally the control input to digital valves are provided by either electrical, pneumatic or mechanical signal to move the plunger of the valve; switching the flow to the outlets. Regardless of different types and position of the plunger, valve switching(fully closed to fully open or vice versa) causes the change in effective area. A certain time is required for opening or closing i.e. depending on the movement of the plunger in the valve. This can be seen as a relative delay to the command signal, depending on the design and architecture of the

valve.
The response time and conductance also depend on the size of the valve. Small valves have fast activation times while the larger valves have high conductance.

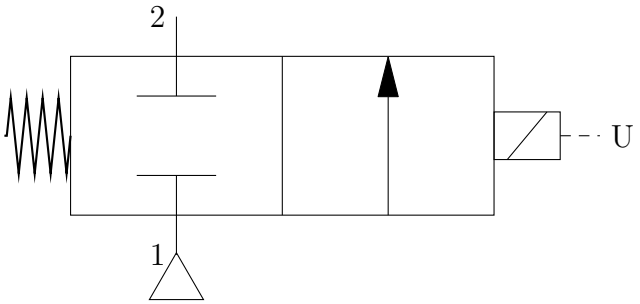

Figure 2.4: Two-way valve symbol

The inlet 1 and outlet 2 are connected via a port whose effective area varies when the valve switches. The term switching means the change of configuration on the left to the one on the right as shown in the Fig.2.4. The effective area between 1 and 2 depends on the control signal U, the physical reference model of two-way valve can be seen as a time variable cross-section resistance shown in Fig.2.5,

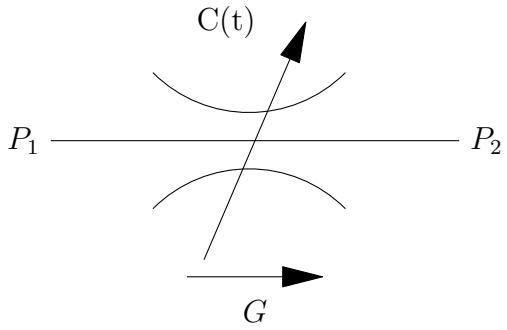

Figure 2.5: Physical reference model of two-way valve

The mass flow rate (G) of the valve is expressed in sonic conditions as well as in subsonic conditions.
For Sonic flow : $0 < \frac{P_D}{P_U} < b$

$$G = C\rho_{ANR}P_U\sqrt{\frac{T_N}{T_M}}sign(P_1 - P_2) \tag{2.38}$$

For Subsonic flow : $b < \frac{P_D}{P_U} < 1$

$$G = C\rho_{ANR}P_U\sqrt{1 - \left[\frac{\frac{P_D}{P_U} - b}{1 - b}\right]^2}\sqrt{\frac{T_N}{T_M}}sign(P_1 - P_2) \tag{2.39}$$

where,

ρ = density at Standard condition $(20^oC, 1bar)$
P_U = upstream Pressure
P_D = downstream pressure
b = critical pressure ratio
C = conductance
G = mass flow rate
T_N = temperature at normal condition
T_N = temperature at upstream conditions.

2.1.3 Connecting rod

The connecting rod couples the piston rod to the cart, making sure that the displacement of the cart and the piston is same. The connecting rod is modelled a spring and damper system.

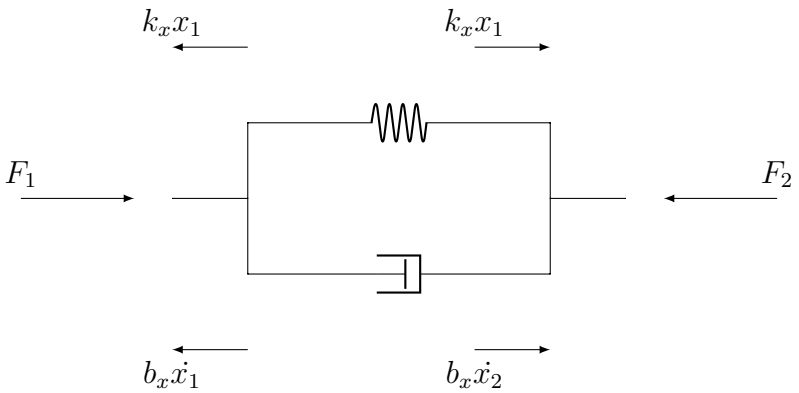

Figure 2.6: Spring and damper model representation of connecting rod

$$F_L = k_x(x_1 - x_2) + b_x(\dot{x_1} - \dot{x_2}) \tag{2.40}$$

where,
x_1 = position of the piston,
x_2 = position of the cart,
k_x = stiffness of the spring,
$\dot{x_1}$ = velocity of the piston,
$\dot{x_2}$ = velocity of the cart,
b_x = damping coefficient of the damper,
F_L = external load to the cylinder motion equation.

2.1.4 Control:

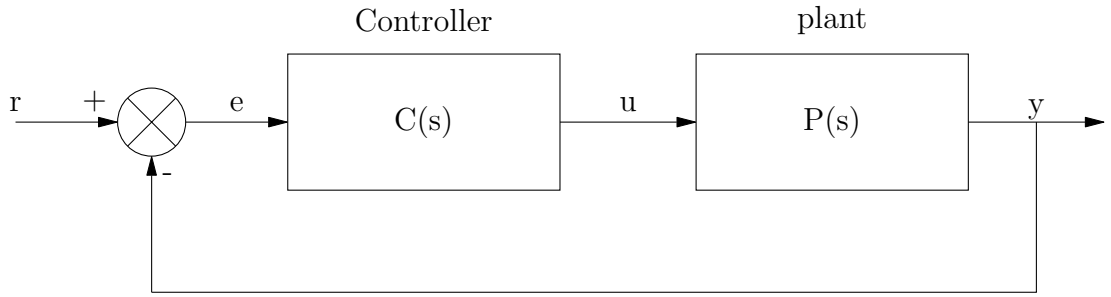

Figure 2.7: Block diagram of closed loop system

The simple feedback compensator is a Proportional-Integral-Derivative (PID) controller. The output of the PID controller is the input to the plant, which is calculated from the feedback error.

The PID controller works in a closed loop system as shown in a Fig.2.7. The variable e represents the error, which is a difference between the desired output r and the actual output y. The controller output is calculated as shown in Eq.2.41. The error signal e is fed to the PID controller, controller signal u is equal to the proportional gain times the magnitude of the error signal plus the integral gain times the integral of the error plus the derivative gain times the derivative of the error signal. The controller output can be expressed as,

$$u(t) = K_p e(t) + K_i \int e(t)dt + K_p \frac{de}{s} \tag{2.41}$$

The control outut signal is fed to the plant and new output signal y is obtained. The new output signal is fed back to find the new error signal e.And controller computes a new control output signal and the cycle continues.

The transfer function of a PID controller is found by taking the laplace transform of Eq.2.41,

$$K_p + \frac{K_i}{s} + K_d s = \frac{K_d s^2 + K_p s + K_i}{s} \tag{2.42}$$

where,

K_p = proportional gain

K_i = integral gain

K_d = derivative gain

Characteristic of P,I and D terms:

With the increase in Proportional gain the controller in the closed loop system reacts more quickly but with the cost of overshoot. The proportional gain reduces the steady state error but wouldn't eliminate the steady state error[23].

The integral term reduces the steady state error. The integral term builds till error reaches zero. A drawback of integral term, it can make the system more oscillatory since when

error signal changes sign, it may take a while for an integrator to "unwind".
The derivative term to the controller adds the ability of controller to predict the error.The control signal can become very big with the error. The derivative acts as a damping to the system, thereby reducing the overshoot. It has no effect on the steady-state error.

CL Response	Rise Time	Overshoot	Settling Time	S-S Error
Kp	Decrease	Increase	Small Change	Decrease
Ki	Decrease	Increase	Increase	Decrease
Kd	Small Change	Decrease	Decrease	No Change

2.1.5 PWM:

[27] PWM is one of the basis of control in electronic systems. The rapid switching on and off of semiconductor material as fast as practically possible reduces the switching transition time and any switching loses. so an ideal PWM will be a one which has zero rising and falling time. Pulse frequency is one of the important parameter in PWM generating methods [28].

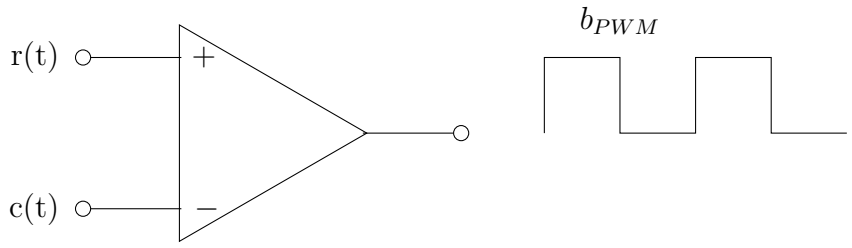

Figure 2.8: Constant-frequency PWM implementation by a comparator

PWM signal can be produced simply by comparing a reference signal $r(t)$ and carrier signal $c(t)$ as shown in Fig.2.8. The binary mathematical PWM signal can be represented as,

$$b_{PWM}(t) = sgn[r(t) - c(t)] \tag{2.43}$$

where sgn is a sign function. The simplest way to generate a PWM signal is the intersective method, which requires only a sawtooth or a triangle waveform (easily generated using a simple oscillator) and a comparator. When the value of the reference signal (the red sine wave in Fig.2.9) is more than the modulation waveform (blue), the PWM signal (magenta) is in the high state(1), otherwise it is in the low state(0).

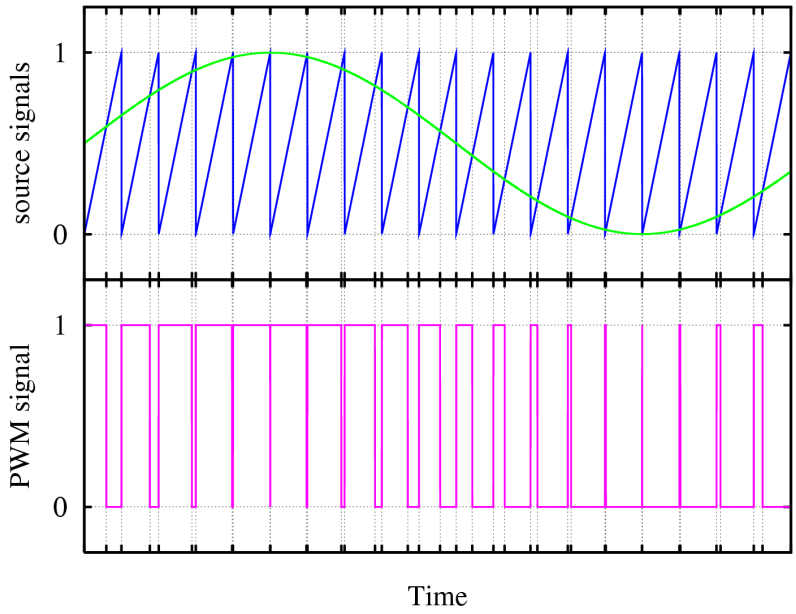

Figure 2.9: Generation of PWM signal

2.2 Computer Aided Modelling

Having an understanding of the mathematical model of the system, we need to take assistance of computer to analyse the system numerically. Computer aided modelling provides fast computation and results. It is helpful for repetitive analysis and optimisation of the system parameters. We be will using couple of numerical computation software:

- Dshplus
- Matlab/simulink
- Altair-Activate

We will be building the complete model in Dshplus as well as in Matlab/Simulink environment. Also we will model subsystems in the environment of Altair - Activate for the co-simulation purposes. Moreover we will be focussing on the results fetched from DSHplus for the real time application, which will be dealt in chapter5.

2.2.1 DSHplus

The DSHplus is software package developed by **FLUIDON GmbH** [29]. DSHplus software package specializes in Hydraulics, Pnuematics, Control and Mechanics. With the help of the building blocks in the Pneumatics, control and mechanics, which will be representing our complete system.

2.2.1.1 Bluiding blocks in DSHplus:

DSHplus has a variety of component blocks to suite the requirements in all the domains mentioned above.Few important blocks used while modelling the system are listed below:

- **Inverted Pendulum:** This block characterizes single pendulum mounted on the cart. The 0° is defined on the positive y axis. The inverted pendulum block comprises of parameters such as stroke length of cart, length of pendulum, mass of cart and pendulum and frictional constants etc..., which are set by the users depending on the requirements of the modelling and simulation.

- **Pneumatic Cylinder:** It is one of block from the list of actuators in the libraries. some of the important input parameters passed to the block are: piston and rod diameter, stroke max and min, mass, stribeck friction constants and polytropic exponent and etc...

- **Valves:** Switching valves 2/2 way were used which were defined by parameters such as switching time(open and close),maximum and minimum opening of the stroke(effective area), conductance, critical ratio(b), relative overlap etc...

- **Pulse Width Modulation:** This block generates the PWM signal with input parameters: Signal period and maximum signal amplitude.

- **PID:** It is parallel block formulation, defined by individual gains of Proportional, Integrator, Derivative and time constant. Additional parameters are present to limit and reset the integrator term.

- **Function Generator:** This block in the model is used to produce signals. Function generator can generate functions like constant, sine, rectangular, ramp etc.... We are using it to change the Set-point and observe system robustness to the changing Set-point i.e. to check the system behaviour while changing the cart position and trying to keep the pendulum stable.

2.2.1.2 General layout of the system

The actuator($P\_cylinder$) used is a pneumatic cylinder without end stop damping. The pneumatic cylinder is coupled with the cart of the inverted pendulum($pend$), the coupling

is done with the help of spring and damper(*conn_rod*). The spring with high stiffness can closely represent a rod. The Fig.2.10 shows the coupling of the inverted pendulum and the pneumatic cylinder's piston rod.

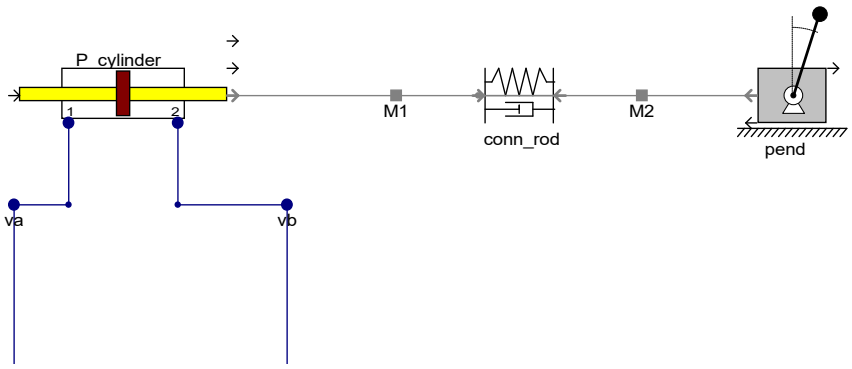

Figure 2.10: Coupling of inverted pendulum and pneumatic cylinder in DSHplus

The Fig.2.11 shows the controller layout, the cart position and pendulum angle position is given out from the inverted pendulum block and is compared with their respective Set-point. The error signals generated out of each comparison is an input to the controller. There are two PID controller used; one for the stroke control while one for the theta control. The each of the PID controller has a multiplication factor and then are summed up to form a value (labeled as *dc* in Fig.2.11), cumulating the values of both the controller. This value can be positive as well as negative. The dc signal is branched into two signals, one of the branch remains unchanged and is connected to PWM signal generator($pwm1$), where the signal *dc* acts as a carrier signal for the $pwm1$. The second branch, the block *g_neg* flips the sign of the signal *dc*(gain of the block *g_neg* is -1), which is further labelled as *dc_neg* and connected to PWM signal generator($pwm2$). The signal *dc_neg* acts as carrier signal for $pwm2$. The Fig.2.12 shows the layout of the pneumatic system. The two 2/2 switching valves are connected to each of the cylinder port. The valve labelled as $solA$ and $solC$ is connected to supply pressure source , while valve labelled as $solB$ and $solD$ are connected to the sink. The pneumatic cylinder piston is set to a initial position at the centre of the stroke length. The triggering of valve($solA$), fills the left chamber of the cylinder, while the triggering of valve($solC$), fills the right chamber of the cylinder. The valve($solB$) is used to discharge the left chamber and valve ($solD$) discharges the right chamber of the cylinder. The block $pwm1$ triggers the valves($solA$ and $solD$), while $pwm2$ signal generator triggers the valve($solC$ and $solB$).

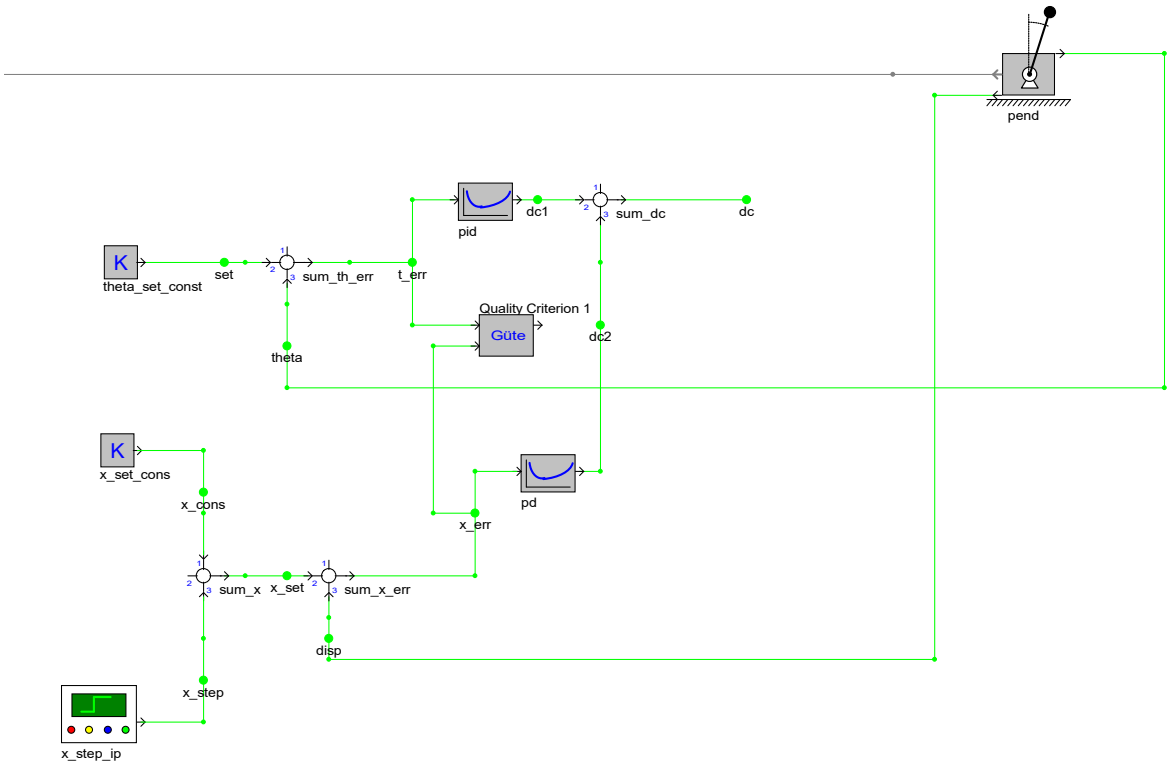

Figure 2.11: Controller layout model in DSHplus

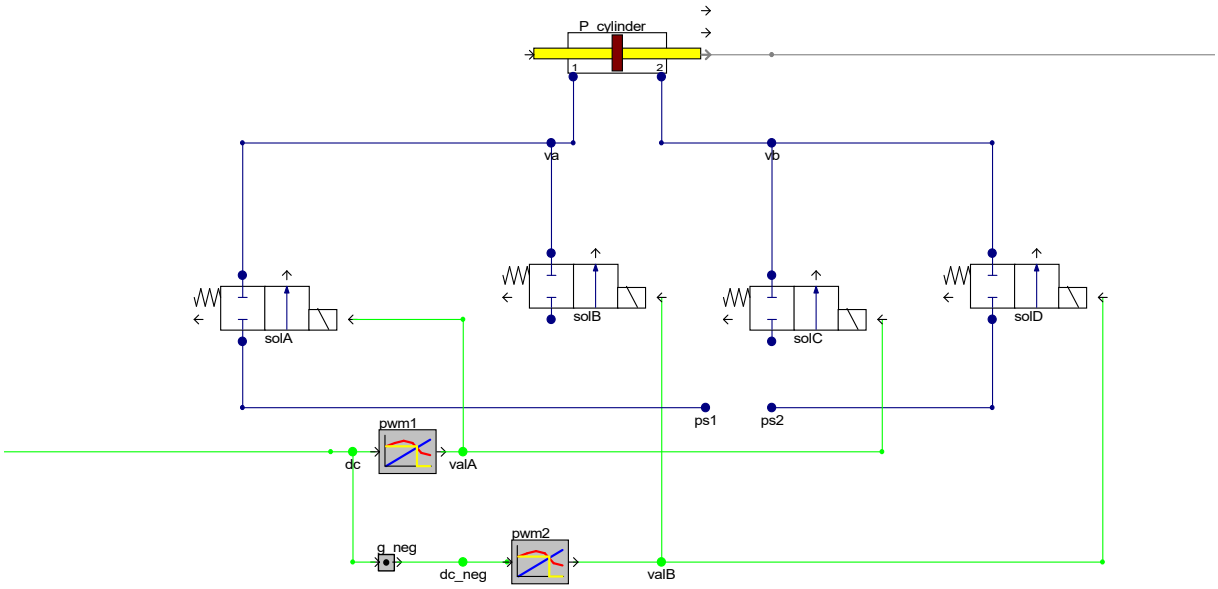

Figure 2.12: Pneumatic system model in DSHplus

The PWM signal generator takes into account only the input of positive value, while the negative value signal is considered as zero. In the figure (2.12), if the sign of *dc* is

positive, then $pwm1$ is active and $pwm2$ is inactive, causing the outward stroke of the cylinder. If the sign of dc is negative, then $pwm2$ is active and $pwm1$ is inactive, causing the inward stroke of the cylinder.
Several models were created for a step by step and systematic understanding of the system. we will only mention the important and focussed set of models which will completely define the scope of this project. Following are the models:

2.2.1.3 Model 1: Only Stroke Control

The model shown in Fig.2.13 emphasizes only on the cart position control, where stroke refers to the displacement of the cart. The stroke of the cart is in the feedback loop and it is compared to the Set-point. Function generator is used to define and acquire a variable Set-point throughout the simulation time. Function generator produces a square waveform with a amplitude of 75 mm and duration of 50 s. Only the stroke error is considered and fed to the controller, the model comprises of 1 PID controller. The pneumatic and mechanical system were described in the previous subsection 2.2.1.2.

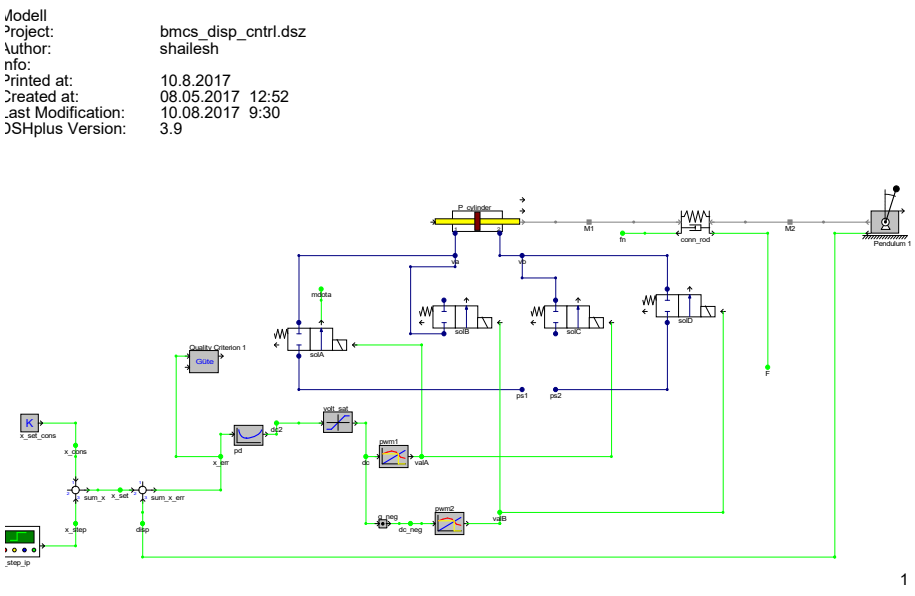

Figure 2.13: Stroke Control model in DSHplus

2.2.1.4 Model 2: Only Theta Control

The model shown in the Fig.2.14 is only meant for the theta control, where theta refers to the angle of the pendulum. The theta is fed back after a comparison to its Set-point($\theta = 0$). Only the theta error (sum_th_err) is fed to the controller, the model comprises of 1 PID controller to control the theta, while position of the cart is not considered. The pneumatic and mechanical system were described in the subsection2.2.1.2.

Modell
Project: bmcs_theta_cntrl.dsz
Author: shailesh
Info:
Printed at: 10.8.2017
Created at: 08.05.2017 12:52
Last Modification: 10.08.2017 9:42
DSHplus Version: 3.9

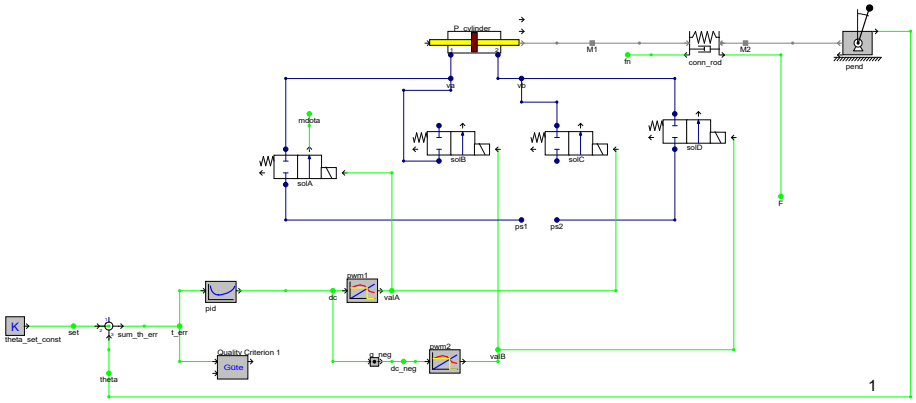

Figure 2.14: Theta Control model in DSHplus

2.2.1.5 Model 3: Stroke and Theta Control

The model manages to control both position (stroke) of the cart and the angular position (theta) of pendulum. From Fig.2.15, stroke and theta values are continuously compared to their respective Set-point. Two PID controllers are used in the parallel form and are summed to generate a input to PWM signal generators. The detailed explanation was described in the subsection 2.2.1.2.

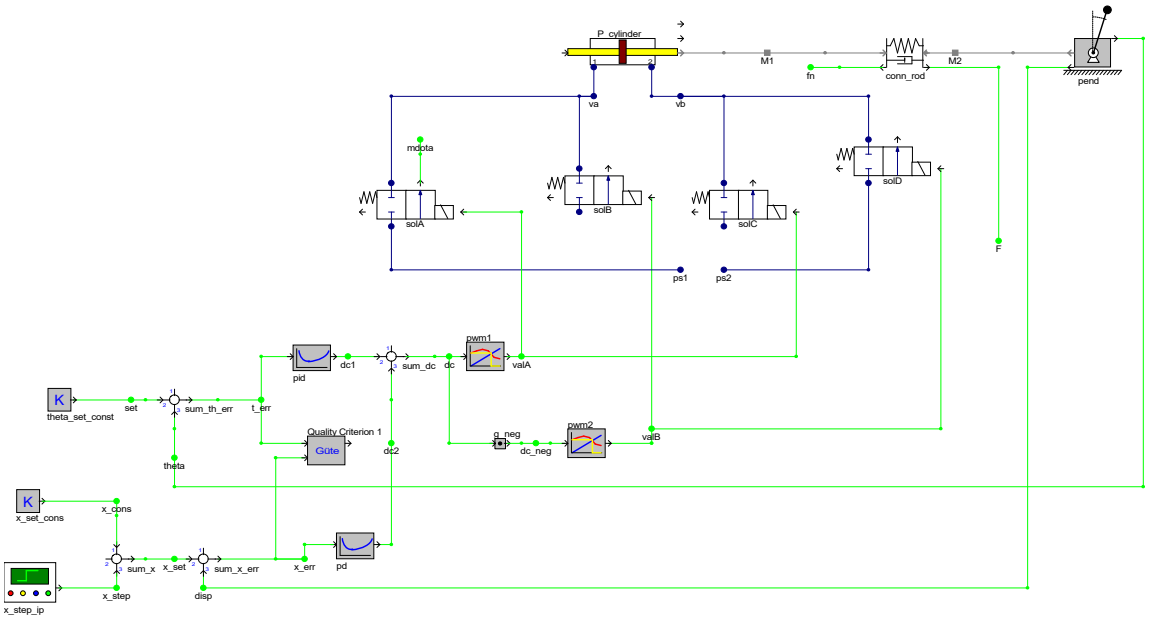

Figure 2.15: Stroke and Theta Control model in DSHplus

2.2.2 Matlab/Simulink

We will build the complete system in Matlab/simulink environment with help of mathematical model developed in the section 2.1. The model will be built with simulink basic blocks and with Simscape package.

2.2.2.1 Inverted Pendulum model with Simulink blocks

The simulink model is shown in the Fig.2.16 is developed on the mathematical model of the inverted pendulum described in subsection 2.1.1.

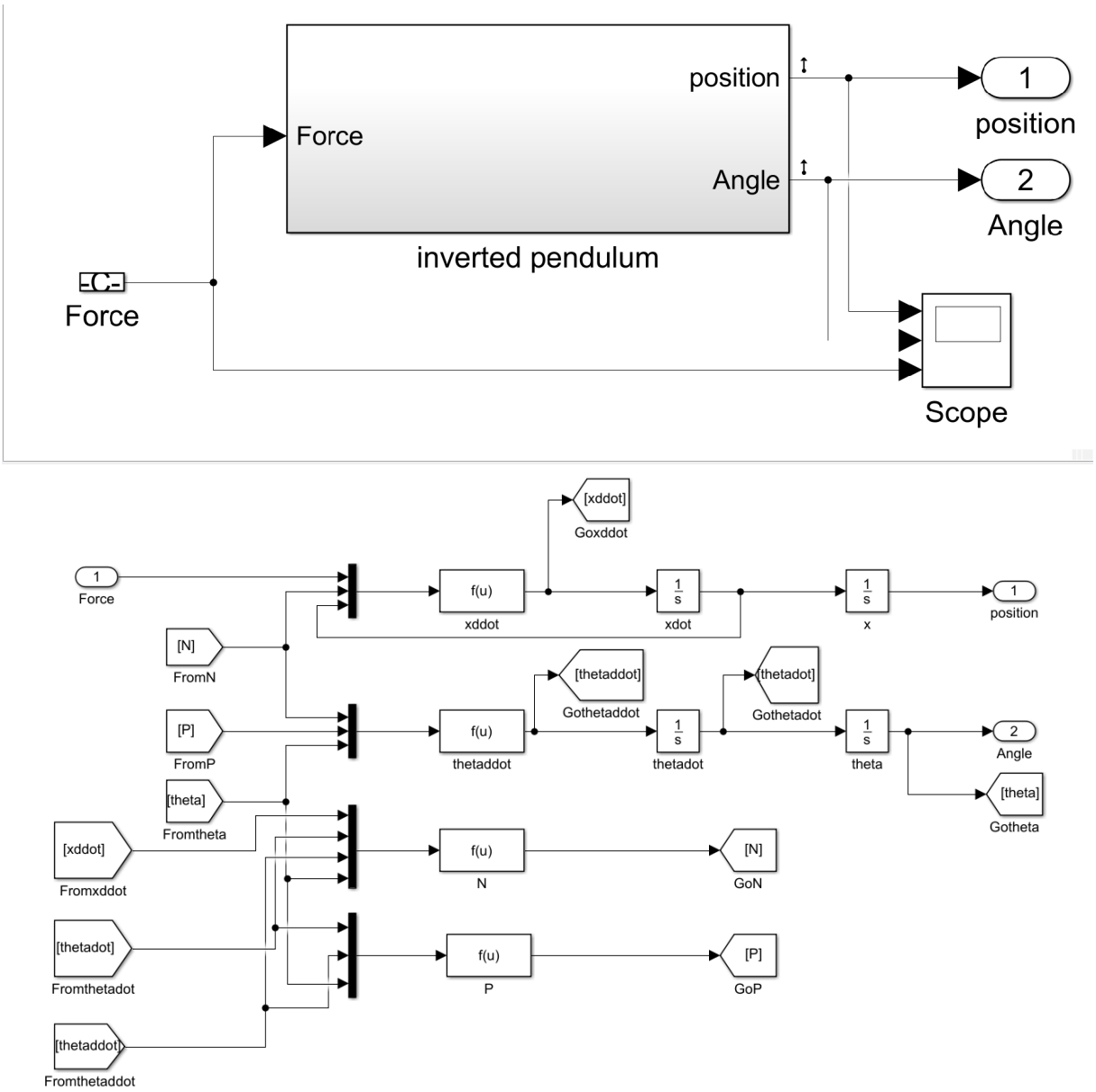

Figure 2.16: Matlab/simulink model of inverted pendulum

2.2.2.2 Inverted Pendulum model with Simscape package

The advantage of this package is the provision to view the model in 3D. And simulating this 3D model gives a fast and better visual understanding of the system behaviour.

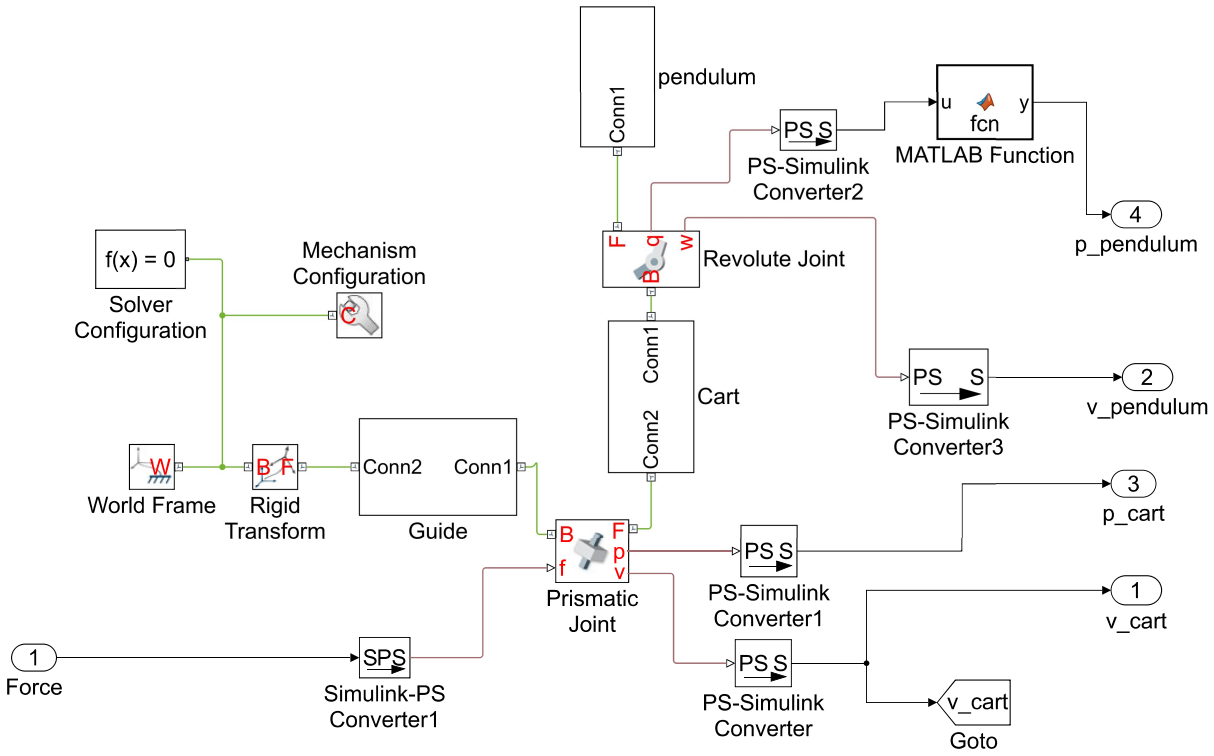

Figure 2.17: Simscape model of inverted pendulum model(cart-pendulum assembly)

Referring to the Fig.2.17 showing the simscape model of inverted pendulum, the *Guide* ((b) in Fig.2.18) is coupled to the *Cart* ((c) of Fig.2.18) with the help *Prismatic Joint*. The *pendulum* ((b) in Fig.2.18) is coupled to the cart by a *Revolute Joint*. The *cart* slides on the *guide* and the *pendulum* is pivoted to the *cart*. The $PS-Simulink\ Converters$ are used to convert the physical signals(signals from simscape blocks) to simulink signals. The 3D model is shown in the Fig.2.19.

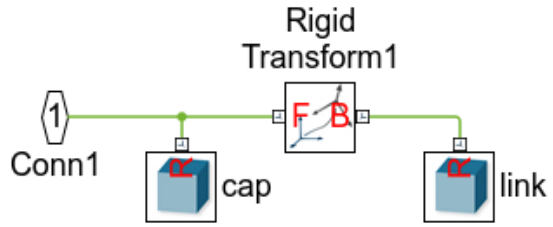

(a) Subsystem:pendulum

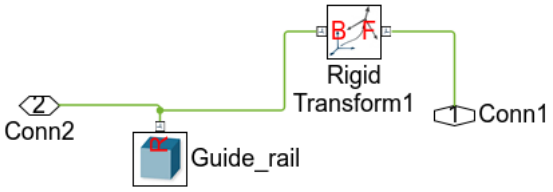

(b) subsystem: Guide

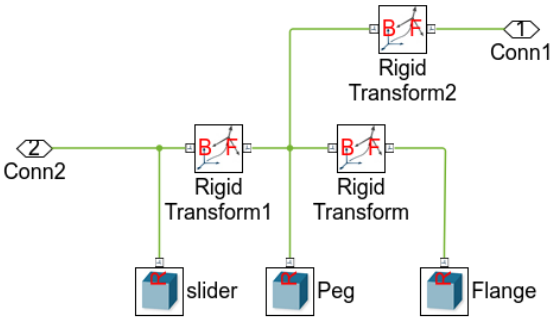

(c) subsystem: Cart

Figure 2.18: Simscape model of guide,cart and pendulum

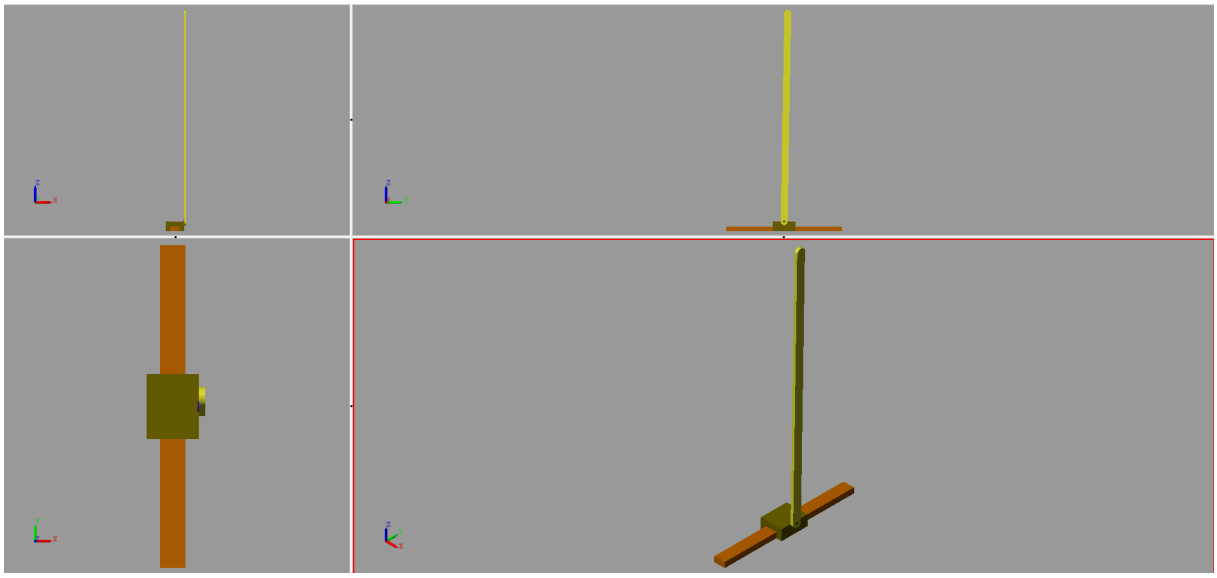

Figure 2.19: 3D model of Inverted pendulum(cart-pendulum assembly)

2.2.2.3 Pneumatic system model with Simulink blocks

The Fig.2.20 shows the complete pneumatic system. It is made up of simulink blocks, the equations mentioned in the section 2.1.2 is extensively used to develop this model. The signal *dc* is generated by the controller, which may be positive or negative in value. This signal is branched out into two signals, one of signal remains unchanged while other signal is multiplied by -1 to flip the sign of the *dc*.

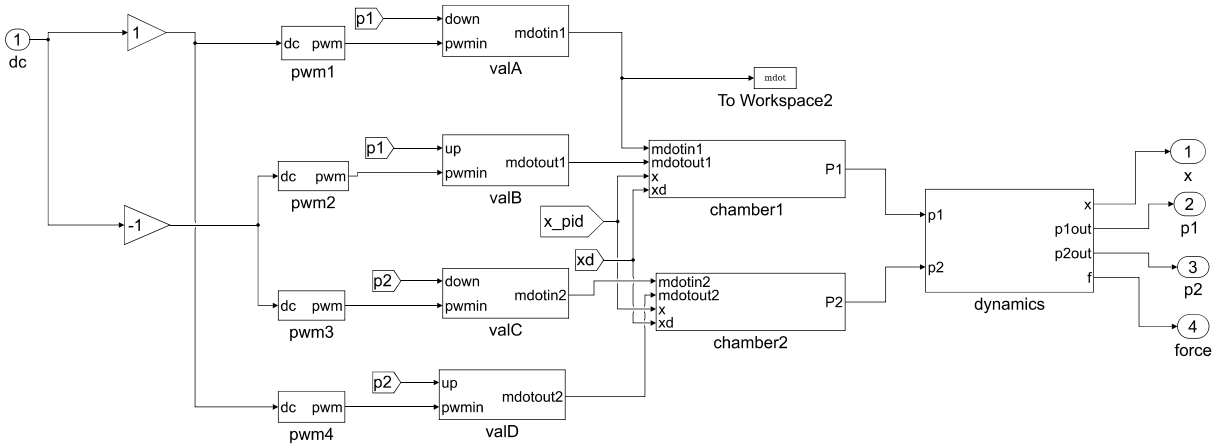

Figure 2.20: Simulink model of complete pneumatic system

When the *dc* is positive, $pwm1$ and $pwm4$ are active and $pwm2$ and $pwm3$ are inactive. If the *dc* is negative in value, then $pwm2$ and $pwm3$ are active and $pwm1$ and $pwm4$ are inactive. In Fig.2.21, subsystem $(Pwm1, pwm2, pwm3, pwm4)$ generates PWM signal for each of the valves$(valA, valB, valC, valD)$. The input to this subsystem is the duty cycle and output is the PWM signal. Sawtooth repeating signal is used as a carrier signal. The period of the PWM signal could be changed by changing the period of the carrier signal(*Repeating Sequence*). Four of these subsystem is required and each of them are driven by controller. The PID will be producing duty cycle for these valves.

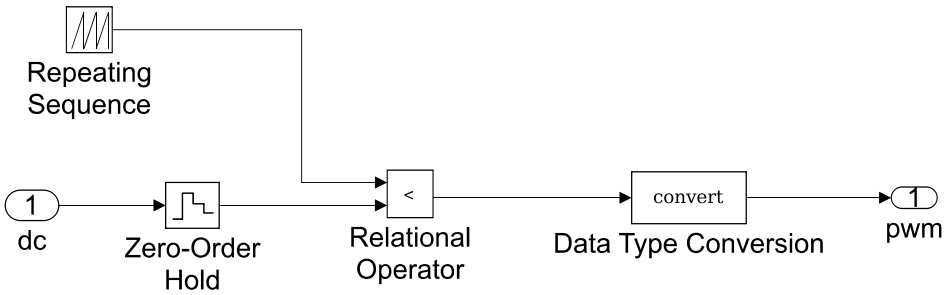

Figure 2.21: Simulink model for PWM generation

The Fig.2.22 shows the cylinder motion dynamics(*dynamics* in Fig.2.20) build with the help of Eq.2.25 mentioned in the subsection 2.1.2. The chamber pressure calculated from the subsystem $Chamber1$ and $chamber2$ is used as an input to this subsystem. The output of the subsystem *dynamics* is the position(x) and velocity(xd) of the piston, which is also an input to the subsystem: $chamber1\&2$ and subsystem:$Connecting\ rod$.

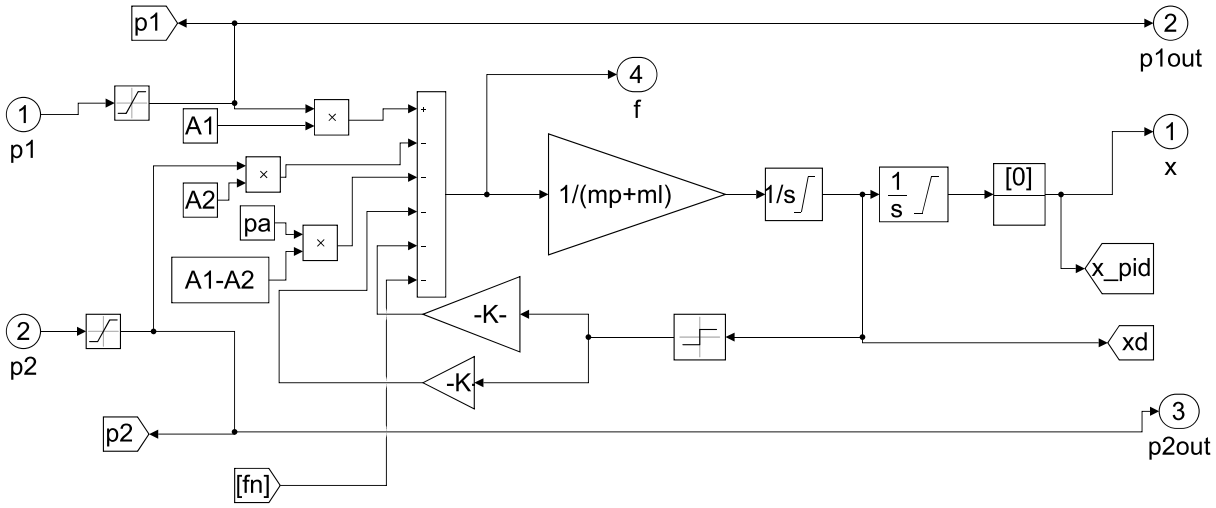

Figure 2.22: Simulink model for cylinder motion dynamics

The subsystem represents a single valve, there are 4 valves of the same type in this system. The left side chamber of the cylinder is *chamber*1 and the right side is *chamber*2. The valve A fills the *chamber*1 and the vale B discharges the *chamber*1. The valve C fills the *chamber*2 and the vale D discharges the *chamber*2. The Fig.2.23 shows the model of mass flow rate for the valve A and C, where the upstream pressure is the supply pressure source and the downstream pressure of valve A is $p1$(pressure of *chamber*1), for valve C it is $p2$(pressure of *chamber*2).

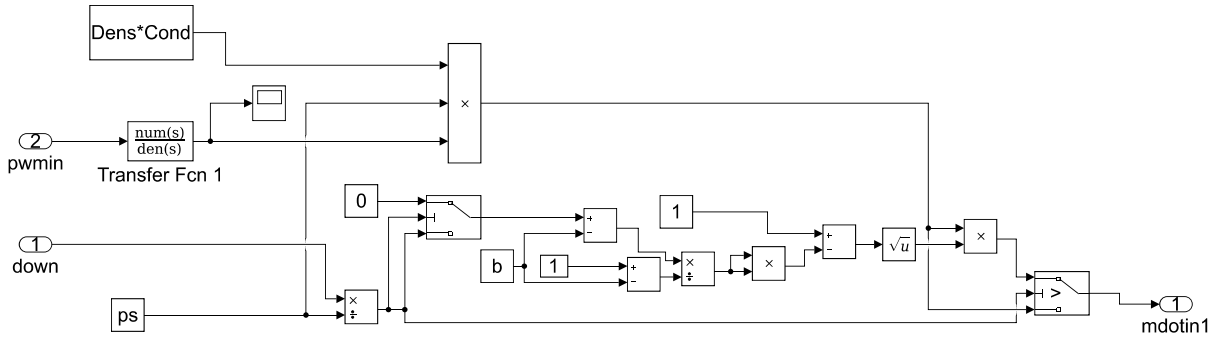

Figure 2.23: Simulink model for the massflow rate of valA and valC

The Fig.2.24 shows the model of mass flow rate for the valve B and D.The upstream pressure is $p1$ and $p2$ for valve B and D respectively, downstream pressure for the both the valves is the ambient pressure.

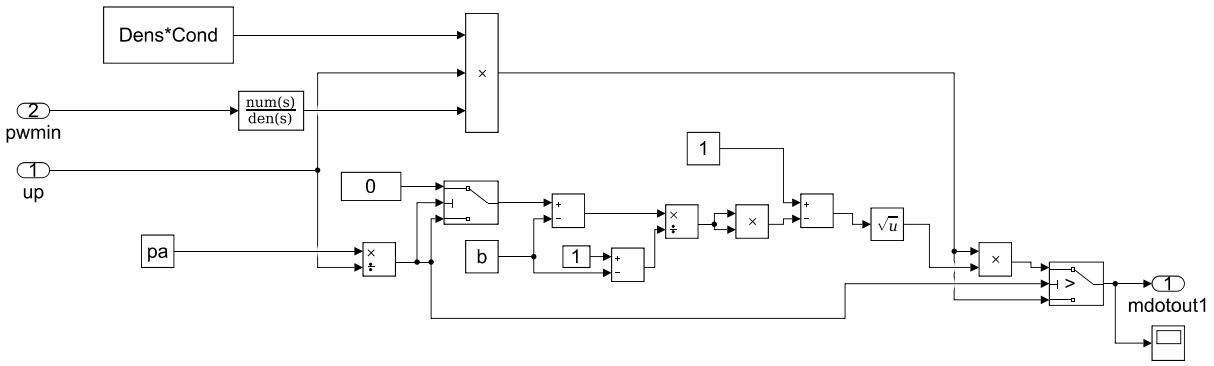

Figure 2.24: Simulink model for the massflow rate of valB and valD

The input being the upstream pressure which is used to calculate the mass flow rate of each valves, upstream pressure is also used to calculate the critical ratio. Critical ratio defines the flow to be sonic or subsonic, depending on which the mass flow rate is calculated. The another input to this subsystem is the PWM signal which controls the opening and closing of the valve. The shifting time of the vale is represented with the help of a transfer function $Transfer\ Fcn$ 1; $\frac{num}{den} = \frac{1}{\tau s+1}$, makes the exponential rise or fall of the PWM signal.

The model to calculate the pressure of the cylinder chambers is based on the Eq.(2.37). The pressure dynamics are shown for the *chamber*1 in Fig.2.25 and for *chamber*2 in Fig.2.26.

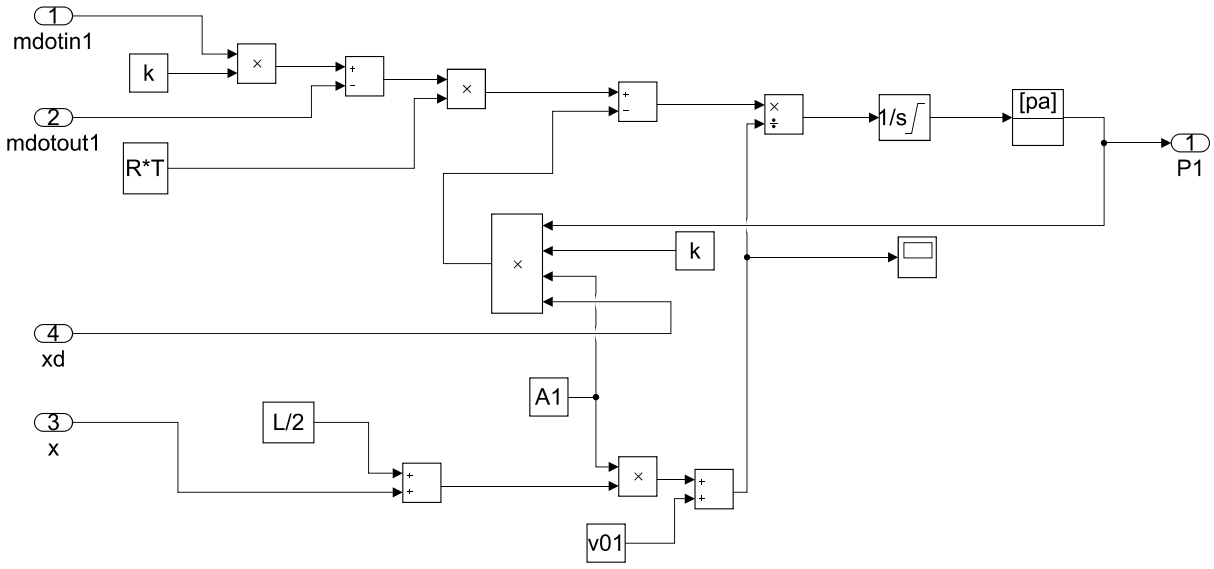

Figure 2.25: Simulink model for pressure dynamics of *chamber*1

The input to these subsystem are the mass flow rate in and out from the valves,

position and velocity of the cylinder piston .The initial condition of the piston is at the centre of the cylinder i.e. half of the stroke length. Mass flow rate into the system is calculated from the valve model connected to the supply pressure, while the mass flow rate out of the system is calculated from the valve model connected to the exhaust/sink. The output of these subsystem (*chamber*1 *and chamber*2) is the pressure of the chamber.

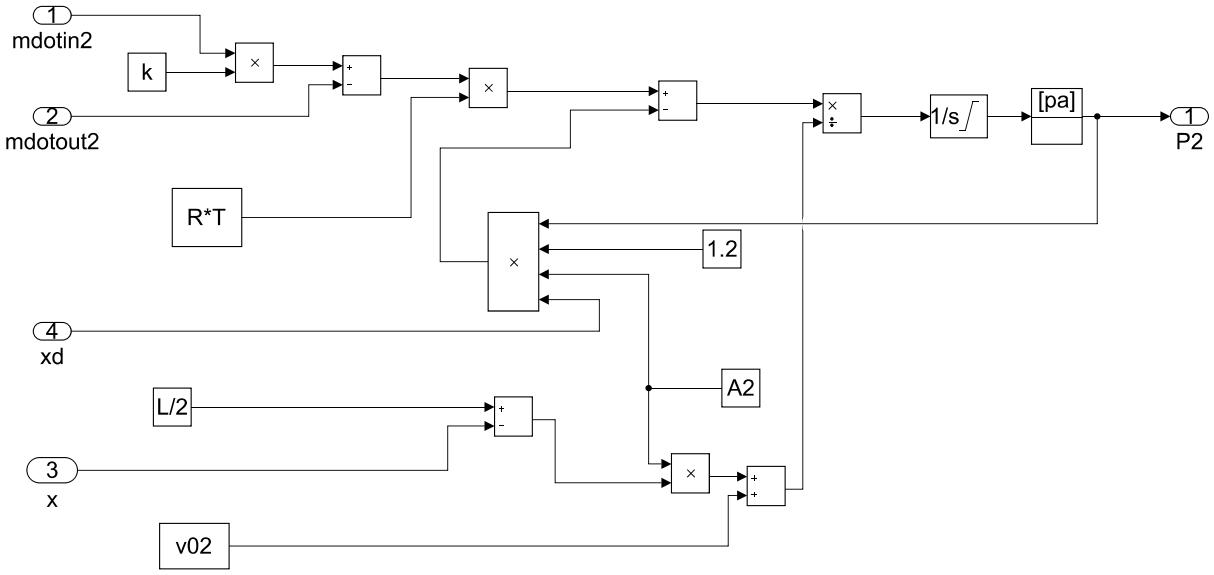

Figure 2.26: Simulink model for pressure dynamics of *chamber*2

2.2.2.4 Connecting rod model

The Fig.2.27 shows the model of connecting rod between the cylinder rod and the cart. It transfers the force from the pneumatic cylinder to the cart, making sure that the displacement of piston rod and the cart has same magnitude and direction. The connecting rod is modelled in such a way that it acts like a mechanical spring and damper with high stiffness. The mathematical model is described in the subsection2.1.3.

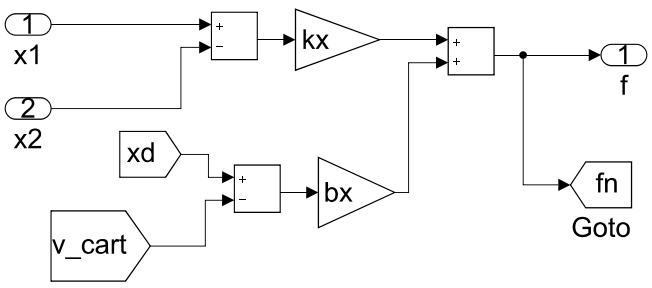

Figure 2.27: Simulink model of connecting rod

2.2.2.5 Pneumatic system model with Simscape package

Alternatively, the pneumatic system can be built with simscape package of simulink. The simscape model of pneumatic cylinder is shown in Fig.2.28.

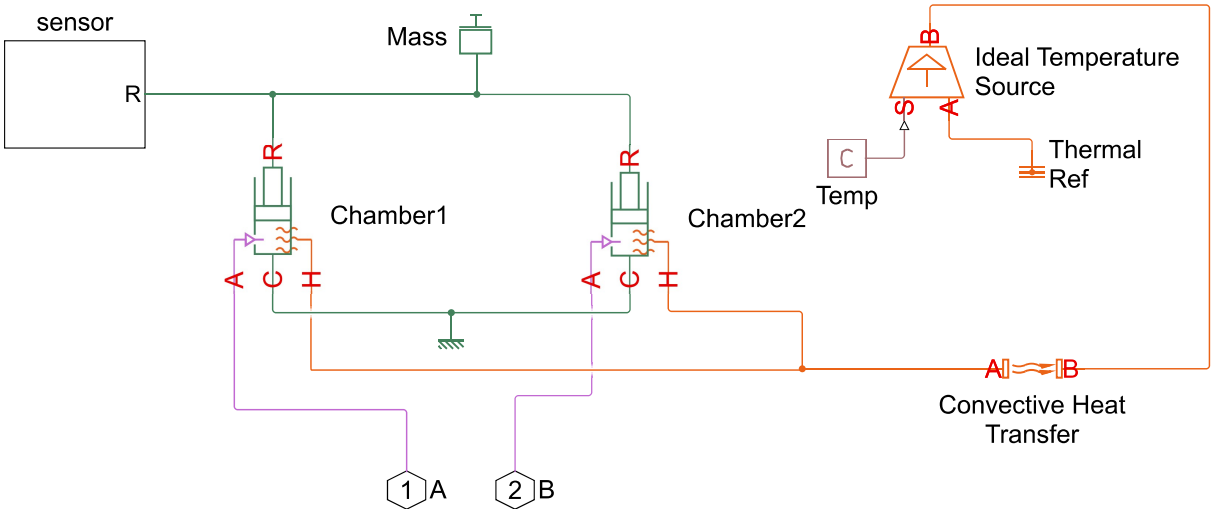

Figure 2.28: Simscape model for pneumatic cylinder

The $Translationalmechanicalconverter(G)$ block is used to represent the $chamber1$ and $chamber2$. The cross-sectional area of the piston, cross-sectional area of the ports, dead volume are some parameters defines the pneumatic cylinder. The mass connected to rod of the cylinder signifies the mass of piston and rod assembly. Heat transfer characteristics are taken into consideration with the blocks; $Convective\ Heat\ Transfer$ and $Ideal\ Temperature\ Source$. The block $Convective\ Heat\ Transfer$ is used to define the heat loss of the cylinder due to convection and the block $Ideal\ Temperature\ Source$ defines the ambient temperature. The $Ideal\ Translational\ Motion\ Sensor$ is used to read the position of the rod and $Ideal\ Force\ Sensor$ is used to measure the force exerted by the rod. The connections of these blocks are shown in the Fig.2.29.

The Fig.2.30 is a 4/3 valve model. 4/3 valve can be broken down to represent four 2/2 valves. P is the pressure source, E is the sink , $A\ and\ B$ are the ports of the pneumatic cylinder. The stroke of the spool(S) is the input to this subsystem, which will be positive or negative in value. It is branched into two signals, one of which is multiplied by -1 ($PSGain$ in Fig.2.30). Both of these signals are converted into orifice area(described in Fig.2.31).The blocks $R1$, $R2$, $R3$, $R4$ are called as variable local restriction, models the pressure loss due to a variable flow area restriction. The ports of this blocks are $A\ and\ B$, AR defines the orifice area. If the orifice area(AR) is zero or negative, signifies no passage between the port $A\ and\ B$ of the variable local restriction block.

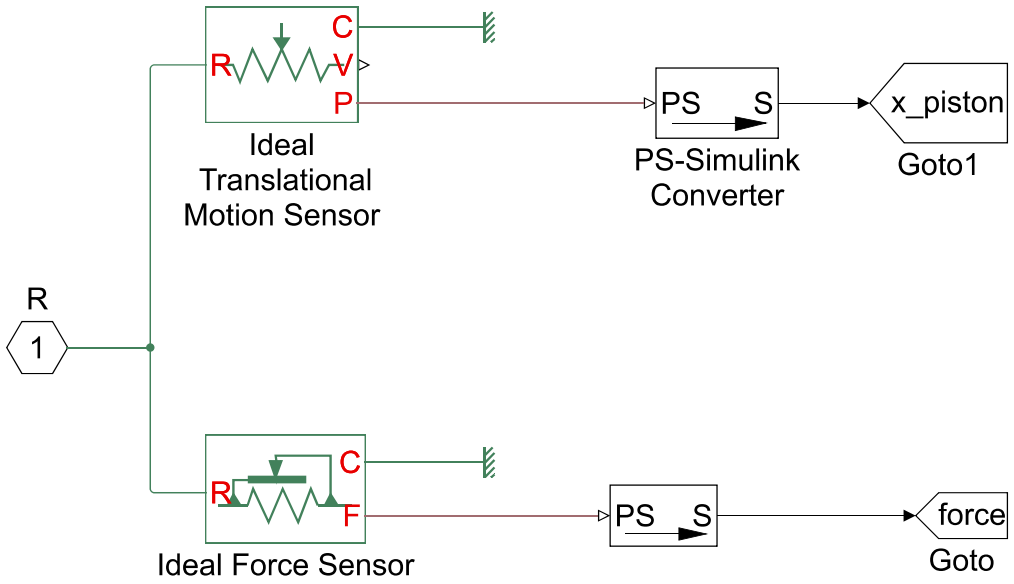

Figure 2.29: Simscape model of position and force sensor

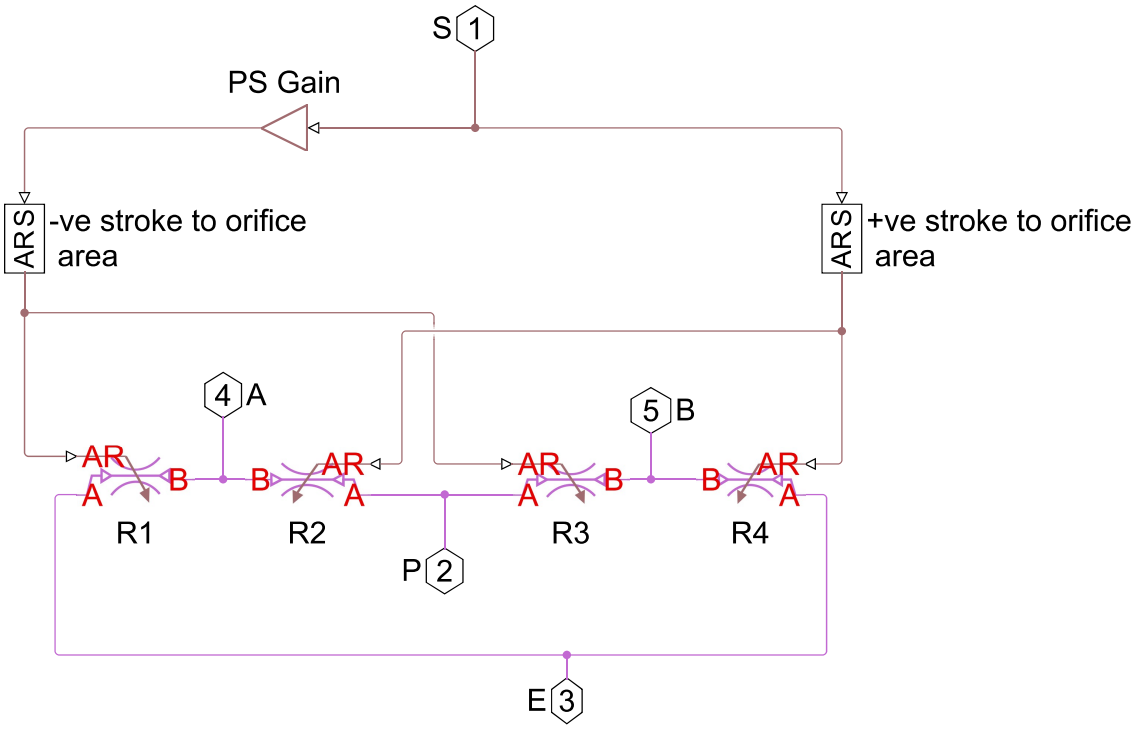

Figure 2.30: Simscape model for pneumatic valve

The model to convert the stroke of the spool into its orifice area is shown in the Fig.2.31, where $PSGain = \frac{A_{max}-A_{min}}{x_{max}-x_{min}}$

A_{max} = maximum area of the orifice,
A_{min} = minimum area of the orifice,
x_{max} = maximum stroke of the spool,
x_{min} = minimum stroke of the spool.

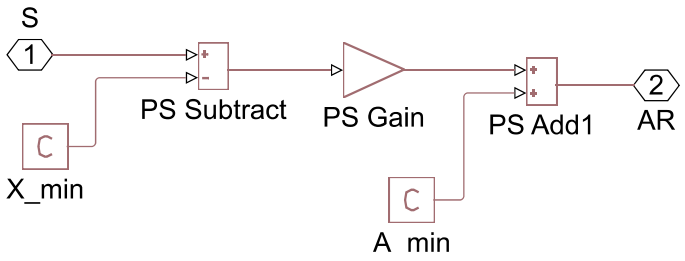

Figure 2.31: Simscape model of stroke to orifice area converter

when S is positive and the magnitude is equal to x_{max}, $R2$ and $R4$ is fully opened while $R3$ and $R1$ is fully closed, causing the flow from P to A and from B to E. The flow rate depends on the stroke of the spool.

The complete model of pneumatic system with simscape package is shown in the figure 2.32.

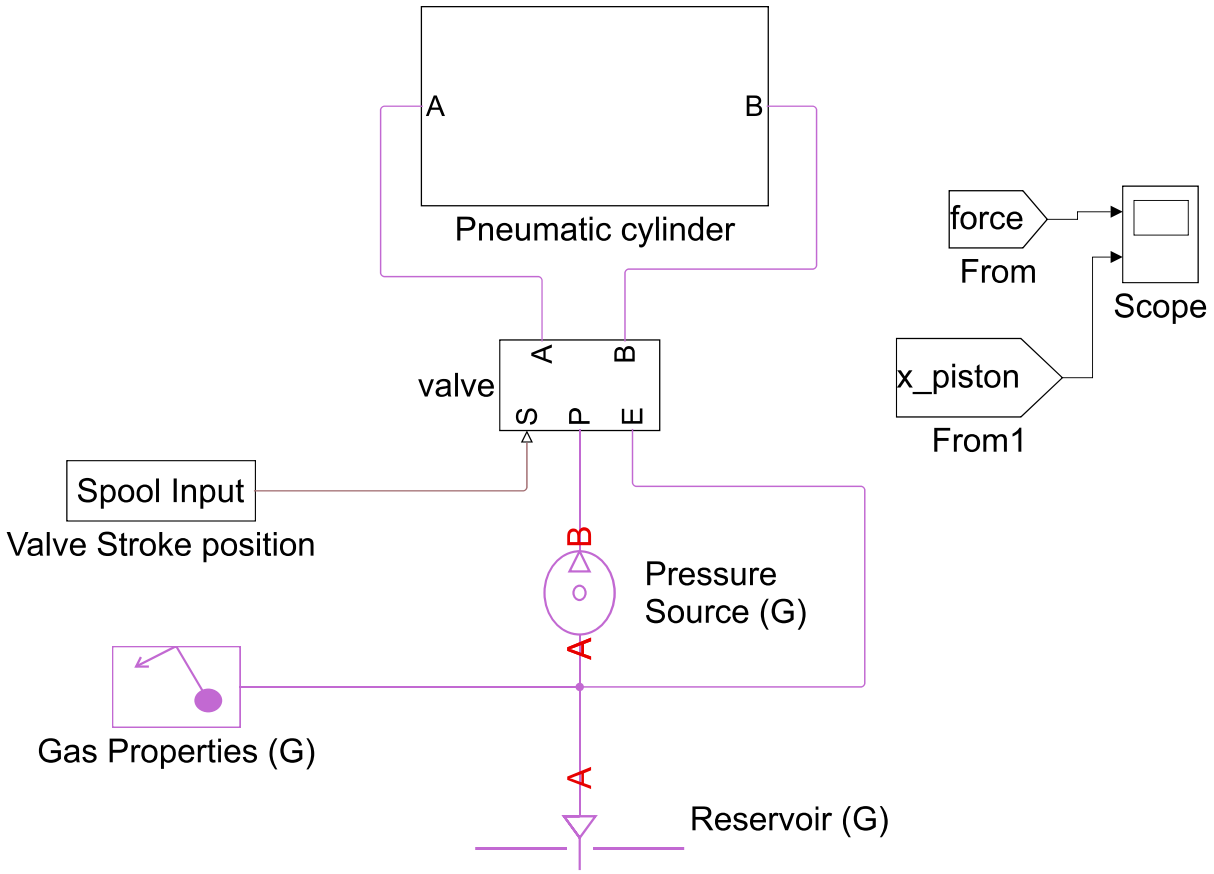

Figure 2.32: Simscape model of complete pneumatic system

As we are trying to model a simple system and to avoid complication while connecting different subsystems, we will prefer continuing the model with the help of basic simulink blocks for the simulation.

2.2.2.6 Only Theta Control

The complete model for the theta control is shown in Fig.2.33. The position of the pendulum is compared with the theta set-point, the error generated is an input to the PID controller. The PID controller output is an input to the PWM signal generator. The pneumatic system model (subsection:2.2.2.3) and the inverted pendulum model(subsection:2.2.2.2) is coupled with the connecting rod(subsection:2.2.2.4).

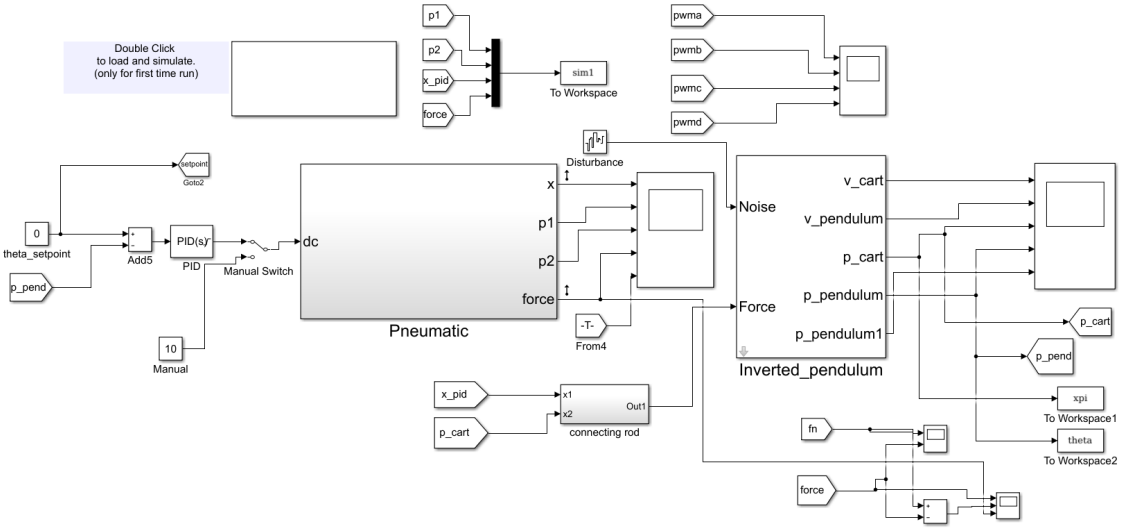

Figure 2.33: Simulink model of the complete system(theta control)

2.2.2.7 Theta and Stroke Control

The Fig.2.34 shows the model for the theta as well as stroke control of the inverted pendulum. The position of the cart(p_cart) and the position of the pendulum(p_pend) is compared to their respective set-point($Stroke\_sepoint1$ $theta\_setpoint$). The error generated are fed to their respective PID controllers, which are parallel to each other. The PID controller output is multiplied by a gain ($Gain1$ $Gain2$), the slight modification of this gain-weightage will help in tuning the system. The resulting output of $Gain1$ is subtracted by the output of $Gain2$. The result of this subtraction is the input to the PWM generator.

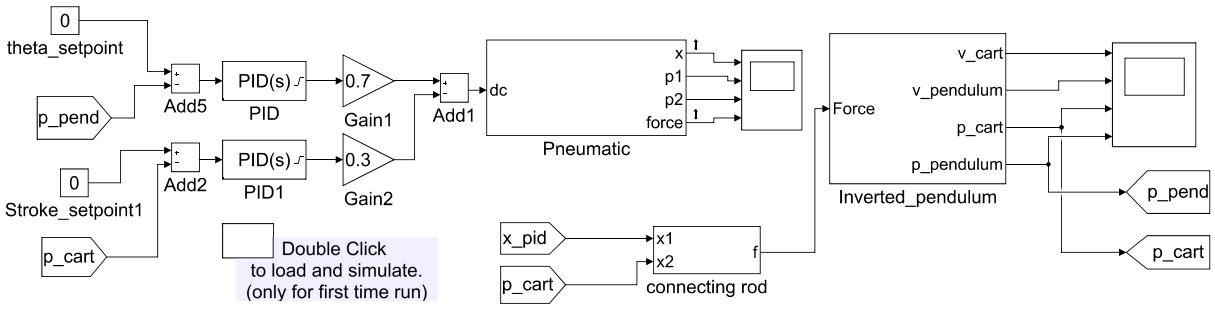

Figure 2.34: Simulink model of the complete system(stroke and theta control)

The modelling for co-simulation in Altair - Activate and Matlab/Simulink will be dealt in the chapter 4.Also we will be more focussing on the results developed out of simulation results from DSHplus. The simulation results and observations are discussed in the next chapter.

Chapter 3

Simulations

The stand alone simulations of the system was carried out in DSHplus and as well as in Matlab. Having understood the Mathematical model and finishing the model in DSHplus and Matlab/simulink of the system in chapter 2.2, we will try to analyse the system behaviour.

3.1 Simulations using DSHplus

Before jumping to the discussion on the simulations, I wish to discuss a tool in DSHplus which helps in optimizing the parameters; which is named **OPTIMIZATION** and the modelling block is **Quality Criterion**. Optimization tool is used to optimize one or more parameters of the model while minimizing the defined target function. The Quality Criterion has 4 methods of computing the numerical value, which uses integral algorithm to do so. This numerical value is minimized by the optimization algorithms. The one used for simulating the model is ITSE(Integral of time multiplied by squared error). OPTIMIZATION module works on Evolution method or gradient search algorithm(Hooke and Jeeves method), depending on the selection. Hooke and Jeeves method is used for this project.

The system parameters are:

- Pneumatic Cylinder

Piston Diameter	0.016 m
Rod Diameter	0.006 m
Stroke max	0.500 m
Stroke min	0.0 m
Mass of Piston	0.5 Kg

Table 3.1: Pneumatic cylinder geometric parameters

- Inverted pendulum

Mass of cart	0.45 Kg
Mass of pendulum	0.89 Kg
Length of pendulum	1 m

Table 3.2: Inverted pendulum geometric parameters

- 2/2 Pneumatic valve

Switching time open	4 ms
Switching time close	7 ms
Conductance	0.283 Nl/s/bar
Critical ratio	0.3

Table 3.3: 2/2 way Pneumatic valve parameters

- PWM signal generator

Carrier frequency	500 Hz
Signal Max	10 V

Table 3.4: PWM parameters

- Pressure source

Ps1	3.45 bar
Ps2	4.2 bar

Table 3.5: Presure source parameters

- Set-point

Position of cart	0.25 m
Angle of pendulum	0°

Table 3.6: Set-point

Let us define the initial condition of the model before starting the simulation trials.
The Initial condition are :

Parameters	Values
Stroke of cart	0.250 m
Velocity of cart	0 m/sec
Angle of pendulum	1°
Angular velocity of pendulum	0 deg/sec

Table 3.7: Initial conditions of the model

We will be simulating three models to do a step by step advancement in controlling the inverted pendulum. The first model is elaborated in below section.

3.1.1 Model 01: Stroke Control Simulation

As we have seen the model of only stroke control in the Chapter.2.2.1.3. We have used a fixed set-point and a variable set-point, which sums up to form the final set-point. The fixed set point is 0.250 m, whereas the variable set point is a square waveform with a amplitude of 75 mm every 50 seconds. The PD controller is used in this model.

The PD gains:

Gains	Values
P	960
I	-
D	130

Table 3.8: Stroke control PID gains

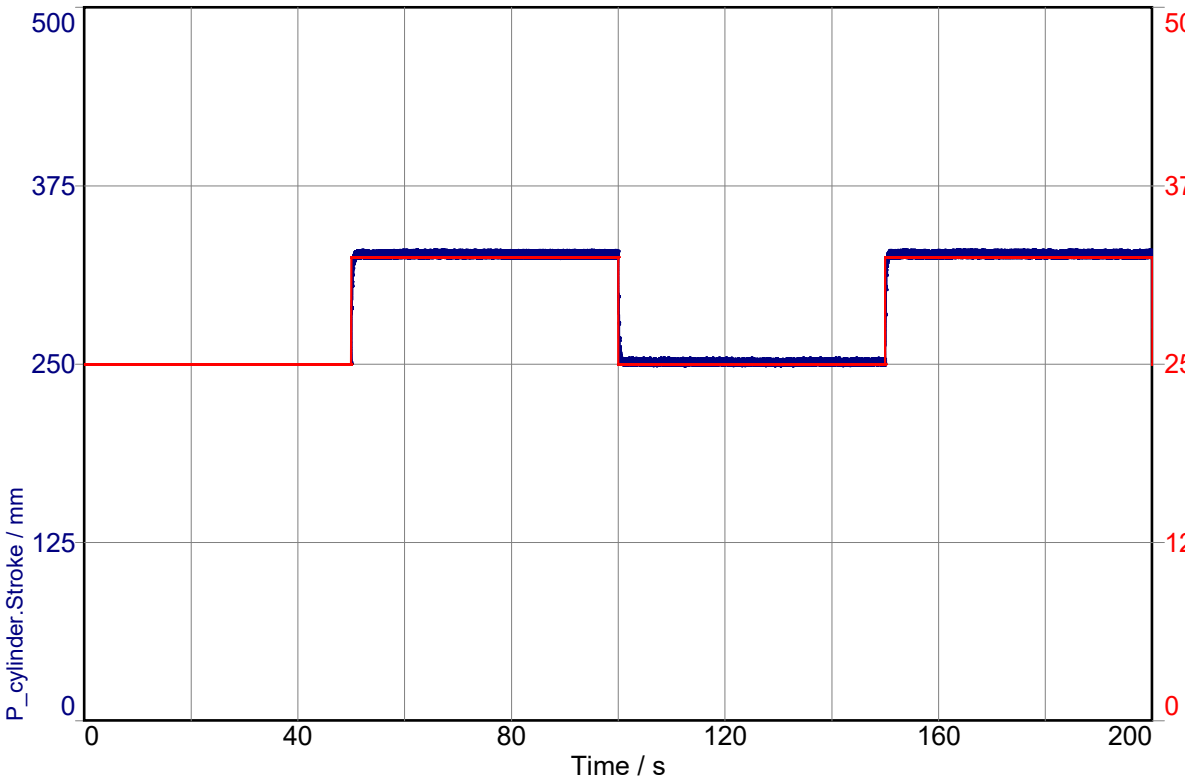

Figure 3.1: Stroke Control plot in DSHplus

The Fig.3.1 shows the displacement of the cart with variable set-point, the stability of the displacement is in the form of an oscillation by ±3 mm about the set point(250 mm).

3.1.2 Model 02: Theta control simulation

We have seen the model for Theta control in the previous Chapter.2.2.1.4. We will be simulating the model with the aim to control the angle of the pendulum i.e $\theta = 0\,\text{deg}$.

The values of PID parameters are shown in Table 3.9,

Gains	Values
P	400
I	1100
D	50

Table 3.9: Theta control PID gains

The Fig.3.2 is a theta plot, shows that the pendulum oscillates with an amplitude of 0.35° about it's set-point and the controller is in attempt to keep the pendulum stable despite of high oscillation amplitude. In Fig.3.3 it can be seen clearly that the stroke of the cart is approaching cylinder stroke end-limits. One PID can only control one parameter which is pendulum angle and not the cart stroke.

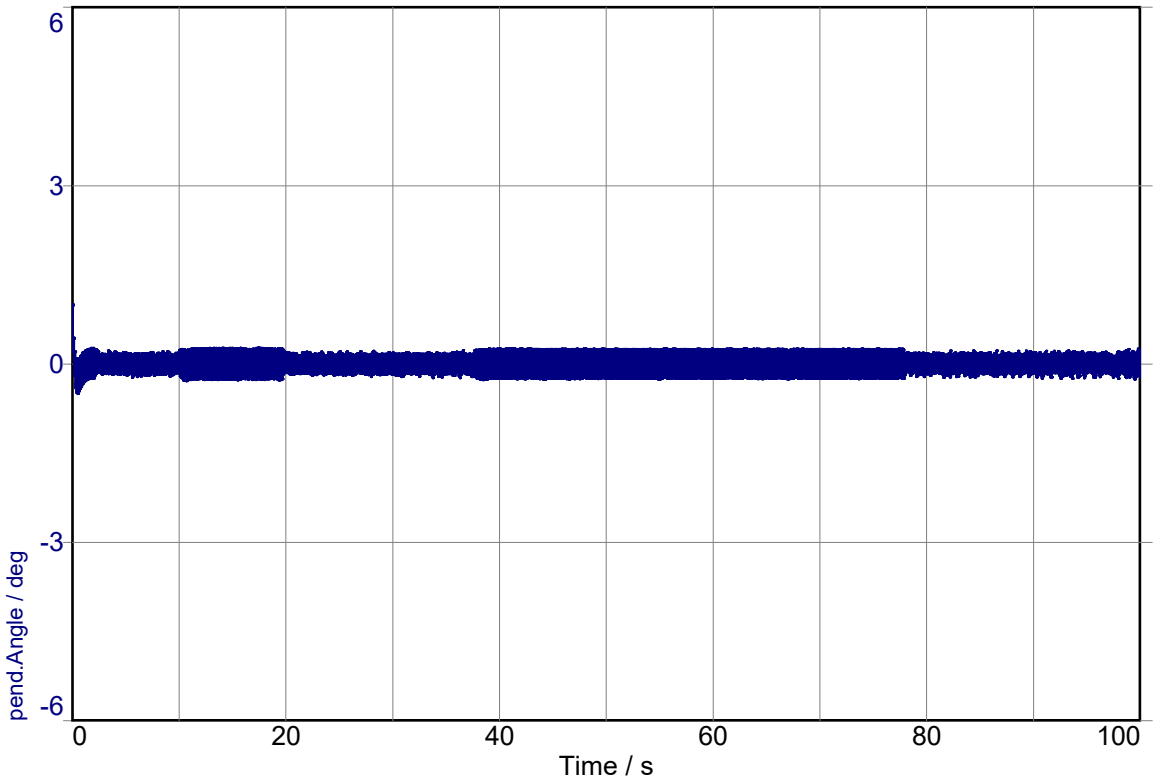

Figure 3.2: Theta plot of Theta control in DSHplus

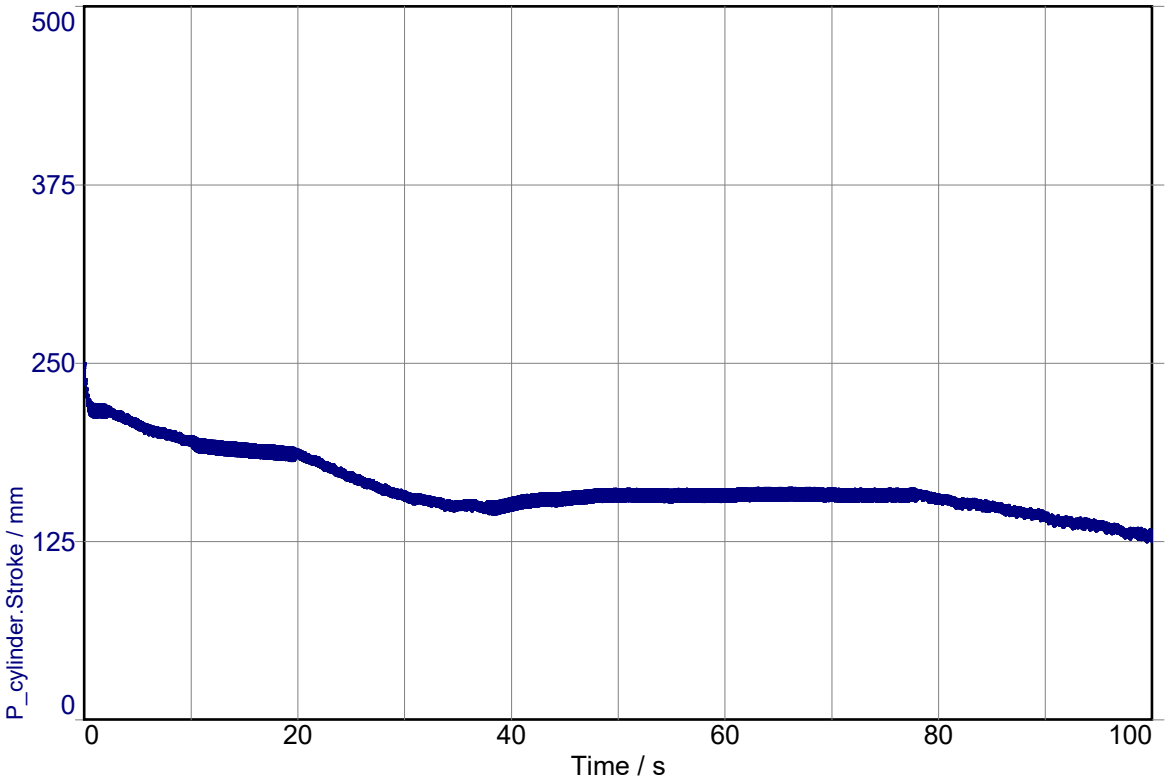

Figure 3.3: Stroke plot of Theta control in DSHplus

3.1.3 Model 03: Stroke and Theta Control Simulation

As we have observed in Theta control simulation model, the piston of cylinder was approaching either ends of the cylinder. The piston of cylinder i.e the cart reaching the end-limit causes the pendulum to fall. Once cart reaches the stroke end-limit, the controller cannot recover and maintain the stability of the system. In this simulation model we will be controlling the cart, while the pendulum is stable. Referring to the model Fig.2.15 in section 2.2.1.5, feedback of stroke and theta is compared to their respective set-point. The error generated are the inputs to their respective PID controllers. The output of the PID controllers are multiplied by their respective weighted gain and then are summed. The result of summation is converted into PWM signal which acts as a plant input. A different weights are helpful to ensure the PID1(for theta) has higher bandwidth, otherwise the control of the cart position may overshadow the error signal of the pendulum angle. The control priority is the control of pendulum angle over the cart position at all times. Basically with weight gain we are ensuring the priority of theta control over the stroke control. The weight gain factor is shown in the Table 3.10,

Weight factor:

Weightage factor	Values
Theta control	0.7
Stroke control	-0.3

Table 3.10: Stroke and Theta control weightage factor.

The Table 3.11 and Table 3.12 specifies the PID gain values of both the PID blocks. The PID1 manages to control the angle of pendulum, while PID2 controls the displacement of the cart.

PID1(for theta):

Gains	Values
P	500
I	1100
D	50

Table 3.11: Stroke and Theta control PID1 gains

PID2(for stroke):

Gains	Values
P	100
I	5
D	30

Table 3.12: Stroke and Theta control PID2 gains

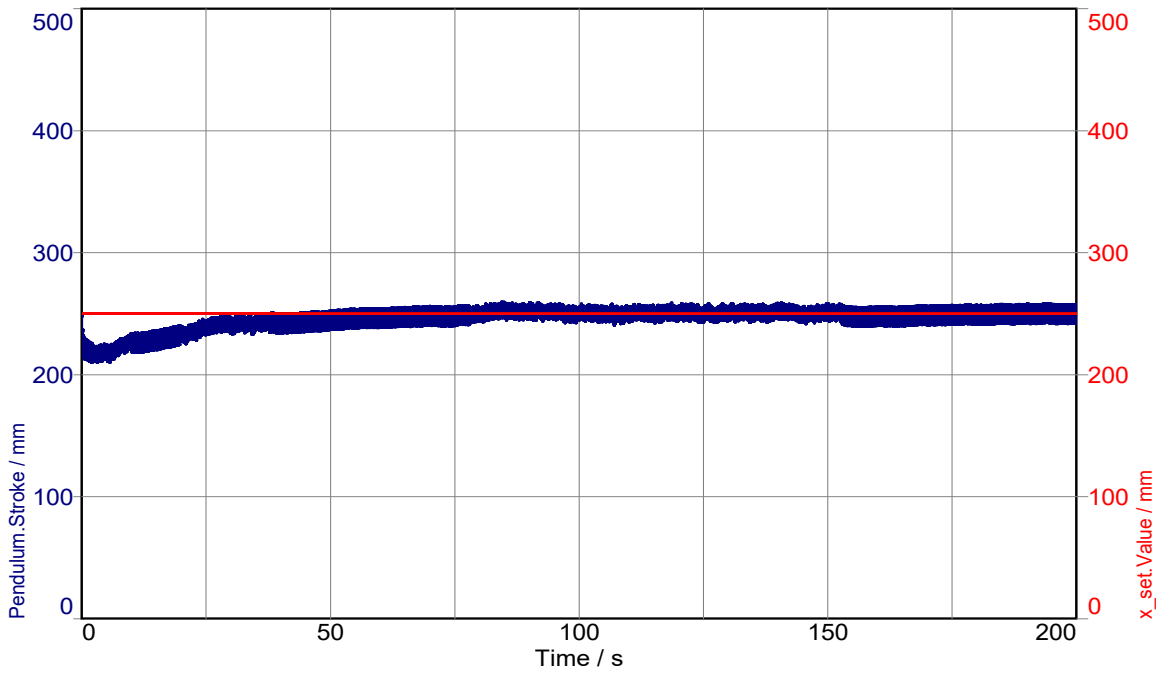

Figure 3.4: Stroke plot of Stroke and Theta control in DSHplus

The Fig.3.4 is the stroke plot of cart, which shows the oscillating stability of the inverted pendulum. Position of the cart oscillates between ±10mm from it's set-point ($250mm$). The Fig.3.5 shows the plot of pendulum angle (Theta), oscillates between ±0.5° from it's set-point(0°).

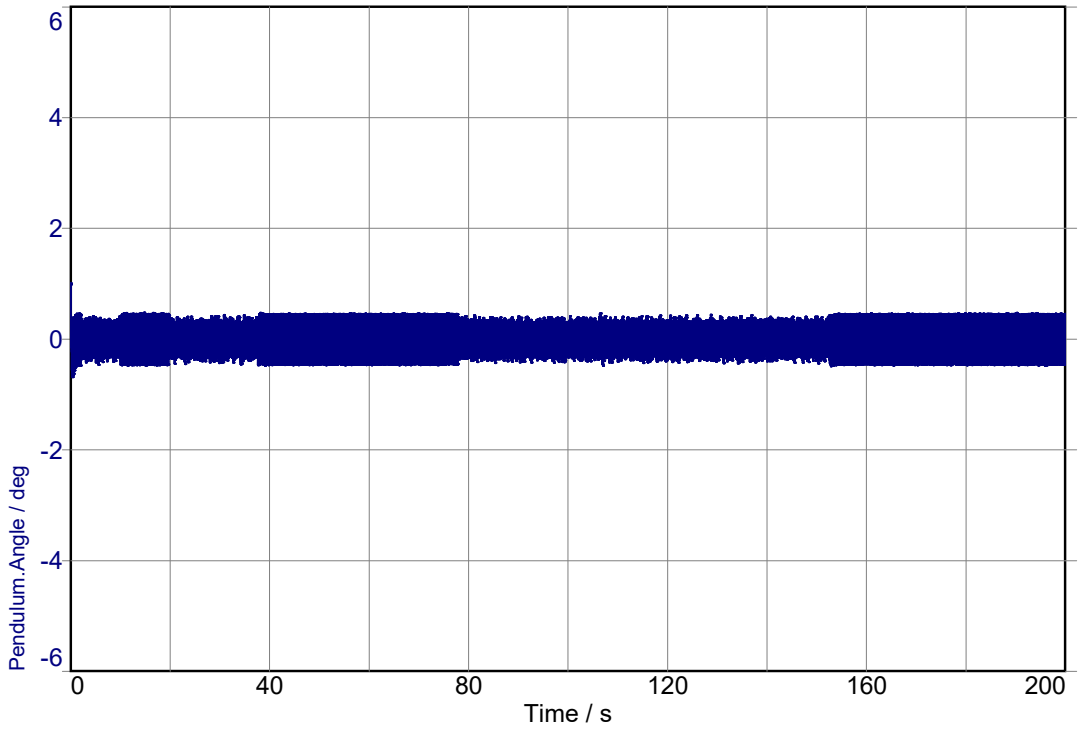

Figure 3.5: Theta plot of Stroke and Theta control in DSHplus

Initial conditions; velocity of cart, angular velocity of pendulum, position of cart and angle of pendulum is defined as 0 m/s, 0 deg/sec, 250 mm and 0 deg respectively, might not be true for all operating situations. And due its oscillating nature of stability, it might be quite difficult to start the system with the desired initial conditions. To check the robustness of the system and to check the capabilities of controller, changing the set-point of the cart seemed a perfect strategy. The set-point was varied in a square wave fashion, with the amplitude of 75 mm. The cart smoothly follows the change in cart position set-point, which can be seen in the Fig.3.6. The cart follows the new set point which is 325 mm and the rise time is 9.16 s. The set-point variation of the cart position has a very negligible effect on the oscillation of the pendulum angle. If the proportional term of PID2 is increased, the rise time can be reduced further. Higher the proportional term of PID2, lower is the rise time. The Fig.3.7 shows the theta plot, where the pendulum angle has an oscillating stability with an amplitude of 0.35° about the set-point(0°).

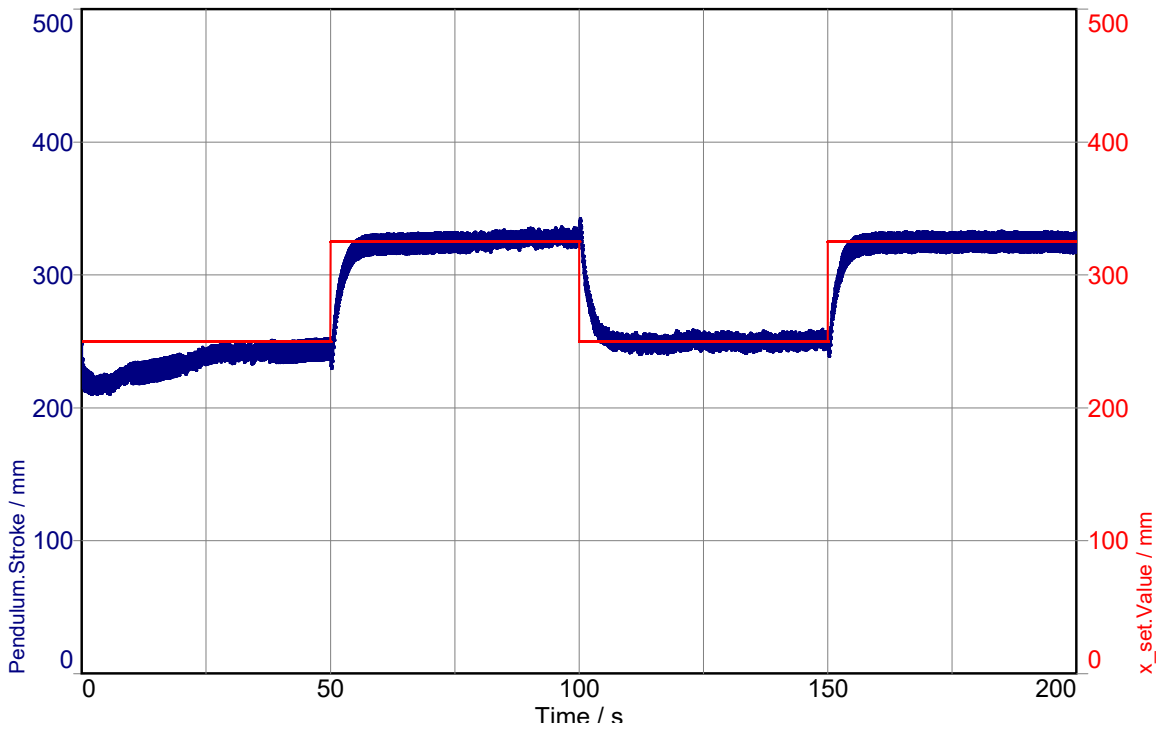

Figure 3.6: Stroke plot with variable stroke set-point

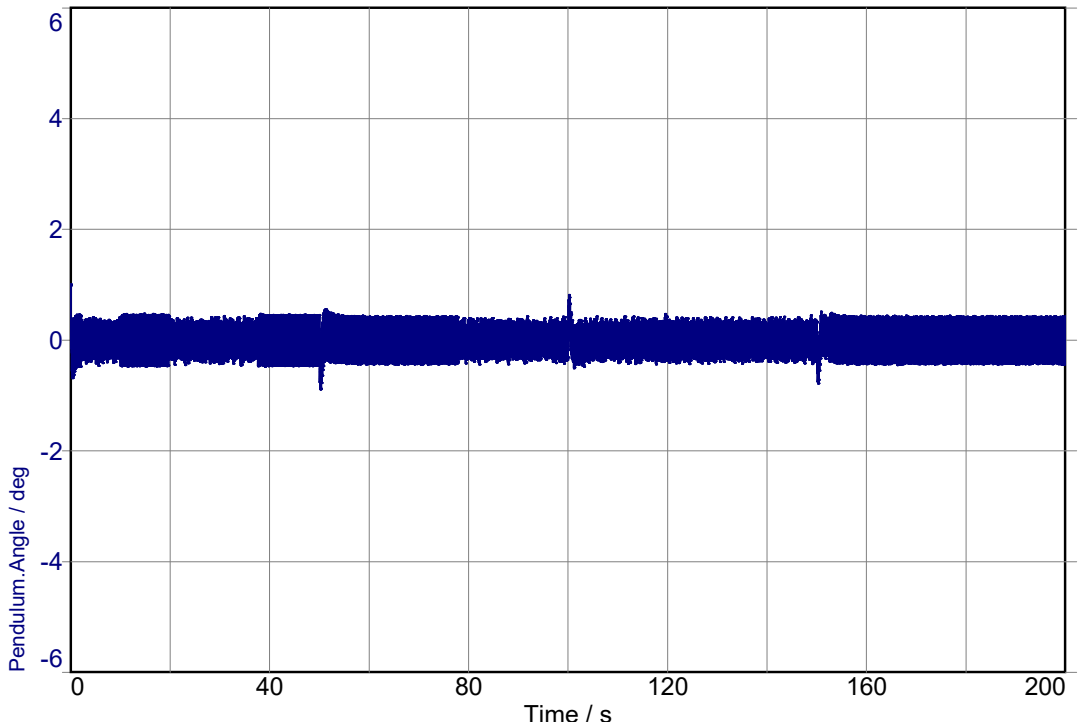

Figure 3.7: Theta plot with variable stroke set-point

In Fig.3.8 and 3.9, the system is able to recover and maintain stability with the initial condition of the pendulum angle set to 6°. The oscillations of pendulum angle and the cart position.

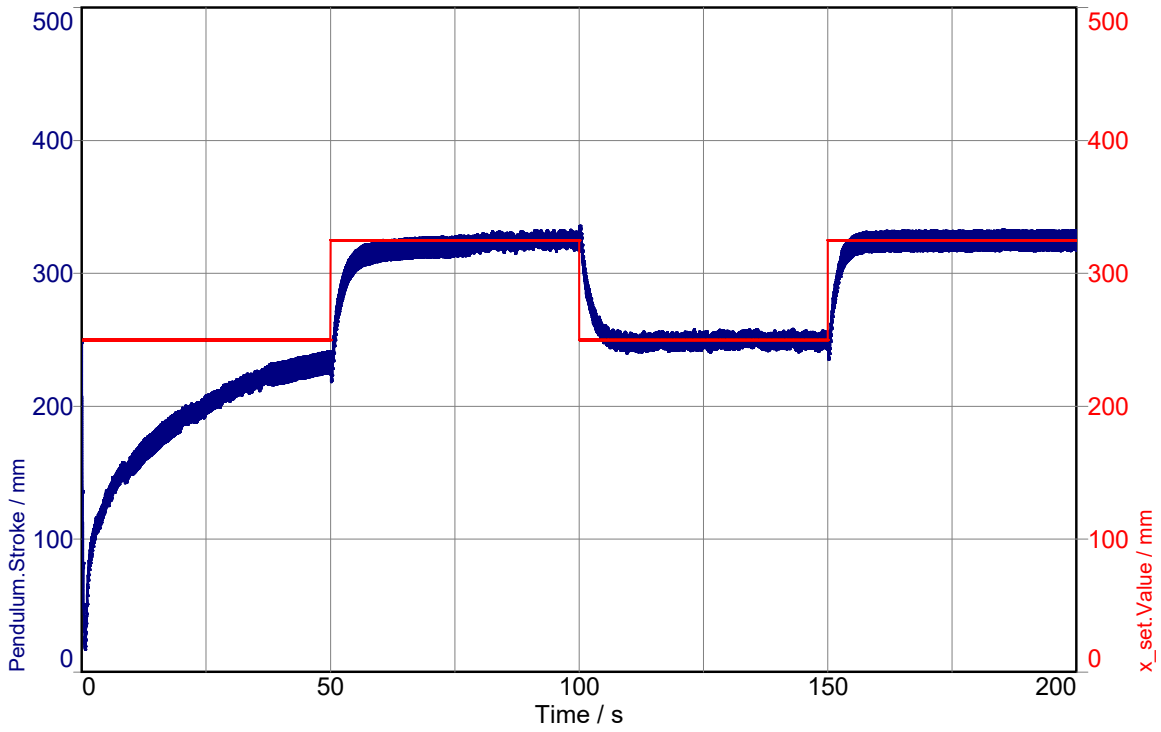

Figure 3.8: Stroke plot(Initial condition:Theta:6°) with variable stroke set-point

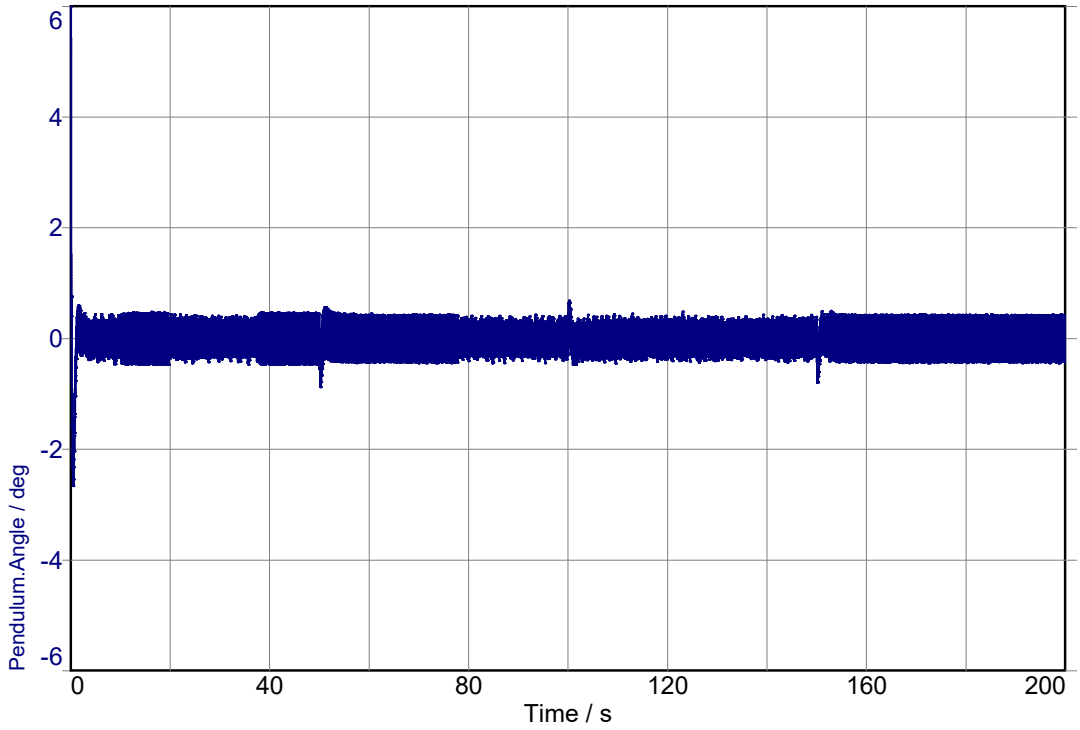

Figure 3.9: Theta plot(Initial condition:Theta:6°) with variable stroke set-point

3.2 Effect of parameters on the system

After couple of simulations by changing the system parameters and observing the results, it was quite obvious that some of the parameters have a major influence on the behaviour of system. Few of the strong influencing parameters being analysed are listed below:

- Supply Pressure.
- Length and mass of the Pendulum.
- Connecting pipe length.
- Valve Timings.
- PWM frequency.

These simulations are carried out on **Model 02: Only Theta Control**, where the pendulum angle has an oscillating stability with amplitude of 0.35° about it's set-point(0°) and the cart is approaching the stroke end limits.

3.2.1 PWM frequency

The PWM frequency has effects on the oscillation of the pendulum angle, if the frequency is low, the oscillation amplitude of pendulum angle is high. The high frequency PWM signal helps in delivering a precise input to the plant. As the frequency is increased, the oscillation amplitude keep on reducing, which can be seen in the Fig.3.10.

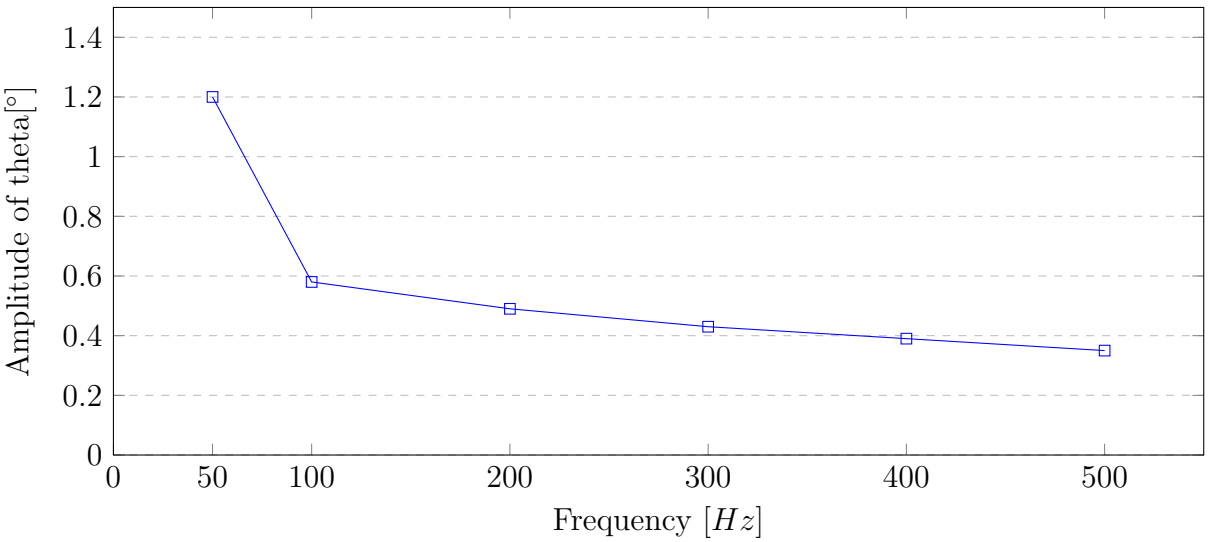

Figure 3.10: Effect of PWM frequency on oscillation of pendulum angle

The PWM signal generator frequency was increased from 50 Hz to 500 Hz, where the the oscillation amplitude of the pendulum angle kept on dropping from 1.2° to 0.35° from

it's set-point. The high frequency PWM signal generator produces better results and stability to the system.

3.2.2 Length of connecting pipes

Both the ports of the pneumatic cylinder is connected to two valves with the help of T-connectors. Effect of the length of connecting pipes between valves and cylinder is quite interesting. Connecting pipes can be seen in a electrical analogy as a RC circuit. The volume of the pipe has an effect on the response time of the system. Higher the volume, higher is time constant of RC circuit and the system turns slow in reacting to changes. This can be seen in the Fig.3.11, plot shows the effect of changing the length of connecting pipes on the time taken the by cart to travel 100 mm away from the stroke set-point(centre of cylinder stroke length: 250 mm).

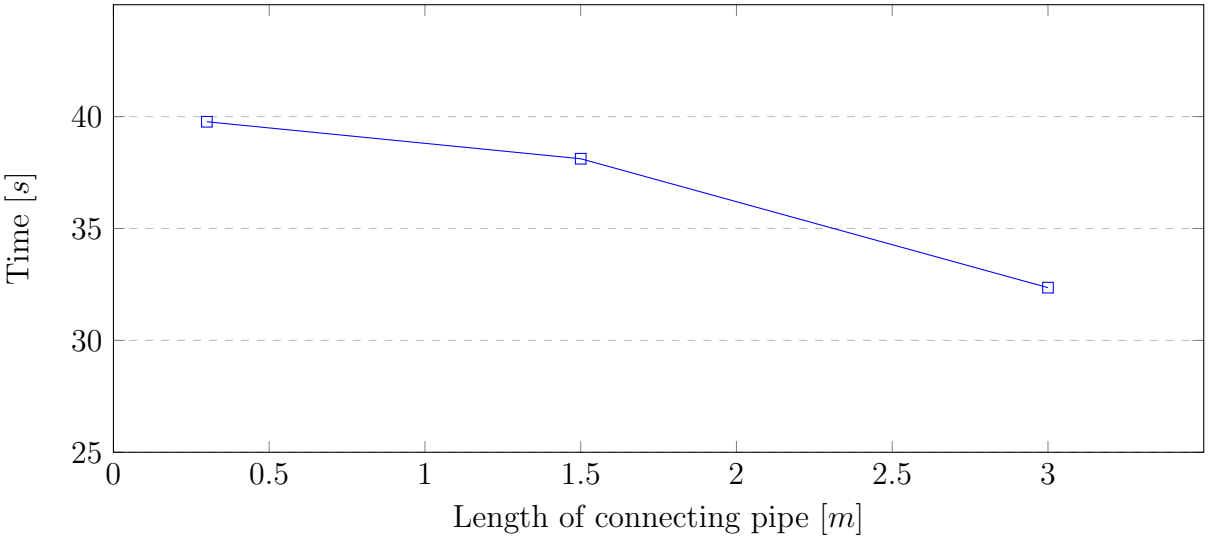

Figure 3.11: Effect of connecting pipe length on stroke of cart

The length of the connecting pipe is chosen to be 3 m then the cart travels 100 mm away from the set-point in 32.35 s and for 0.3 m of the pipe length, cart takes 39.77 s to travel 100 mm away from the set-point(250 mm). The time required by the cart to reach stroke end increases by reducing the length of the connecting pipe. So the length of the connecting pipe are kept small for better control over of the system and for the ease of controller design.

3.2.3 Mass of pendulum

The mass of the pendulum has a significant effect on the stability of the whole system. The mass of the pendulum is assumed to be at the centroid of pendulum. Let us simulate the system by varying the mass of pendulum from 1.2 kg to 0.3 kg. With the decrease of pendulum mass, cart tends to move towards the end of the stroke limit, though the

inverted pendulum angle is stable. There is not much significant change in the oscillation of the pendulum angle due to pendulum mass. The Fig.3.12 shows the effect of changing the mass of pendulum on the time taken by cart to travel 100 mm away from the stroke set-point(centre of cylinder stroke length:250 mm)

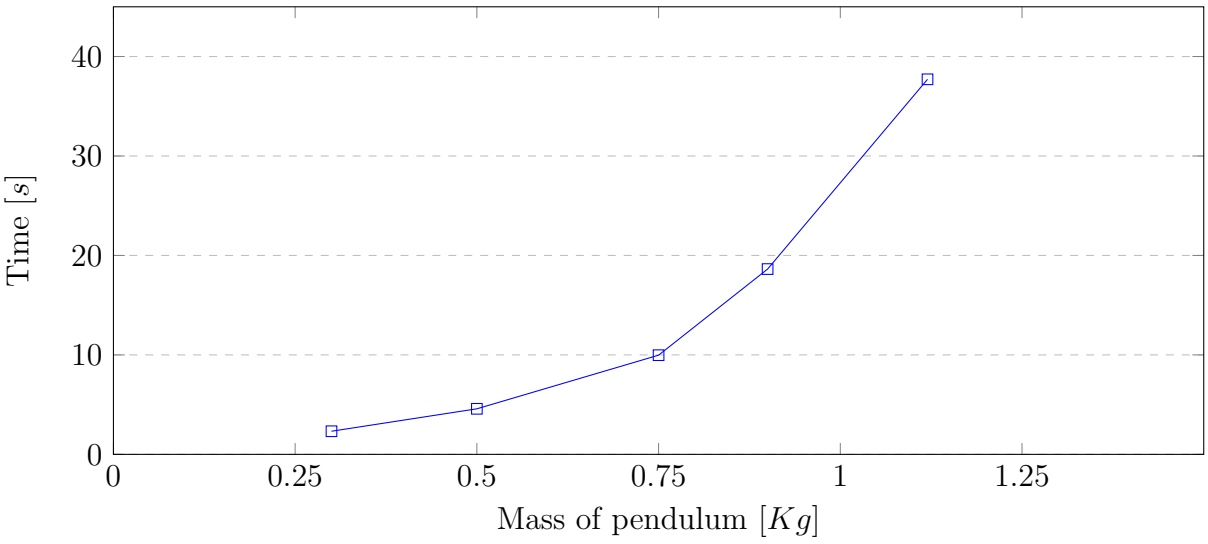

Figure 3.12: Effect of pendulum mass on stroke of cart

The mass of pendulum is chosen to be 0.3 Kg then the cart travels 100 mm away from the set-point in 2.325 s and for pendulum mass of 1.2 Kg, cart takes 37.71 s to travel 100 mm away from the set-point. The time required by the cart to reach stroke end increases by increasing the mass of pendulum.

3.2.4 Length of pendulum

Length of the pendulum is measured from the pivot on the cart to the mass of the pendulum. Changing the length of the pendulum from 1 m to 0.3 m. The effect of the pendulum length can be seen in the Fig.3.13. The impact of the reducing pendulum length has a same impact that of decreasing the pendulum mass. The length of pendulum is chosen to be 0.3 m then the cart travels 100 mm away from the set-point(250 mm) in 4.25 s and for pendulum length of 1 m, cart takes 37.71 s to travel 100 mm away from the set-point(250 mm). The time required by the cart to reach stroke end increases by increasing the length of pendulum. Longer the pendulum, better is the stability of the system.

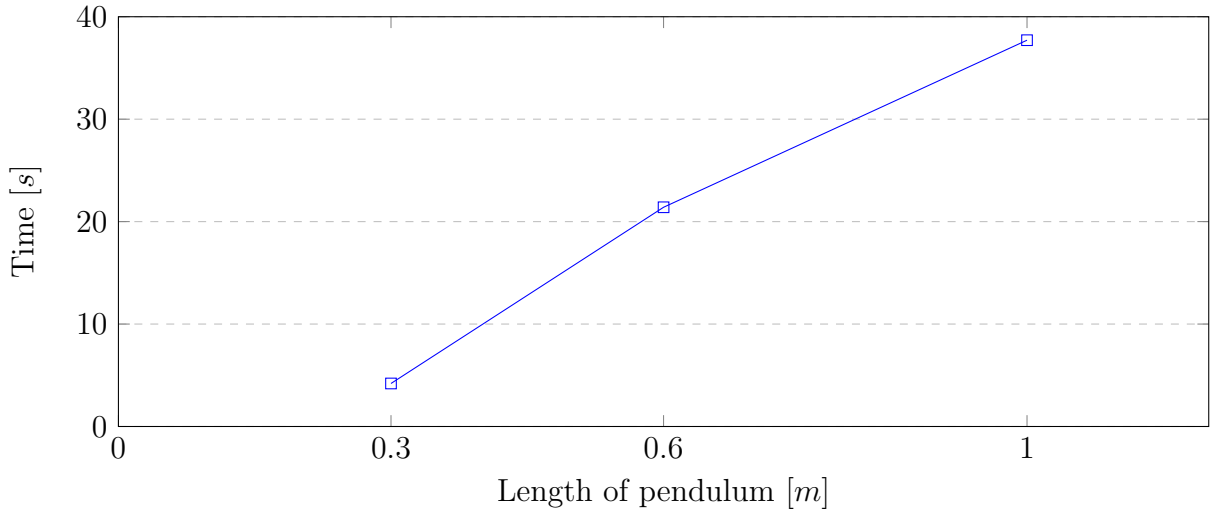

Figure 3.13: Effect of pendulum length on stroke of cart

3.2.5 Mass of cart

The effect of changing the mass of the cart has very small effect on the stability of the system. The change of cart mass from 0.7 kg to 0.3 Kg as shown in the Fig.3.14, cart mass has negligible effect on it's rate of moving towards the end stroke limit.

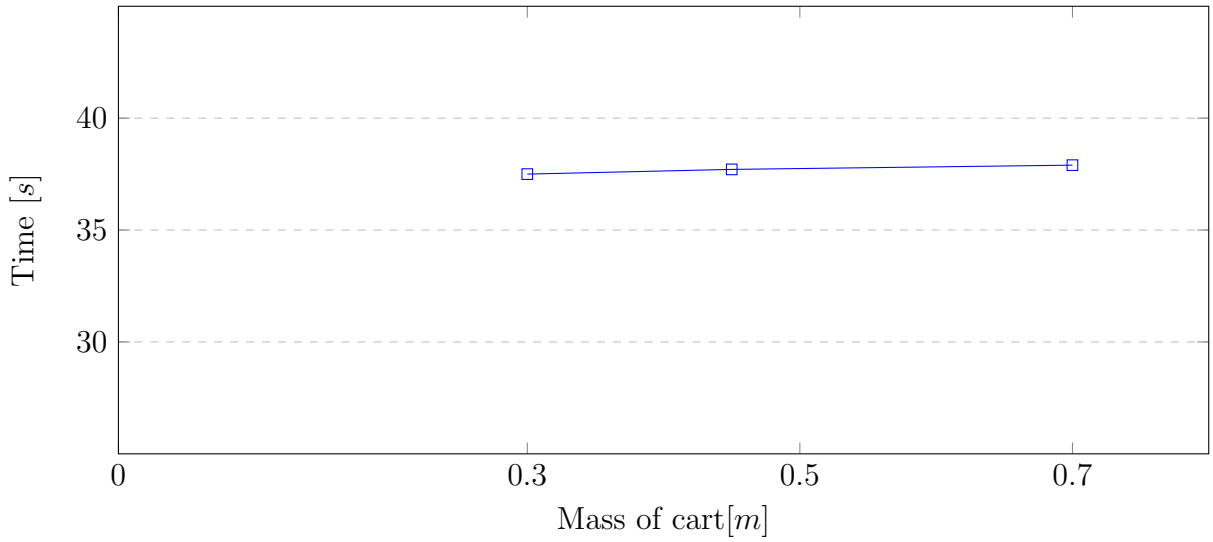

Figure 3.14: Effect of cart mass on stroke of cart

3.2.6 Valve Timings

The valve timing are defined for the opening and closing of the valve, which is the change in the effective cross-sectional area of the port. The opening of the valve is actuated by electromechanical assistance, while the closing of the valve is forced by a mechanical spring. The valve open timing being varied from 4 ms to 40 ms and valve close timing varied from 7ms to 70 ms has a similar effect of cart approaching the cylinder end stroke

limit at a faster rate. The Fig.3.15 shows the effect of valve timings on the oscillation amplitude of pendulum angle.

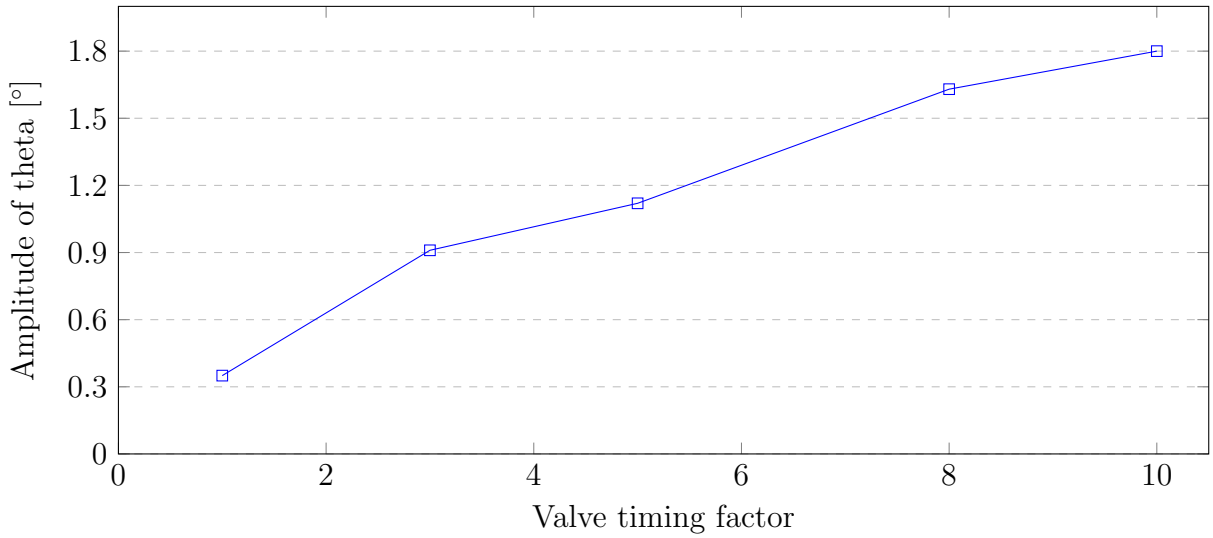

Figure 3.15: Effect of valve timings on pendulum angle

For valve open time of 4 ms (4*$\mathbf{1}$) and close time of 7 ms(7*$\mathbf{1}$), the oscillation amplitude of pendulum angle is 0.35°, while for valve open time of 40 ms (4*$\mathbf{10}$) and close time of 70 ms(7*$\mathbf{10}$), the oscillation amplitude of pendulum angle is 1.8°

3.2.7 Supply Pressure

Changing the supply pressures; PS1(3.45 bar) from 0.8 times to 1.2 times of 3.45 bar and similarly for PS2 (4.2 bar), the amplitude of the pendulum angle oscillation is increased from 0.25° to 0.43°. The supply pressure can be seen as a proportional gain factor.

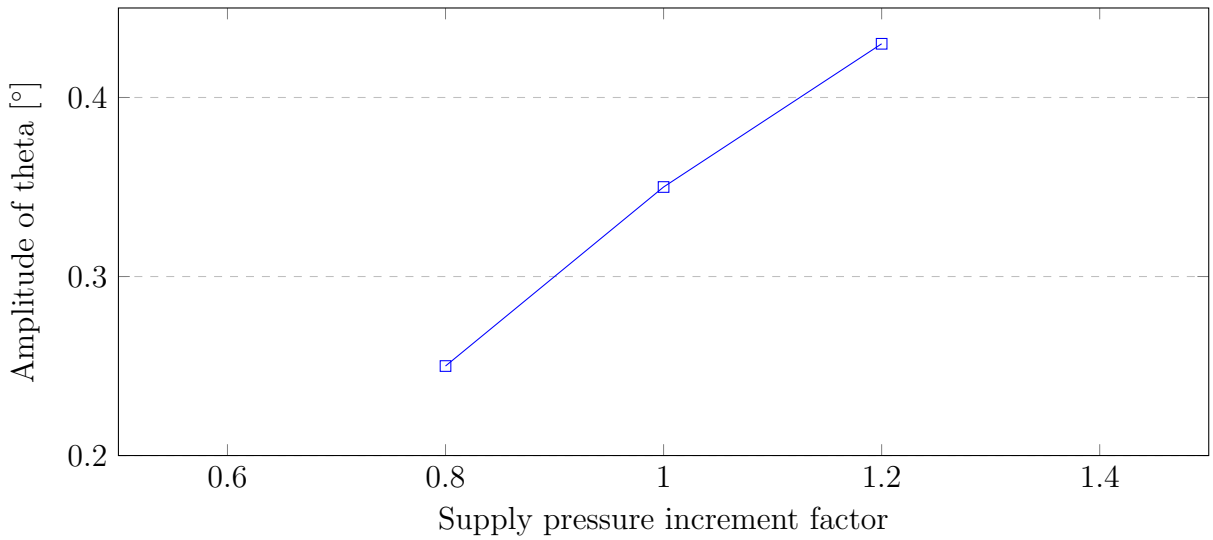

Figure 3.16: Effect of supply pressure on pendulum angle

3.3 Simulations using Matlab/Simulink

The stand-alone simulations in the Matlab/Simulink environment lets us cross verify our results with DSHplus environment to some extent. The parameters of the system are:

Piston Diameter	0.016 m
Rod Diameter	0.006 m
Stroke max	0.250 m
Stroke min	-0.250 m
Mass of Piston	0.7 Kg
PWM signal genertor frequency	500Hz
critical ratio of valves	0.3
Conductance of Valves(C)	0.283 Nl/s/bar
Time constant of valve (τ)	0.005
Supply pressure	4.2 bar
Density of air	1.225 kg/m^3
Mass of cart	0.45 Kg
Mass of pendulum	0.89 Kg
Length of pendulum	1 m

Table 3.13: Geometric parameters

The Initial conditions are :

Parameters	Values
Stroke of cart	0.250 m
Velocity of cart	0 m/sec
Angle of pendulum	1°
Angular velocity of pendulum	0 deg/sec

Table 3.14: Initial conditions of the matlab model

Set-point:

Position of cart	0.25 m
Angle of pendulum	0°

Table 3.15: Set-points of matlab model

3.3.1 Model 01: Theta Control Simulation:

The model used for the simulation is described in the section 2.2.2.6. Main focus is to control the pendulum angle(set-point= 0°). The values of PID parameters are shown in Table 3.9,

Gains	Values
P	0.3
I	1.2
D	0.06

Table 3.16: Theta control PID gains

The Pendulum angle has an oscillating stability about 0° with an amplitude of 0.2°.

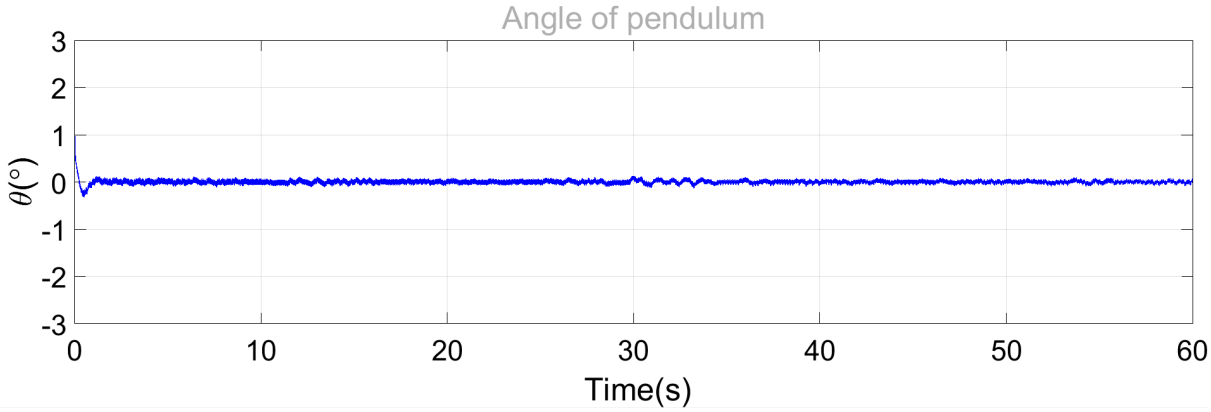

Figure 3.17: Theta plot of Theta control model in Matlab/Simulink

The cart travel towards the stroke end limits, which can be seen in Fig.3.18. One PID controller is able to keep the pendulum stable, while unable to control the cart position. For this very reason, Two PID controller is required for the overall stability of the system.

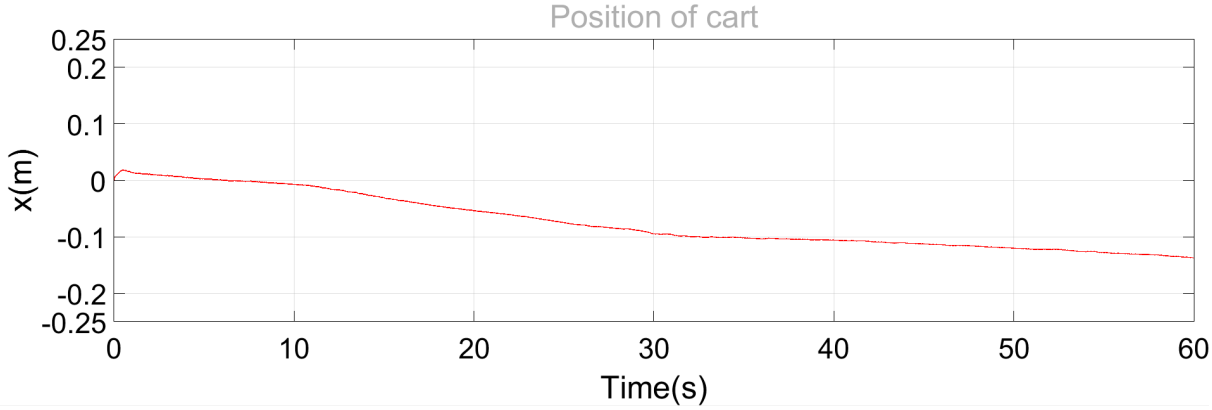

Figure 3.18: Stroke plot of Theta control model in Matlab/Simulink

3.3.2 Model 02: Stroke and Theta Control Simulation

Two parallel feedback loop PID controller is used to individually control the cart position and the pendulum angle.The model used for the simulation is described in the section 2.2.2.7. The weight gain factor multiplied to the output of the PID controller ensuring the PID controller for theta to have a higher bandwidth. The initial condition; Pendulum

angle is set to 5°. The weight gain factor is shown in the Table 3.17,

Weight factor:

Weightage factor	Values
Theta control	0.7
Stroke control	-0.3

Table 3.17: Stroke and Theta control weight factor.

The Table 3.18 and Table 3.19 specifies the PID gain values of both the PID blocks. The PID1 manages to control the angle of pendulum, while PID2 controls the displacement of the cart.

PID1(for theta):

Gains	Values
P	0.3
I	1.2
D	0.06

Table 3.18: Stroke and Theta control PID1 gains

PID2(for stroke):

Gains	Values
P	15
I	12
D	1

Table 3.19: Stroke and Theta control PID2 gains

The Pendulum angle has an oscillating stability about 0° with an amplitude of 0.2° as shown in Fig.3.19. The PID2 controller manages to keep the cart at the set-point (centre of stroke length) as shown in Fig.3.20.

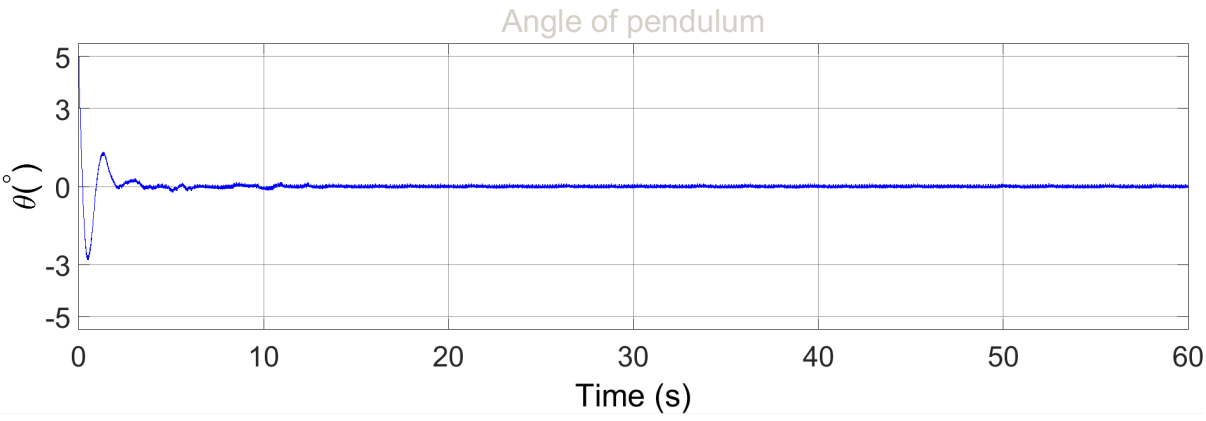

Figure 3.19: Theta plot of Stroke and Theta control model in Matlab/Simulink

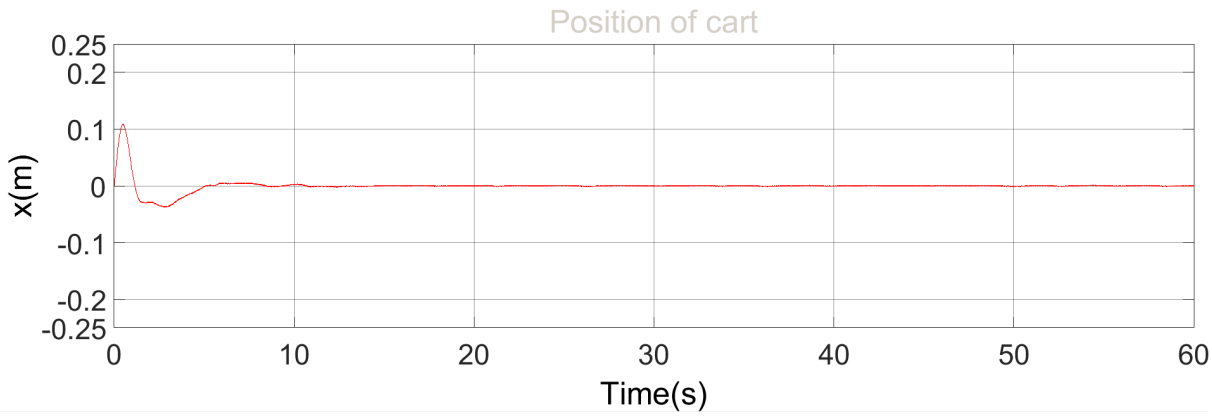

Figure 3.20: Stroke plot of Stroke and Theta control model in Matlab/Simulink

The Two parallel feedback loop PID controller is able to recover the system with initial condition; pendulum angle of 5° and is successful to maintain the cart position to it's set-point.

All the analysis, observations and results in this chapter will be helpful for real time control of the system. Now that we have understood the effect of some important variables on the whole system, which will be useful to tune the parameters in the real time environment.

Chapter 4

Co-Simulation

In co-simulation the different subsystems which form a coupled problem are modelled and simulated in a distributed manner. Hence, the modelling is done on the subsystem level without having the coupled problem in mind. Furthermore, the coupled simulation is carried out by running the subsystems in a black-box manner. During the simulation the subsystems will exchange data. Co-simulation can be considered as the joint simulation of the already well-established tools and semantics; when they are simulated with their suitable solvers[30].

4.1 Co-simulation Model 1: DSHplus and Matlab/ Simulink

In this co-simulation model we will interacting between two environment; Simulink and DSHplus. The pneumatic system and the inverted pendulum is developed in DSHplus while the controller implementation is done in Matlab/Simulink. The layout of the whole system is same as mentioned in the section 2.2. Communication between the environment for Co-Simulation is done via *SignalInput/SignalOutput* components which acts as an interface. A documented guide to setup the co-simulation is provided in the Appendix A. The Pneumatic system and Inverted pendulum is modelled in the DSHplus environment. The DSHplus model can be seen in the Fig.4.1.

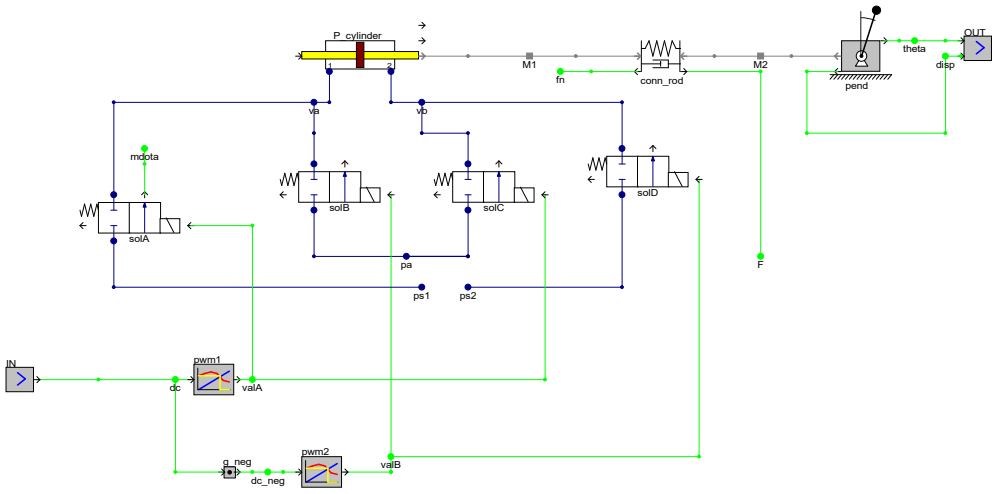

Figure 4.1: Co-simulation model:1a in DSHplus

The implementation of the control strategy in the Matlab/Simulink environment is shown in the Fig.4.2. The DSHplus model acts as a blackbox. The simulink blocks are connected around the blackbox generated by DSHplus. The output of the blackbox are the cart position and the pendulum angle. These signals are compared to their respective set-point. The sum of the outputs from the PID controller is an input to the blackbox. The numerical computation of the model is partially done in their respective environment.

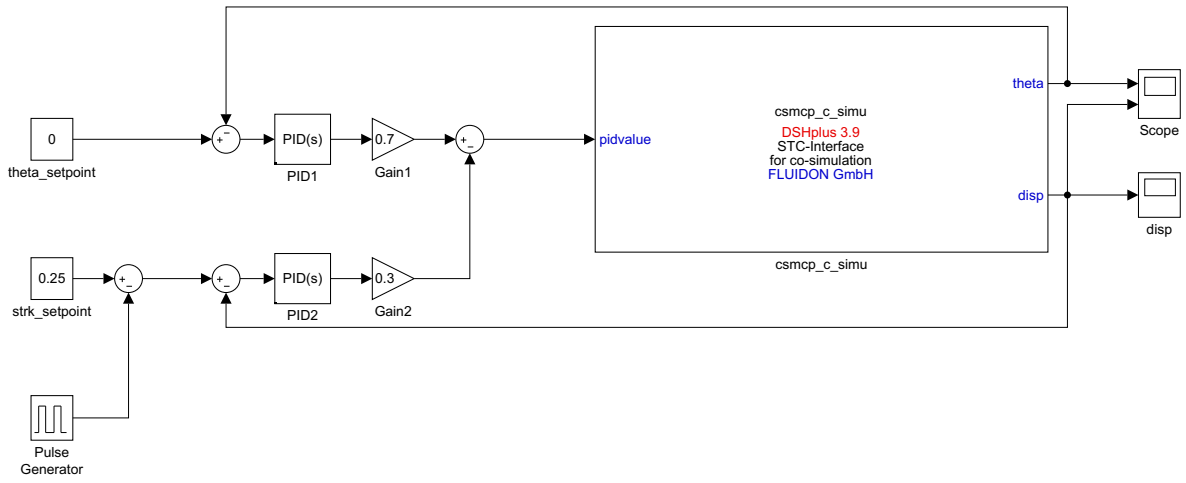

Figure 4.2: Co-simulation model with variable stroke setpoint in Matlab

The PID gains, initial conditions and other system parameters remain unchanged from the chapter 3. The set-point of the pendulum angle is 0° and the set-point of the cart position is changed to -75 mm after 50 seconds from the start of simulation. The simulation results are quite similar to the one published in the chapter 3. The stroke plot and the Theta plot is shown in the Figs.4.3 and 4.4. The results show an oscillating stability, where the oscillation amplitude is 15 mm about the set-point for the cart position and 0.5° for the pendulum angle(set-point = 0°).

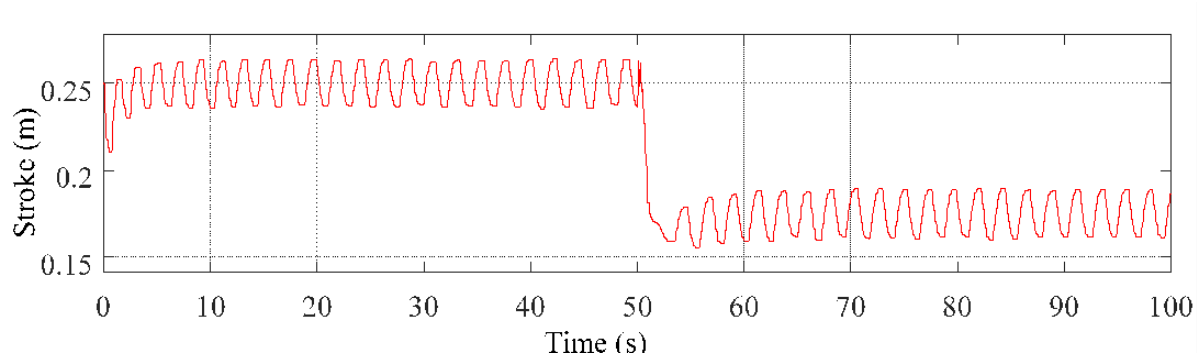

Figure 4.3: stroke plot of Co-simulation model:1

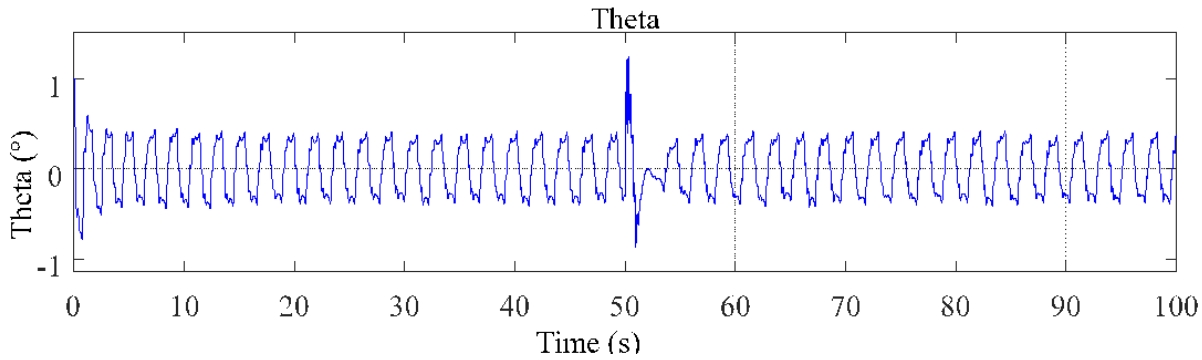

Figure 4.4: Theta plot of Co-simulation model:1

4.2 Co-simulation Model 2: DSHplus and Altair Activate

The DSHplus model is the same from the subsection 4.1, was co-simulated with the Altair-Activate environment. The PID controller was modelled in the Altair-Activate environment. The PID gains, initial conditions and other system parameters remain unchanged from the chapter 3. The Fig.4.1 shows the DSHplus model, The PID controller is build in the Acivate-Altair,the set-point of the pendulum angle is 0° and the set-point of the cart is fixed to 0.250 m. The Fig.4.5 shows the black box produced by the DSHplus and around which the controller is build using Altair-Activate blocks.

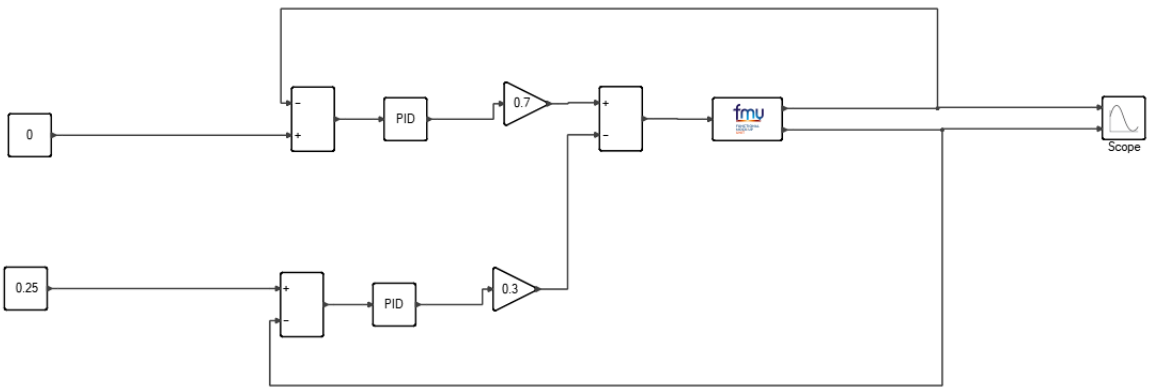

Figure 4.5: Co-simulation model in Atair Activate

The cart stroke plot is shown in Fig.4.6 and the pendulum theta plot is shown in the Fig.4.7, the simulation shows an oscillating stability of inverted pendulum with an amplitude of 0.5° for the pendulum angle(set-point = 0°) and an oscillation of 15 mm about the set-point of 0.25 m for the cart position.

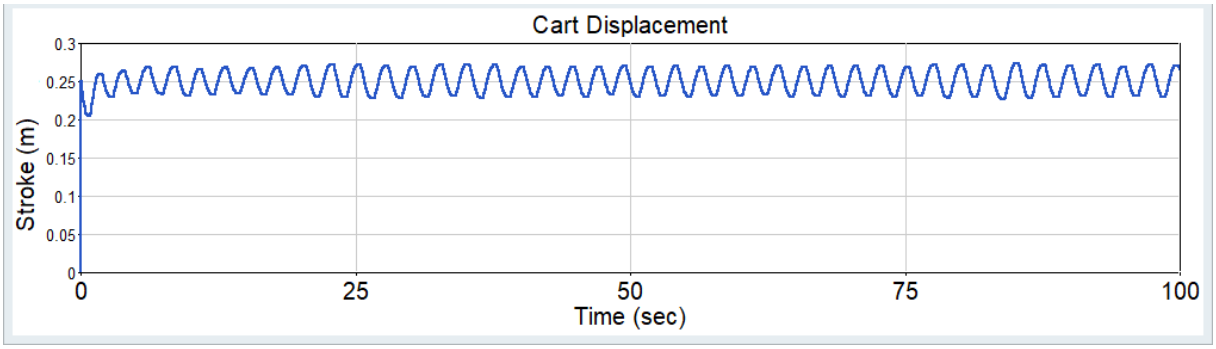

Figure 4.6: Stroke plot of Co-simulation model:2

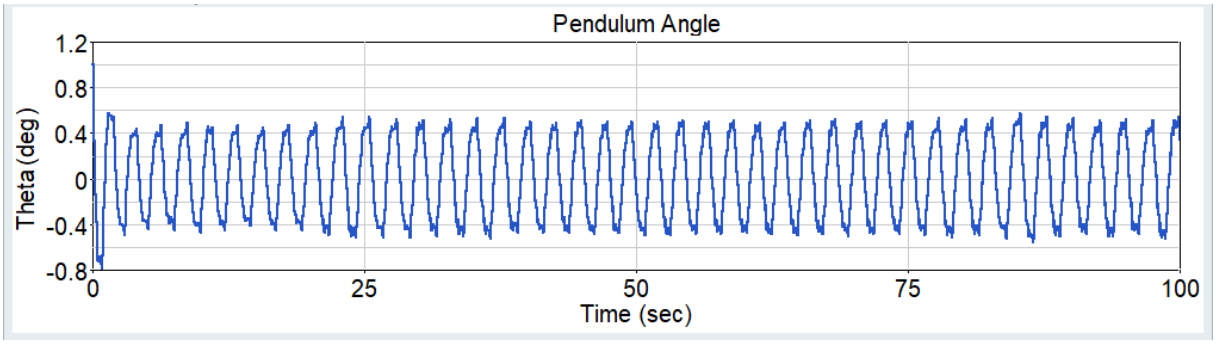

Figure 4.7: Theta plot of Co-simulation model:2

The previous co-simulation in the section 4.1 have produced identical results and system behaviour, which ensures the correct coupling of DSHplus with different environments.

4.3 Co-simulation Model 3: DSHplus and Simulink simscape

This model produces a 3D animation of the inverted pendulum dynamics. The controller and Pneumatic system were modelled in the DSHplus environment shown in the Fig.4.8. The PID gains, initial conditions and other system parameters remain unchanged from the chapter 3. To setup the co-simulation refer Appendix.A

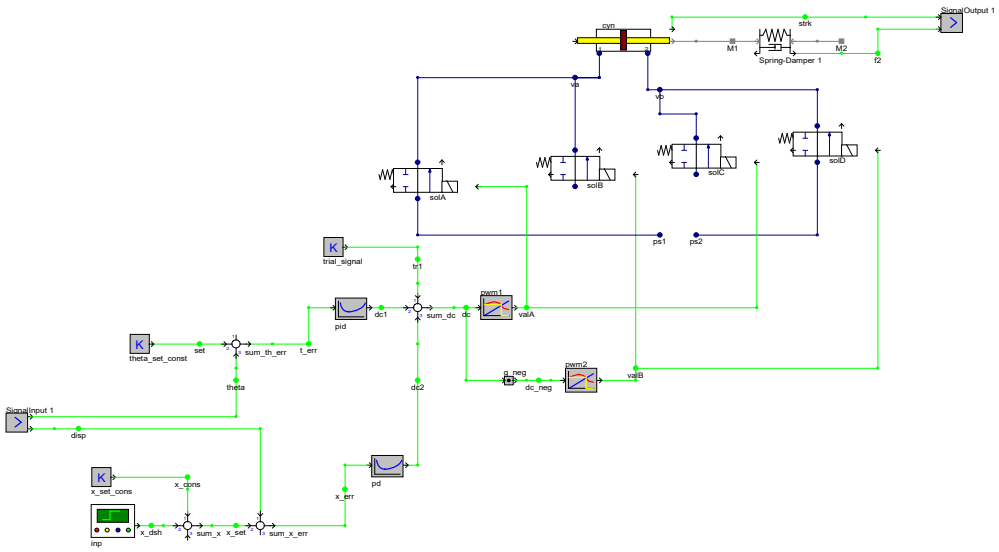

Figure 4.8: Co-simulation model:3 in DSHplus

The inverted pendulum is modelled with the help of Simscape package, the subsystem *connectingrod* couples the pneumatic system with the inverted pendulum model as shown in the Fig.4.9,

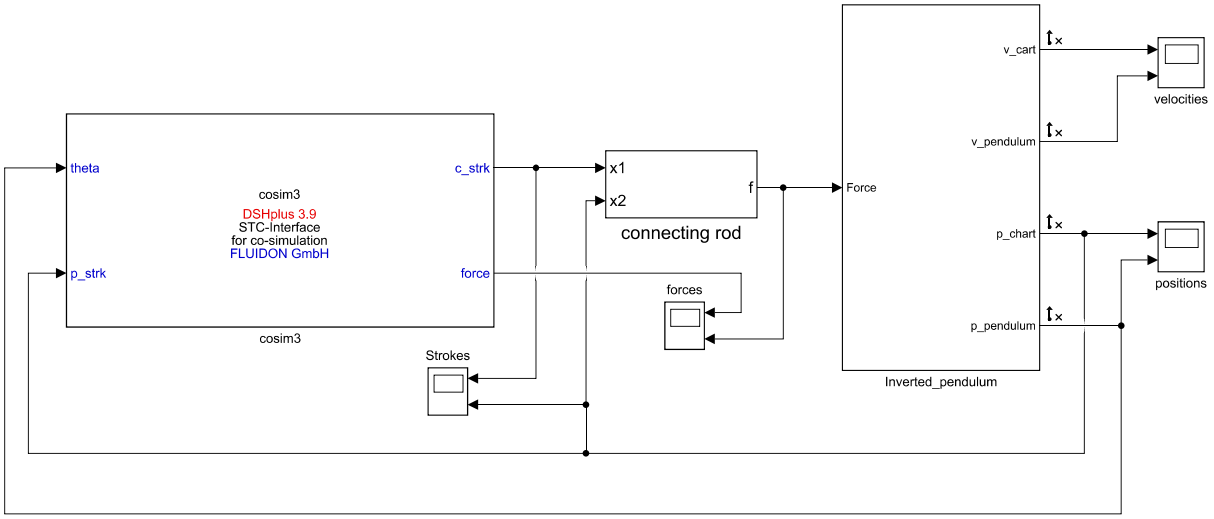

Figure 4.9: Co-simulation model:3 in Matlab

The stroke plot and the Theta plot is shown in the Figs.4.10 and 4.11. The results show an oscillating stability, where the oscillation amplitude is 10mm about the set-point of 0 mm for the cart position and 0.4° about the set-point of 0°) for the pendulum angle.

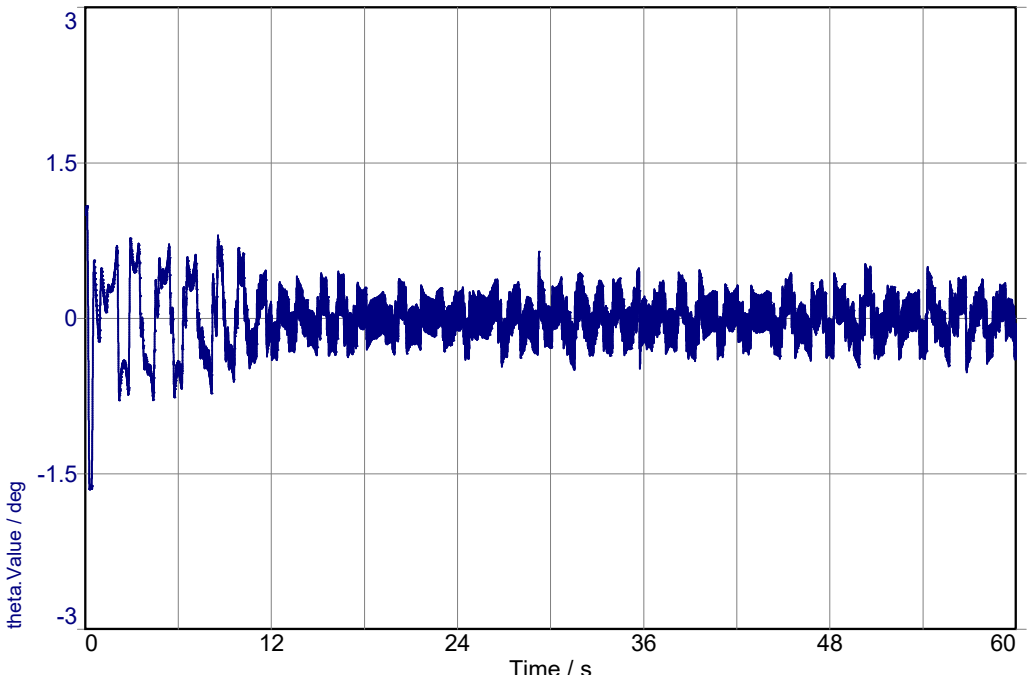

Figure 4.10: Theta plot of Co-simulation model:1

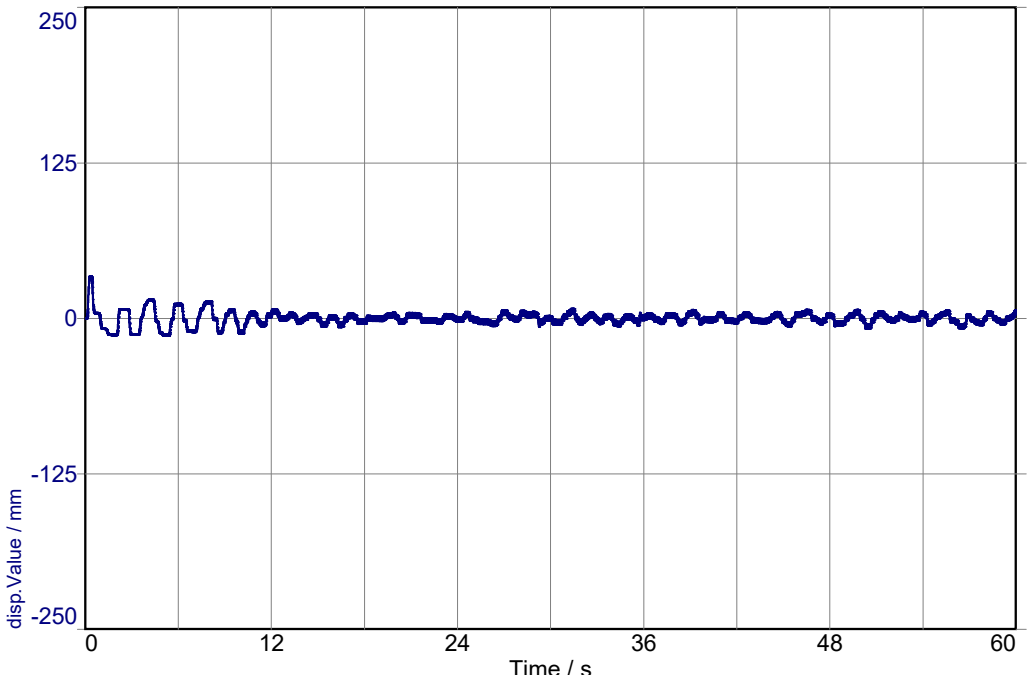

Figure 4.11: Stroke plot of Co-simulation model:3

The development of co-simulation models will be helpful in further development and improvement in the control strategies to be developed in the Matlab/Simulink environment, while the pneumatic system modelled in DSHplus environment.

Chapter 5

Hardware-In-the-Loop testing

5.1 Test bench description

The proposed controller design was also verified on experimental setup of pneumatically actuated inverted pendulum with the help of switching 2/2 digital valves. The components of the test bench were setup with the help of the study in the chapter 3. Having understood the crucial parameters of the system and their effect on the system behaviour, we have finalised the parameters of the test bench. The test bench can be seen in the Fig.5.1. The technical specification of the components in the system are mentioned in Appendix B.

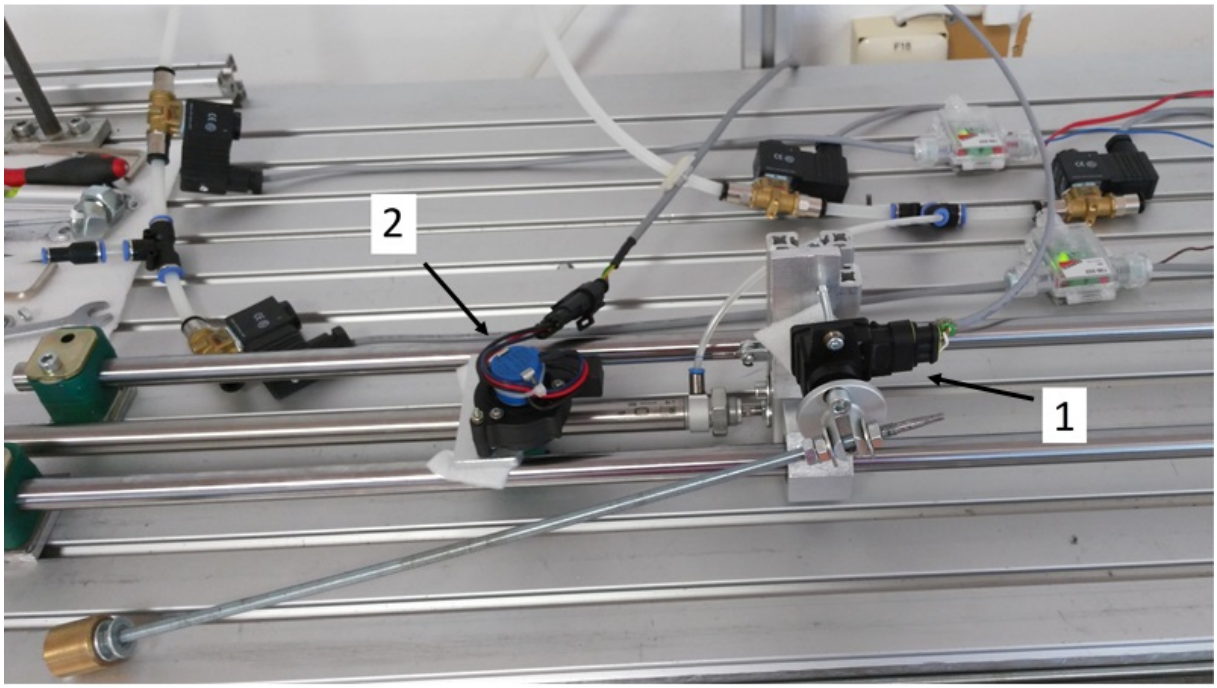

Figure 5.1: Test bench

The cart of Inverted pendulum is built with the help of T-slot extrusion(1), linear guide rail(2), Linear Slide Bearings(3) shown in the Fig.5.2 and the pendulum is a 1/4" lead screw coupled to the Angle sensor((1) in Fig.5.1).

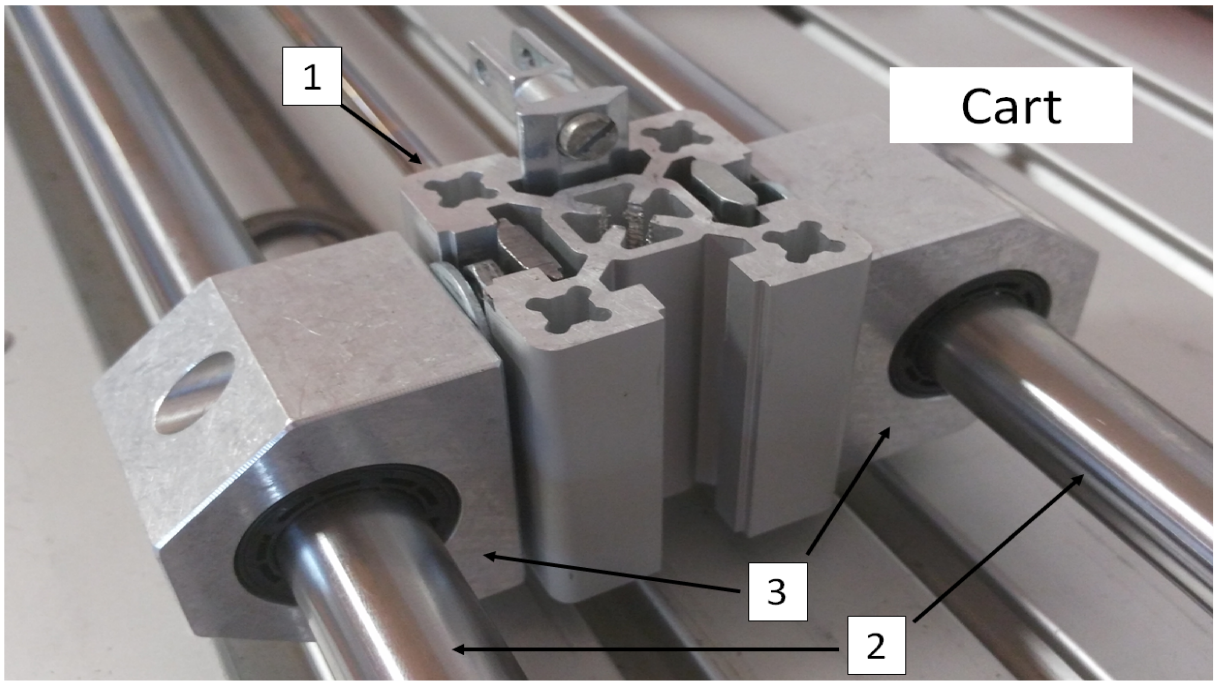

Figure 5.2: Cart assembly

The pneumatic cylinder(Appendix B.1) is fastened to the T-slot extrusion. With reference to Fig.5.3, the pneumatic cylinder(1) is connected to a pressure source of 4 bar. A pair of 2/2 switching valves (Appendix B.2); one for the exhaust and one for filling the chamber, are connected to each of the cylinder port. For further reference, Valve C and Valve D are connected to the port on the piston rod side, while valve A and valve B on the other side. The Valve A(2) and valve C(3) are connected to the source, while valve B(4) and valve D(5) is connected to the exhaust, more likely triggering of valve A and valve D will cause the outward stroke of the cylinder piston rod, while the triggering of valve C and B will cause the inward stroke of the cylinder piston rod. The PWM signal to each of the valves are given by the electronic control devices(Appendix B.3) connected to it. The electronic control device (ECD) are labelled as ECD-A(6), ECD-B(7), ECD-C(8), ECD-D(9) for further references, labelled according to their respective connections to the valves. The operating frequency of this device is 495 Hz. The input power supply given to it on the test bench was 24 V DC. The analog input ranges from 0 to 10 V. The NI myrio 1900 board (Appendix B.5) is used as a controller in this Hardware-in-loop testing. The NI myrio board has an analog output pins labelled as C/AO0 and C/AO1, generates an analog output through MXP connectors(Appendix B.5.2); ranging from 0 V to 10V . The input of the The ECD-A and ECD-D are connected to pin C/AO0 while ECD-C and ECD-B is connected to pin C/AO1. Each of the ECD are connected to a power supply of 24 V DC. The Honeywell Angle sensor(Appendix B.4.1) is mounted on the T-slot extrusion and coupled to the pendulum, reading the angular position of the pendulum. The Angle sensor is connected to the pin B/AI0(pin 3), MSP analog input

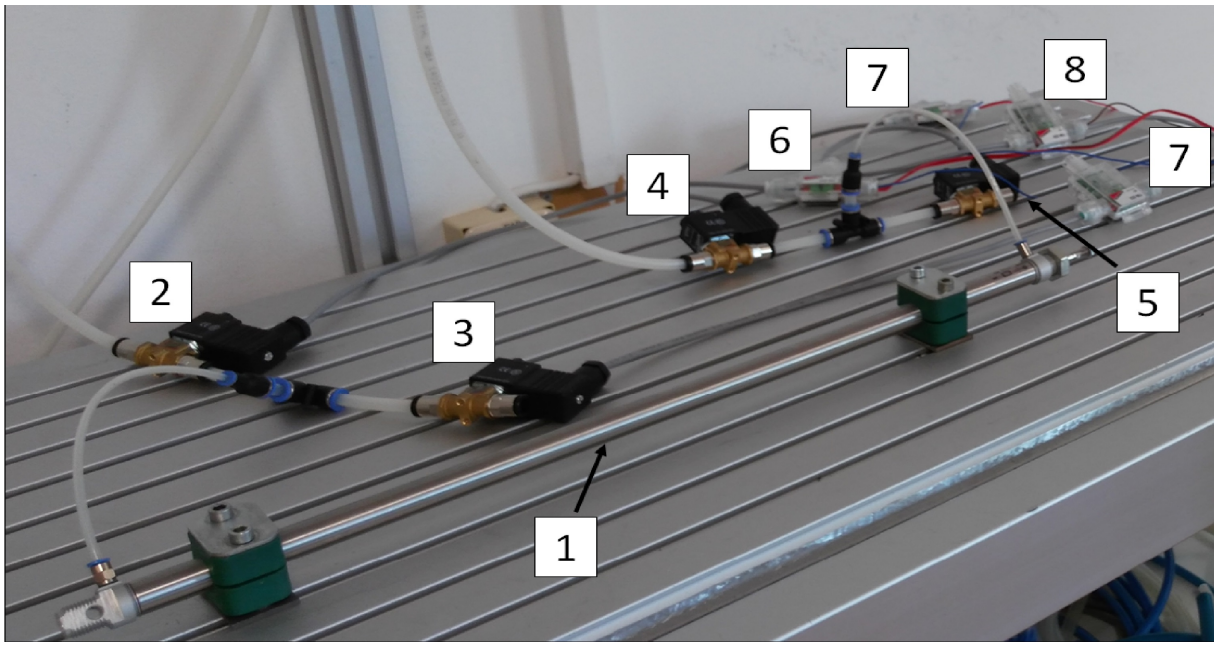

Figure 5.3: Pneumatic system assembly

connectors of the myrio board. It is connected across 24 V DC and neutral. While the draw wire sensor ((2) in Fig.5.1, Appendix B.4.2)is fastened to the T-slot extrusion(cart). It is connected to the analog input pin B/AI1(pin 7), a MSP analog input connectors on the myrio board. It's V_{cc} is connected to 5V supply generated by the myrio board. The ground of the myrio board and the DC power supply unit are connected to create a common ground.

5.2 Implementation

After the hardware assembly of the test-bench, let us configure the controller. The controller NI-myrio 1900 software deployment is done with the help of LabVIEW. First we will validate the sensor configuration. To test the draw wire sensor (linear displacement measurement) which is connected to B/AI2(pin 7), we manually moved the cart to a known position and measured the voltage generated by the sensor. The front panel and the block diagram is shown in the Figs.5.4, 5.5 and 5.6.

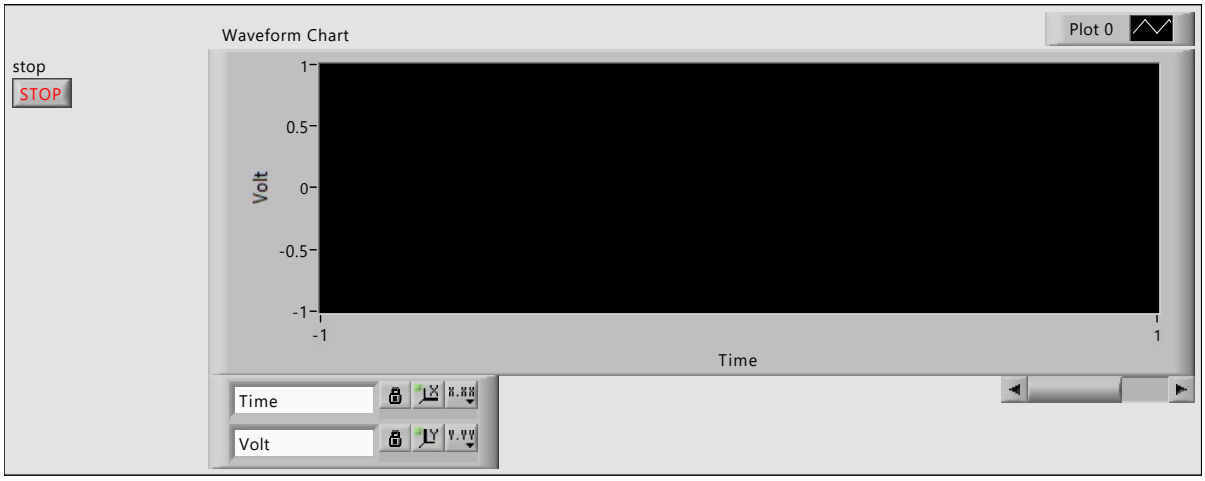

Figure 5.4: Labview model to test the Linear position sensor's analog signal(Front Panel)

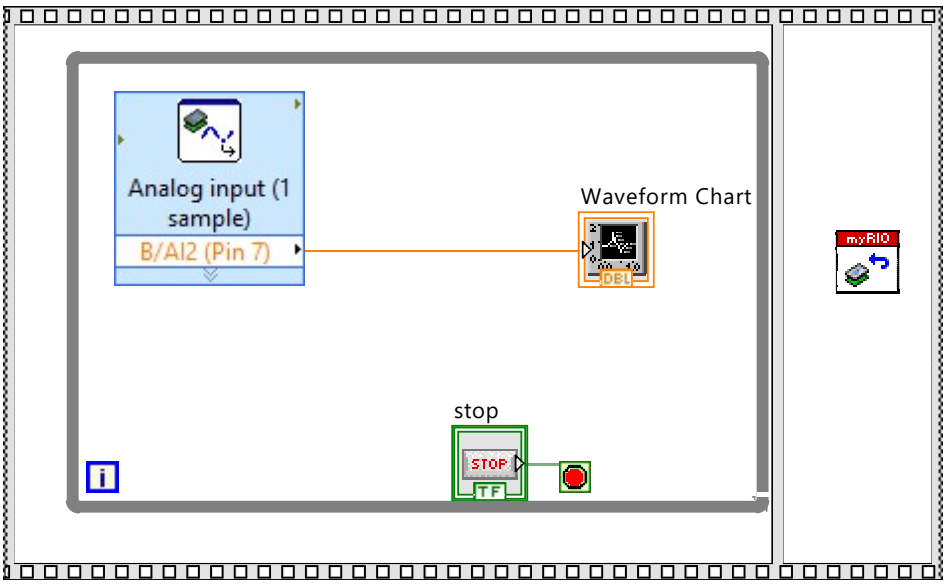

Figure 5.5: Labview model to test the Linear position sensor's analog signal(Block diagram)

The table 5.1 shows the position of the cart and the output voltages of the draw wire sensor.

Sr. no.	Displacement(mm)	Voltage(V)
1	0mm	0.0378
2	100mm	0.359
3	200mm	0.719
4	300mm	0.9405
5	400mm	1.1135
6	500mm	1.553
7	600mm	1.927

Table 5.1: Test data of linear position sensor

To convert the sensor output(V) into position(mm) of the cart, we use the Eq.5.1,

$$y = 500 * \frac{x}{1.927 - 0.0378} \tag{5.1}$$

where,
y = cart displacement in mm
x = sensor output voltage in volts
To measure the angle of the pendulum, angle position sensor is used. The labview front panel and block diagram are shown in Fig.5.6,

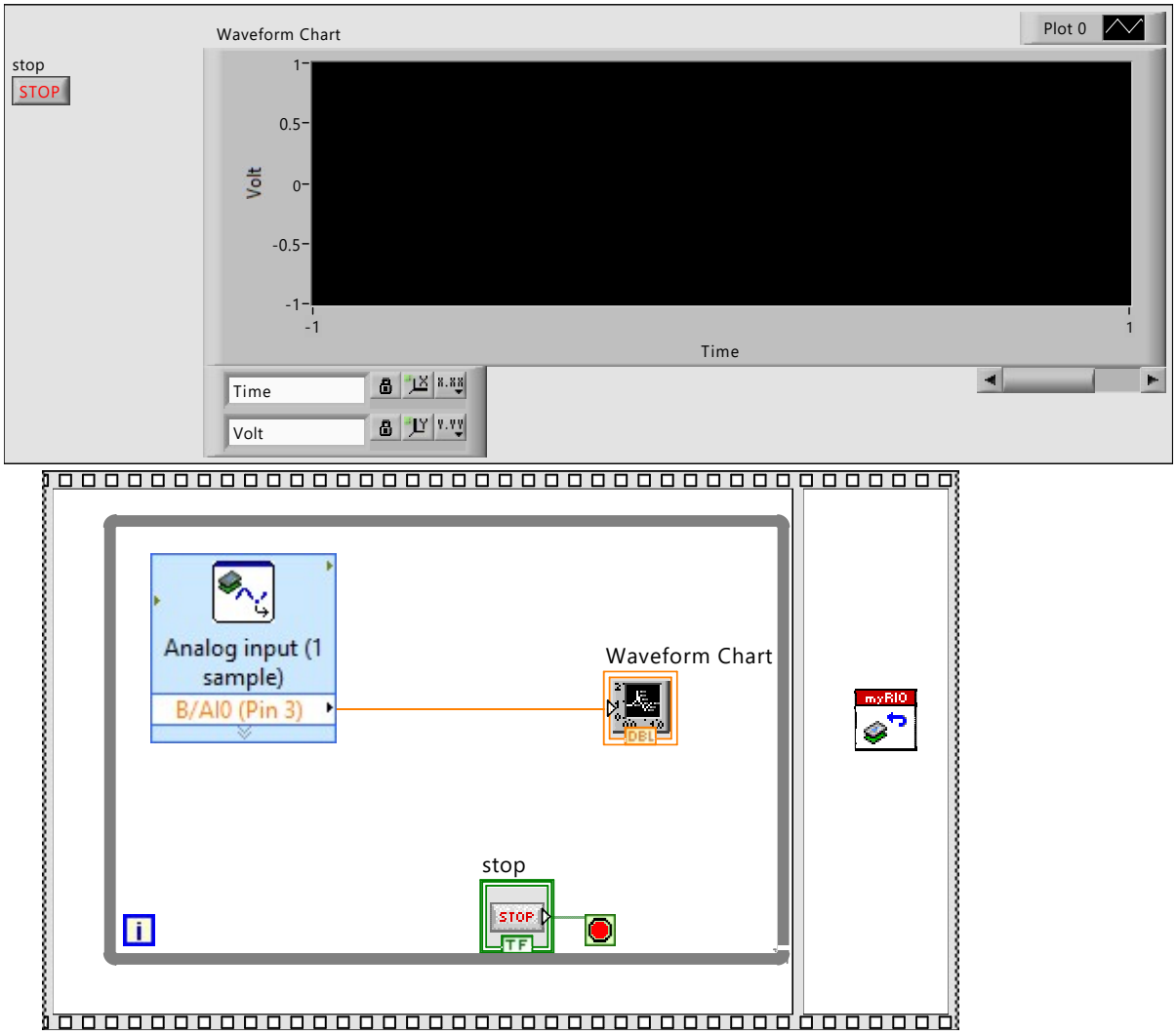

Figure 5.6: Labview model to test the Angle position sensor's analog signal

The results of the test, the output voltage of angle position sensor,

Sr. no.	Displacement(mm)	Voltage(V)
1	-45°	4.75
2	0°	2.85
3	45°	0.23

Table 5.2: Test data of Angle position sensor

To convert the sensor output(V) into angle position(deg) of the pendulum, we use the Eq.5.2,

$$y = x * \frac{4.75 - 2.85}{45} \tag{5.2}$$

where,

y = pendulum angle in degrees

x = sensor output voltage in volts

The cylinder actuation is controlled with two Analog output pins of the controller. The pin C/AO0(AO0) actuates two valves(Valve A and Valve D) responsible for the outward stroke of the cylinder, while C/AO1(AO1) actuates other two valves(Valve C and Valve B) responsible for the inward stroke of the cylinder. These pins are capable of generating analog output from 0 to 10V. The Fig.5.7 shows the front panel and block diagram in labview for the test.

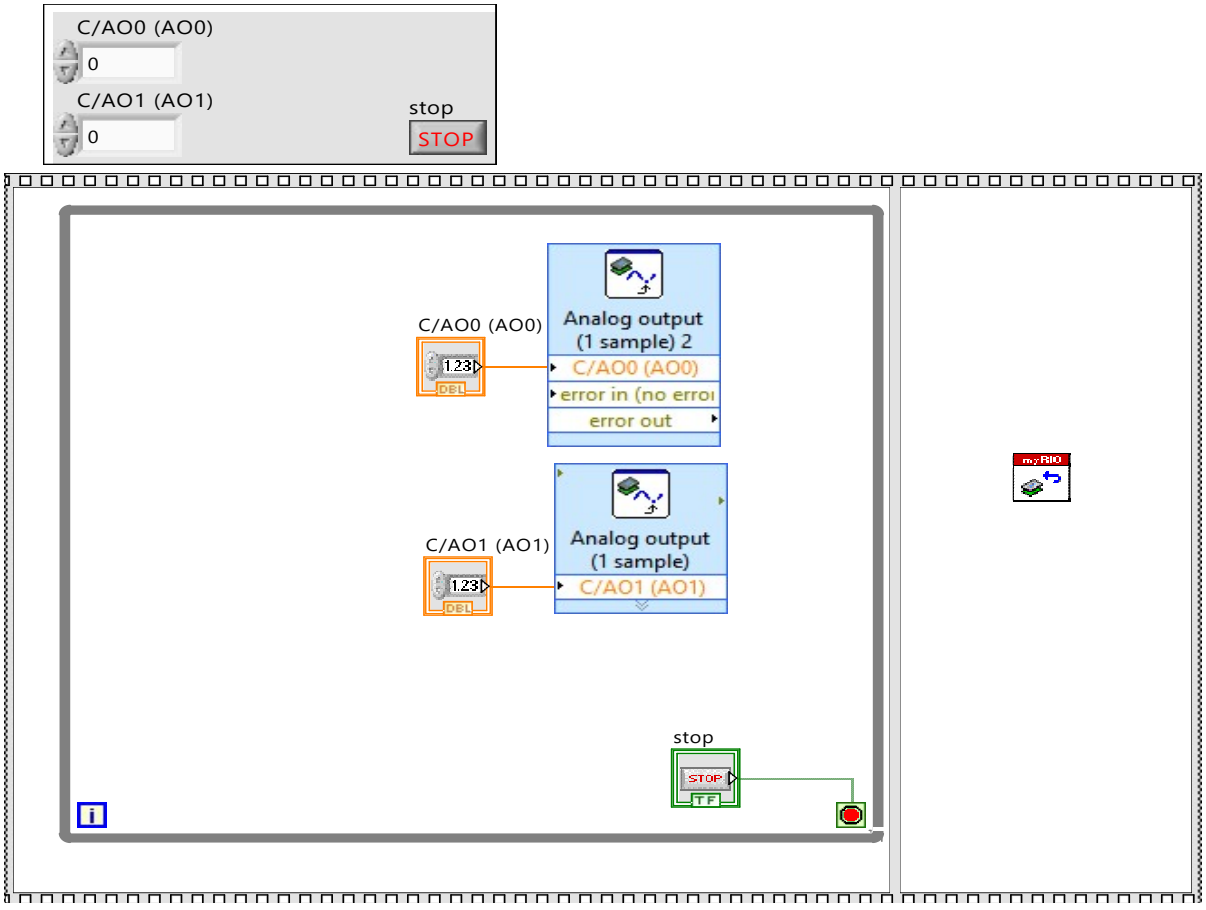

Figure 5.7: Labview model to test the actuation of pneumatic cylinder and valves

During the test, it was observed that the cylinder piston rod doesn't start moving until the analog output is greater or equal to 5V.

5.2.1 Model 01: Stroke Control

Aim of the model is to control the cart position. The set-point is $250mm$(center of the stroke length). The block diagram and the front panel of the model is shown in the Figs.5.8 and 5.8. The Position of the cart is read in volts from the pin 7(B/AI2) is subtracted by $0.23V$(position of the cart when the piston is fully retracted), further converted to mm with the help of a factor developed in the Eq.5.1.

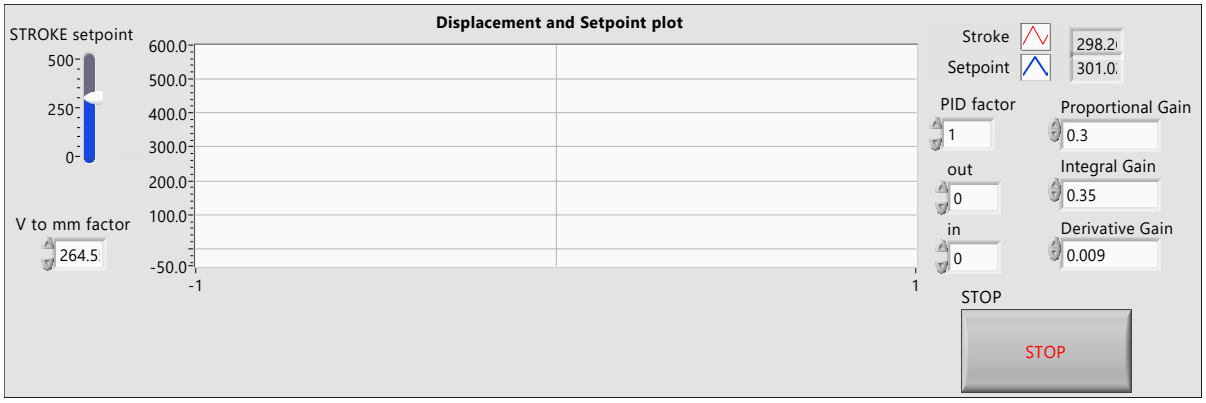

Figure 5.8: Labview model to implement Stroke control(Front panel)

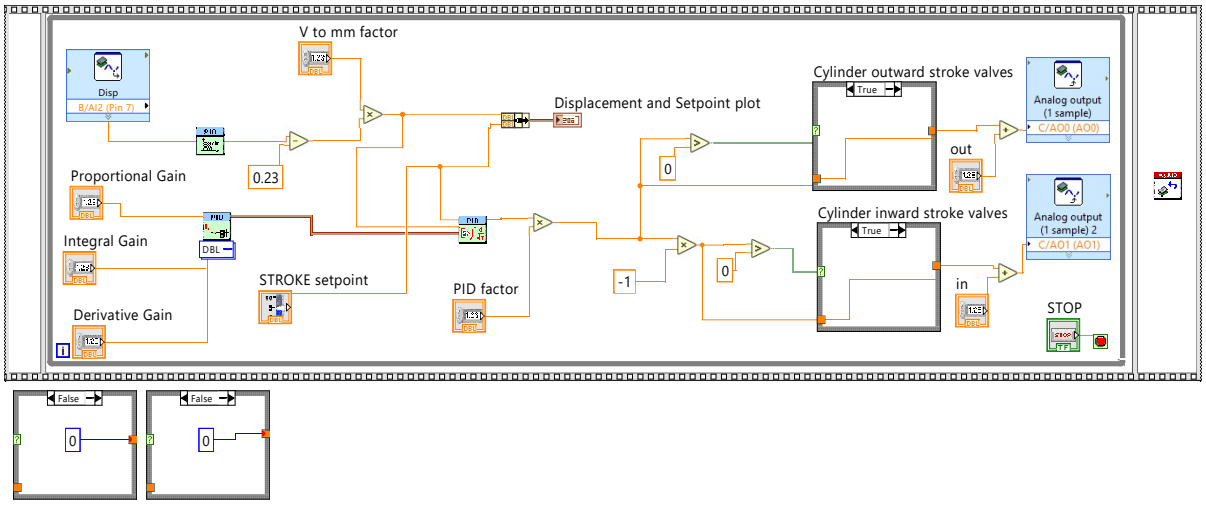

Figure 5.9: Labview model to implement Stroke control(Block diagram)

The error generated after the comparison with the set-point is fed to the PID controller. The PID gains used for this model is shown in the Table 5.3.

Gains	Values
P	0.3
I	0.35
D	0.009

Table 5.3: Stroke control PID gains

There are two case structures used to implement the correct logic. The PID controller outputs will be positive or a negative valve. The output of the PID controller is split into two branches, one of which is connected to the case structure *Cylinder outward stroke valves*, while other branch is multiplied by -1 and is connected to the case structure *Cylinder inward stroke valves* . Both the case structures are true when their respective input is greater than zero, and then the output of the case structure is equal to its input. If the case struture turns out to be false (input is less than zero) then their ouputs are zero. The case structure *Cylinder outward stroke valves* is connected to the analog output pin (C/AO0) and *Cylinder inward stroke valves* is connected to the analog output pin (C/AO1).

5.2.2 Model 02: Theta Control

Aim of the model is to control the pendulum angle. The set-point is zero. The Figs.5.10 and 5.11 shows the front panel and the block diagram of the controller in labview,

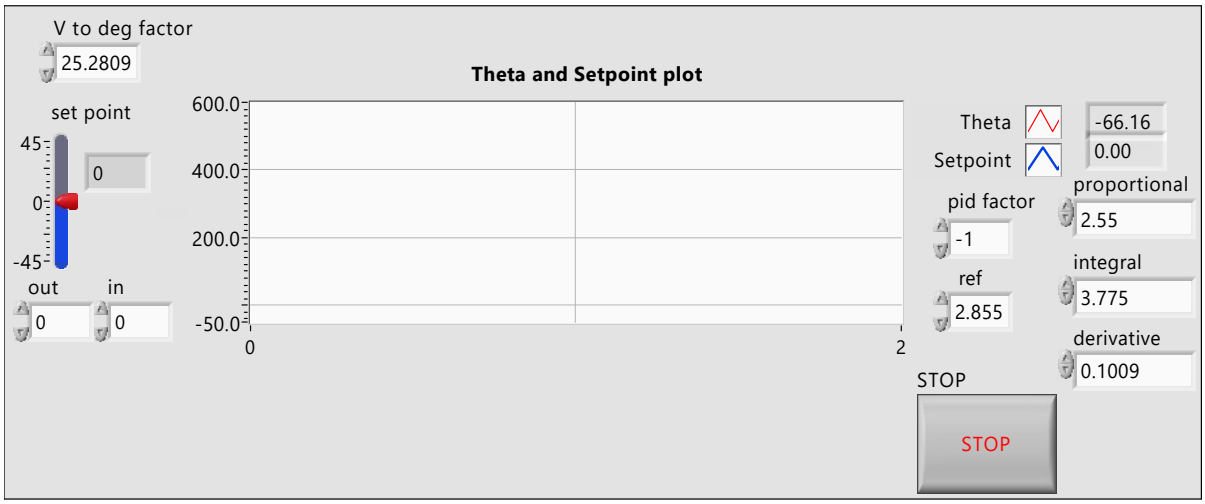

Figure 5.10: Labview model to implement Theta control(Front panel)

The Position of the pendulum is read in volts from the pin 3(B/AI0) is subtracted by 2.855 V(output voltage at 0°) and then converted to degree with a factor calculated from Eq.5.2, by this we make sure that 0° of the pendulum axis is aligned with the positive y axis. The calculated degree is compared to the set-point which is 0°. The error generated from the comparison is fed to the PID controller. The logical blocks from the

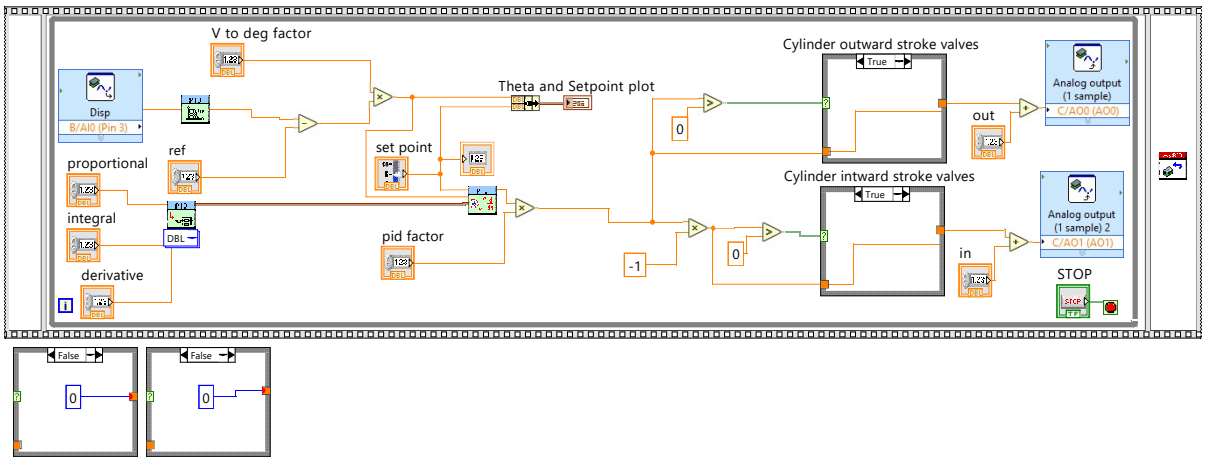

Figure 5.11: Labview model to implement Theta control(Block diagram)

PID controller to the analog pins are similar to the previous model. The values of PID parameters are shown in table 5.4,

Gains	Values
P	2.550
I	3.775
D	0.100

Table 5.4: Theta control PID gains for Real time simulation

The Theta pid factor is -1, used for tuning the system as well as for the ease to set the pid gains as a positive term.The PID is able to control the pendulum angle, while the cart tends to move away from the center of the stroke length.

5.2.3 Model 03: Stroke and Theta Control

Aim of the model is to stabilize the angle position of the pendulum, while controlling the position of the cart. The Figs.5.12 and 5.13 shows the front panel and the block diagram of the controller in labVIEW. This model is the combination of model 01 and model 02, where Two PID controllers are used in parallel loops.The output of the PID controller are multiplied by a gain shown in the Table.5.5.

Weightage factor	Values
Theta control	-0.56
Stroke control	0.4

Table 5.5: Stroke and Theta control weightage factor

The Table.5.6 and 5.7 specifies the PID gain values of both the PID blocks. The PID1 manages to control the pendulum angle, while PID2 controls the cart position.

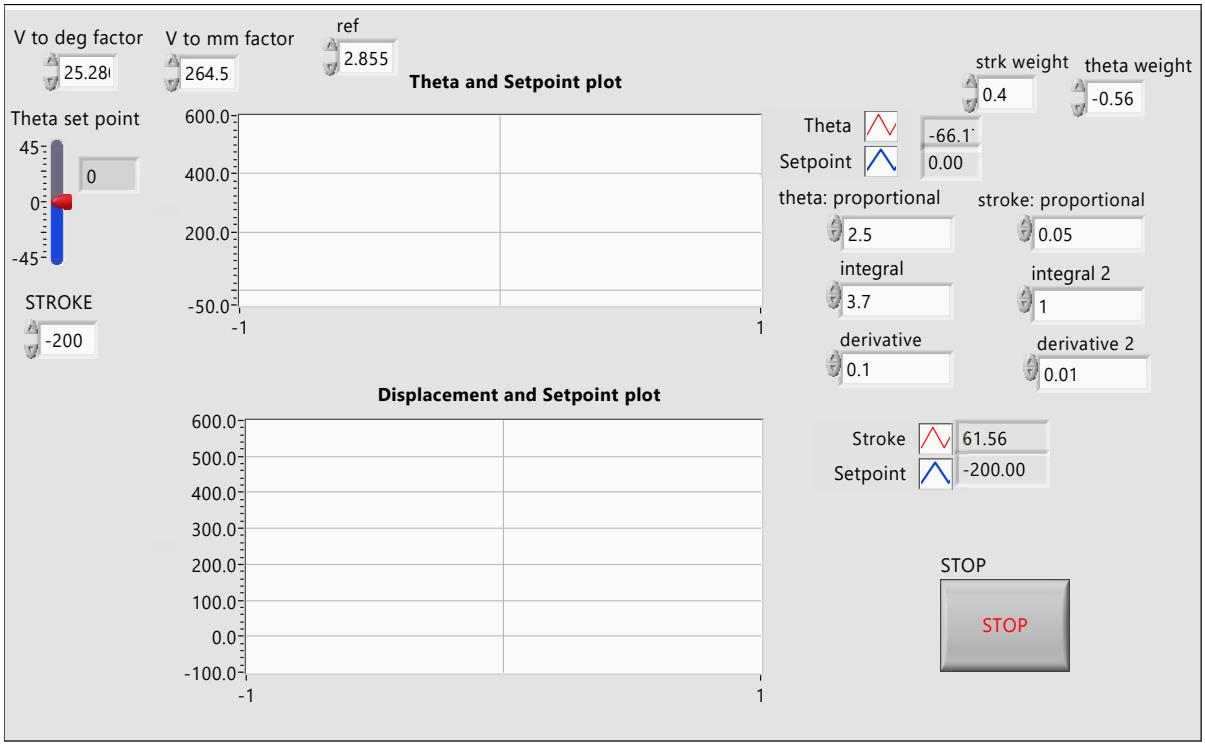

Figure 5.12: Labview model to implement Stroke and Theta control(Front panel)

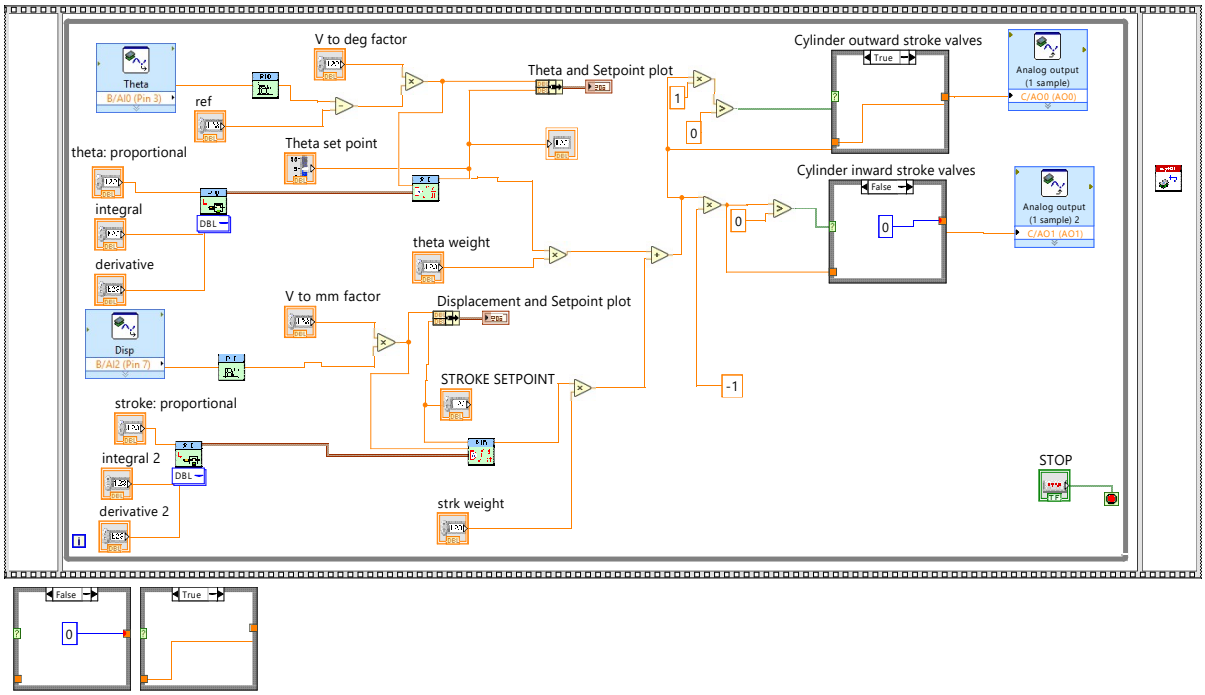

Figure 5.13: Labview model to implement Stroke and Theta control(block diagram)

PID1(for theta):

Gains	Values
P	2.5
I	3.7
D	0.1

Table 5.6: Stroke and Theta control PID1 gains

PID2(for stroke):

Gains	Values
P	0.05
I	1
D	0.01

Table 5.7: Stroke and Theta control PID2 gains

The PID controllers are able to stabilize the angle position of the pendulum and the position of the cart with respect to their reference set-point. The inverted pendulum looses its stability while changing the reference set-point of the cart. For the time being, the Data logging couldn't be carried out. With HIL simulation data, the real time system can be further analysed and will be helpful to understand the non-linearities in the system.

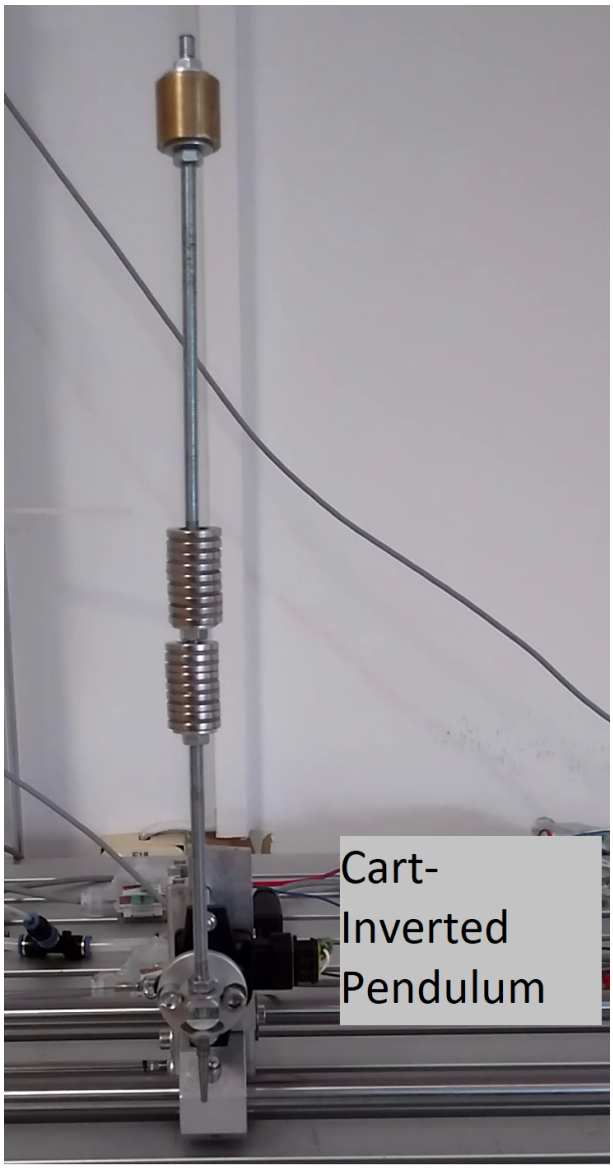

Figure 5.14: Stabilized inverted pendulum in real time control

Chapter 6

Conclusion

6.1 Conclusion

The thesis presents the stabilization of inverted pendulum with a low cost pneumatic actuator and interfacing elements. The simulation and the real time experiment showcased the potential of the pneumatic 2/2 on-off solenoid valves and the pneumatic actuator. The modelling of the system in different software environment helps us in understanding the pros and cons of the environment. The modelling and validation of the system in Simulink environment was tedious, whereas DSHplus provides an easy implementation of the pneumatic system. The modelling of Inverted pendulum with the Simscape package enables the 3D simulation. The step by step modelling the system was advantageous in defining the PID gains and the weightage factor of the Two-loop PID controller. The two loop PID controller was enough to stabilize the system in simulation as well as in the real time. Though in real time control the inverted pendulum looses its stability by changing the reference set point of the cart.These design methods have been successful in meeting the stabilization goal.

The Implementation with 1 PID(pendulum angle in the feed-loop) shows that the pendulum oscillates with an amplitude of 0.35° about it's set-point (0°) and the controller is in attempt to keep the pendulum stable despite of high oscillation amplitude. It is seen that the stroke of the cart is approaching cylinder stroke end-limits. One PID can only control one parameter which is pendulum angle and not the cart stroke.
The Implementation Two parallel closed-loop PID controller(pendulum angle and cart position in the feed-loop) produces an oscillating stability of the inverted pendulum. Position of the cart oscillates between ±10mm about it's set-point ($250mm$) and the pendulum angle(Theta), oscillates between ±0.5° about it's set-point(0°). To check the robustness of the system, the set-point was varied in a square wave fashion, with the amplitude of 75 mm. The cart smoothly follows the change in cart position set-point. The cart follows to the new set point which is 325 mm and the rise time is 9.16 s. The set-point variation of the cart position has a very negligible effect on the oscillation of the pendulum angle. If the proportional term of PID2(stroke control) is increased, the rise time can be reduced further. The system is able to recover and maintain stability with the initial condition of the pendulum angle set to 6°.

Simulations by changing the parameters such as Supply Pressure, Length and mass of the Pendulum, Connecting pipe length, Valve Timings, PWM frequency ensured a better understanding of the system behaviour, which helped in tuning the parameters during the real time control.

The co-simulation of models between DSHplus, Simulink and Altair Activate will be a foundation for the future development, where the study can be extended with implementation of advanced control strategies. while the Advanced control strategies can be taken care by minimal efforts with the help of dedicated Simulink packages.The co-simulation models confirms to produce the same results.
The specifications of NI myrio 1900 was sufficient enough for the data acquisition and to generate the required output. The implementation was quite successful apart from the shortcomings in data logging.

6.2 Thesis outcomes

- Mathematical modelling of the inverted pendulum and the pneumatic system.
- The study of two-loop PID controller approach.
- Modelling and simulations in DSHplus, Matlab/Simulink, Simscape, Altair Activate.
- The co-simulation between DSHplus, Simulink and Altair Activate.
- HIL testing with NI myrio.

6.3 Future scope of development

- Other Control Designs
  The use of Model predictive control or Fuzzy logic control may provide a better solution.
- Controller
  The Replacement of NI myrio 1900 with a Siemens PLC S1200 may turn out to be a better solution for data acquisition and data logging.

Appendices

Appendix A

Guide to setup Co-Simulation

Quick-start guide Co-Simulation with Matlab and DSHplus

1. Model export for Matlab

- Open model in DSHplus.
- Data exchange for Co-Simulation is done via SignalInput/SignalOutput components (see library Modules\Interfaces).

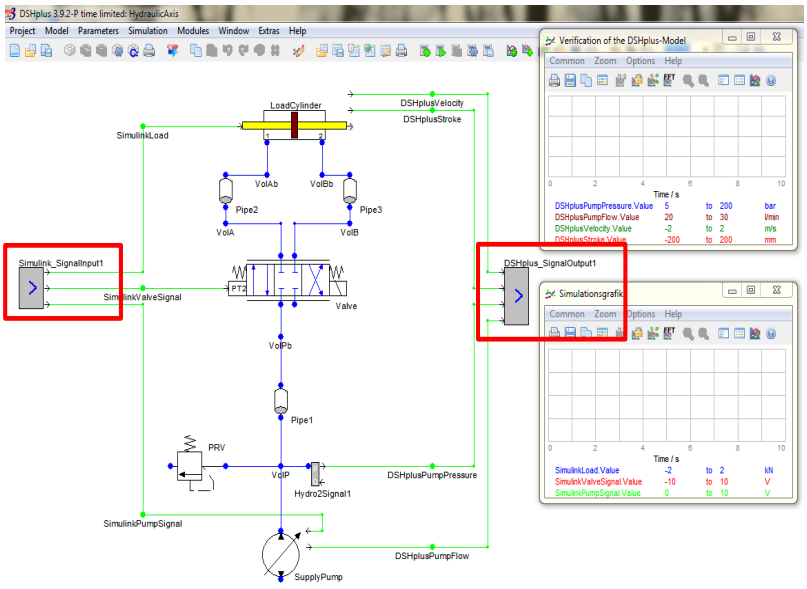

- In the dialog of the SignalInput/-Output elements you can specify channel names which will then be used to name the S-Function in-/outputs.
- Select „Export model…“ within Modules menu, a window opens where the type of Co-Simulation can be selected. Click „Export“ and specify a directory (wether to use 32- or 64-bit depends on the Matlab-Installation).

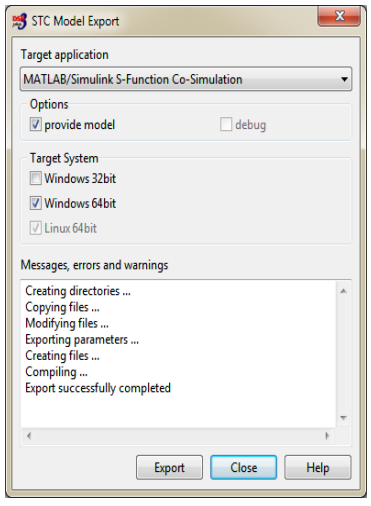

- DSHplus creates a subfolder „win32“ or „win64“, which contains the necessary files:

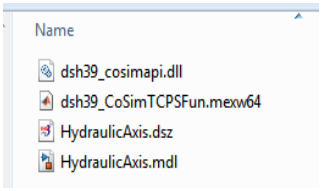

- Checking “provide model” creates a copy of the DSHplus-model. „HydraulicAxis.mdl“ is the Simulink-block for data exchange with DSHplus (see below).
- The DSHplus-model file name is also used for the S-Function. Beware: Matlab will not accept special characters within the name of the mdl-file, therefore avoid using blanks and the like within your DSHplus-model file name.
- In the case of **Embedded Co-Simulation** additional files for the model parameters are created:

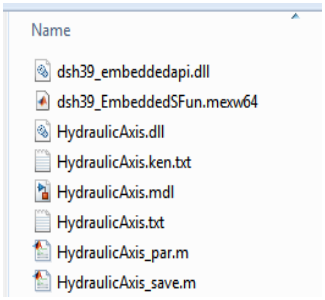

- Make sure to use this directory itself or copy all files into your preferred Matlab working directory.

2. Preparation of the Matlab-model

- Open the mdl-file in Matlab:

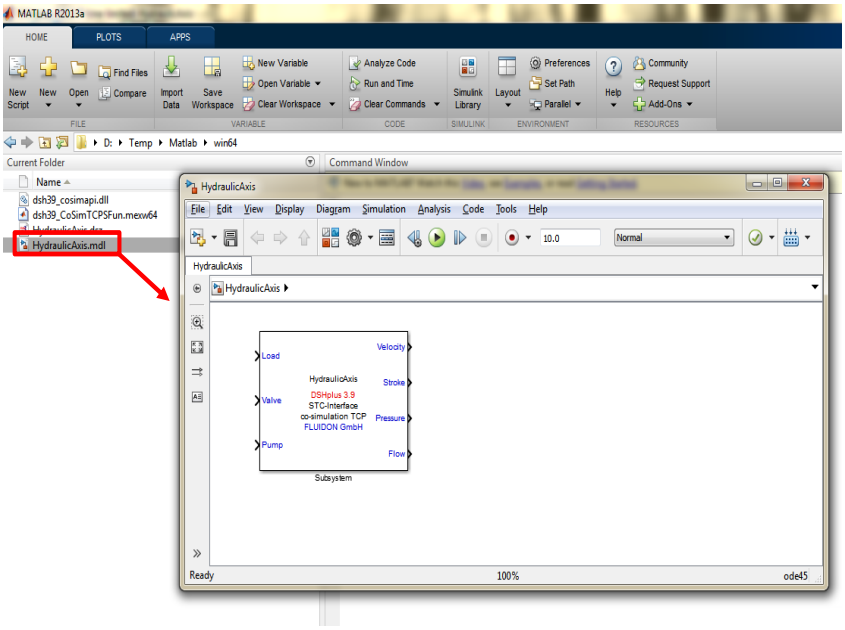

- Simply drag & drop the function block into your Matlab-model window:

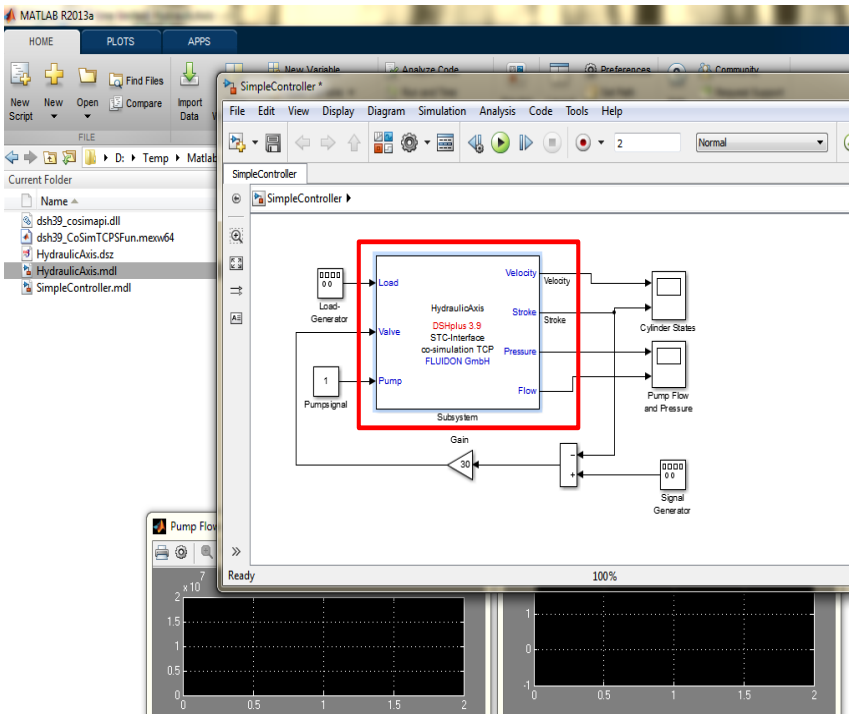

3. Embedded Co-Simulation

- You can run the Matlab-model right away without any further steps.
- If several sets of parameters are to be used, you can export the respective sets from DSHplus (menu Parameters\ASCII-Export…). Then open the DSHplus-subsystem in Matlab and therein

the dialog of the inner DSHplus-block to change the parameter files (both files are mandatory even when the *.ken.txt-file does not contain any data):

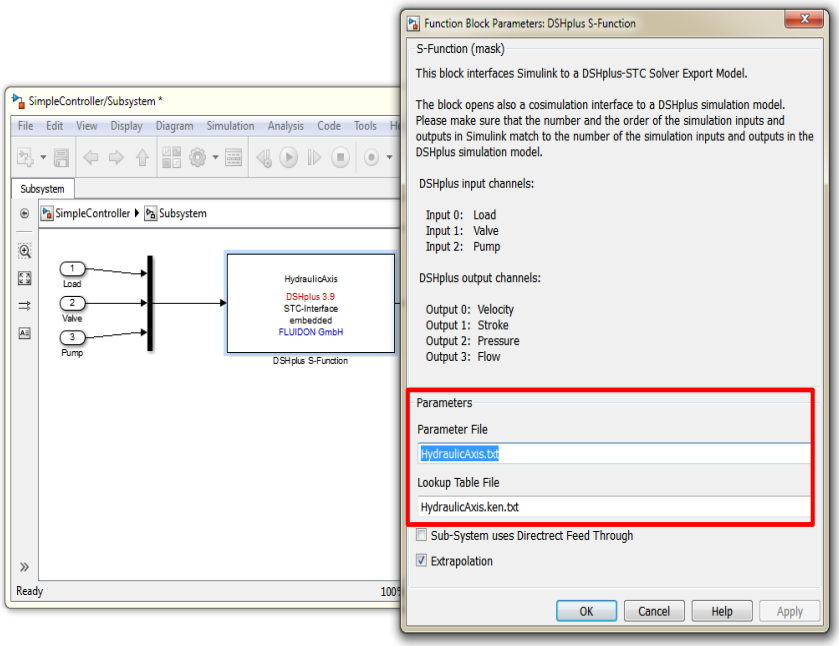

4. Online Co-Simulation

- Open the DSH-model from the export directory and select the Co-Simulation Interface in the dialog.

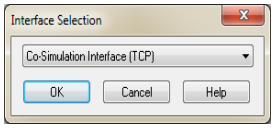

- Change communication parameters as necessary:

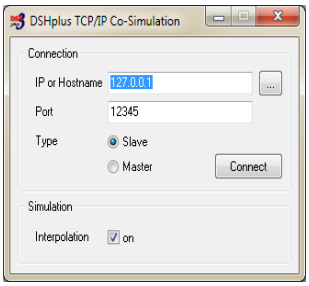

- In Matlab communication parameters are specified by opening the DSHplus-subsystem and therein the DSHplus-block:

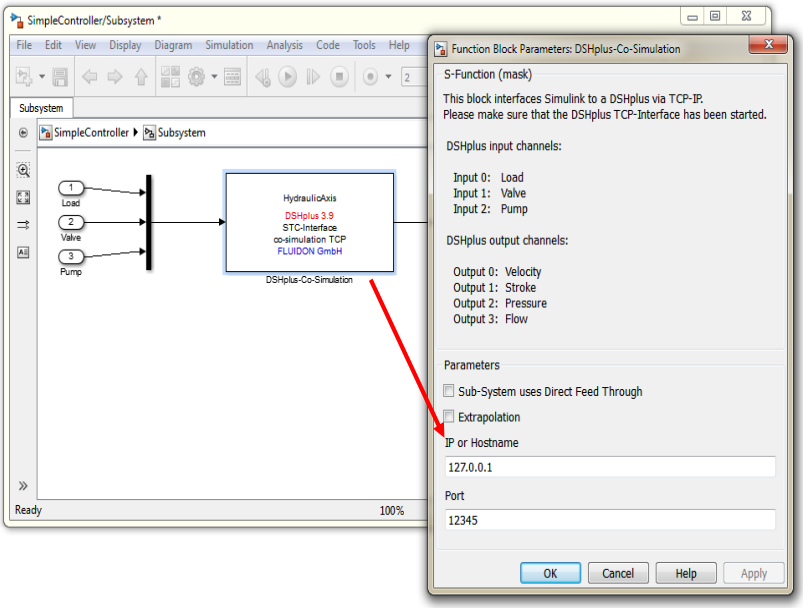

- First select „Connect“ in DSHplus and then start your simulation in Matlab:

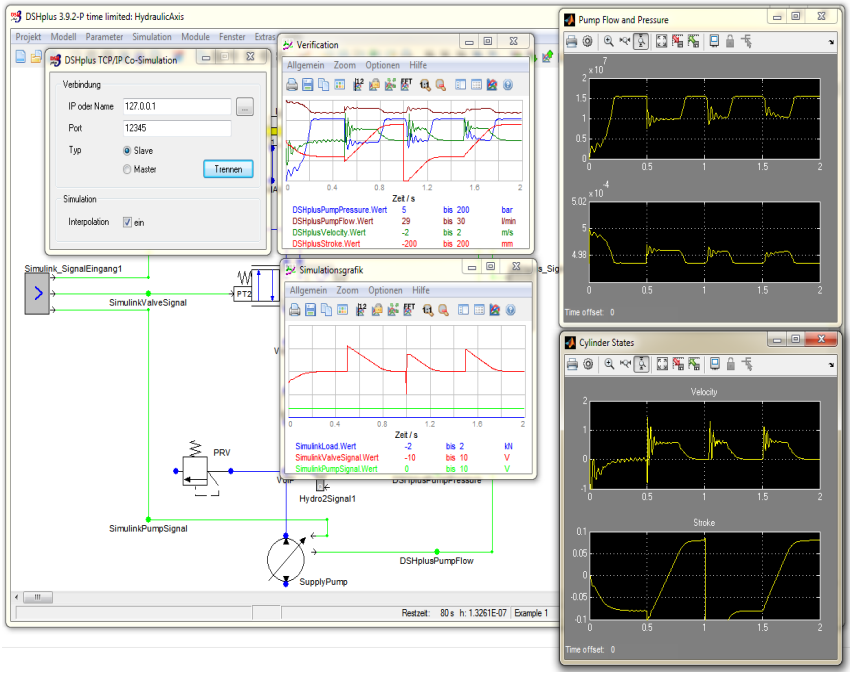

Appendix B

Test bench component technical specification

B.1 Pneumatic cylinder

The pneumatic cylinder is a comozzi product label as **24N2A16A500**.
Product description:
Type of construction: Crimped,
operation: Double acting,
Materials: Anodized aluminium end-caps; stainless steel barrel and rod; aluminium piston - NBR/PU seals,
Bore:Series 24: ϕ 16m,
Min. Races - max: Series 24 - ϕ 16: 500 mm,
Operating temperature: 0° C to 80° C (with dry air -20° C)
Working pressure: 1 to 10 bar ,
Fluid: filtered air, without lubrication.
Speed: 10 to 1000 mm / sec (without load).

B.2 Switching digital valves

Function:2/2 NC,
Operation:proportional directly operated,
Ports: M5 - G1/8,
Nominal diameter(ϕ):
Nominal flow (Qn - Kv):
Maximum operating pressure:
Hysteresis: $< 7\%$,
Repeatibility: $< 5\%$,
Operating temperature: 0 to 60°C,
Medium Installation: filtered compressed air, unlubricated, according to ISO 8573-1 class 3.4.3, inert gas in any position,
Materials: body = brass / PVDF, seals = NBR,
Nominal resistance: 85 ohm,

Rated current: 271 mA.

B.3 Electronic control device

Material of container: Polycarbonate,
Electrical connections: screw,
Environmental temperature: 0 to 50°C,
Mounting: in any position,
Power supply: 6 V to 24 V DC (± 10%), Consumption: 0.4 W (without valve),
Analogical input: 0 to 10 V, 4 to 20 mA,
Input impedence: >30 Kohm with inlet under voltage <200 ohm with inlet under current,
Output PWM: 120 Hz to 11.7 KHz (fixed, according to the valve chosen),
Maximum current (valve): 1 A,
Protection: Polarity inversion, short circuit of the outlet.
External diameter of cable jacket: 5 to 7.5 mm with seal only, 4 to 6 mm with reducer and seal,
Conductor section: 26 to 16 AWG / 0,13 to 1,5 mm^2,
Maximum length supply/signal cable: 10 m,
Maximum length valve cable: 5 m,
IP protection class according to EN 60529: IP 54,
Ramp function: Adjustable time from 0 to 5 s,
Regulation min. current (Offset) 0% to 40% F.S.,
Regulation maximum current 50% to 100% F.S.

B.4 sensors:

B.4.1 Honeywell Angle sensor:

Supply voltage:10 Vdc to 30 Vdc,
Supply current: 20 mA max,
Output 0.5 V to 4.75 V,
Output load resistance (pull down to ground): 10 kOhm,
Operating temperature range: -40°C to 125°C [-40°F to 257°F],
Storage temperature range: -40°C to 125 °C [-40 °F to 257 °F]

B.4.2 Waycon Position Sensor:

Model: LX-PA-50,
Sensor element: Potentiometer,
Measurement range: 1250,
Output [mV/V/mm]** : 0.8,
wire rope tension [N]: 2.2,
Linearity [% MR]: ±1, f or MR up to 120 mm,
±0.5, f or MR up to 625 mm,
±0.25, f or MR up to 1250 mm,
Working temperature [°C]: -25 to +75,
Output signal: 0 to 1 kOhm, ±15% ,
Resolution: depends on the signal quality of the reference voltage,
Voltage supply [V]: 5 ±0.25,
Protection class: IP40,
Weight [g]: 85,
Housing material: thermoplastic body,
Wire rope : standard: jacketed stainless steel, ϕ 0.46 mm,
** At 1 VDC Excitation Voltage. To calculate nominal output voltage in application, multiply nominal output shown by excitation voltage of application.

B.5 Controller

The NI myRIO-1900 provides analog input (AI), analog output (AO), digital input and output (DIO), audio, and power output in a compact embedded device. The NI myRIO-1900 connects to a host computer over USB and wireless 802.11b,g,n.

B.5.1 Connector Pinouts

Connector Pinouts NI myRIO-1900 Expansion Port (MXP) connectors A and B carry identical sets of signals. The signals are distinguished in software by the connector name, as in ConnectorA/DIO1 and ConnectorB/DIO1.

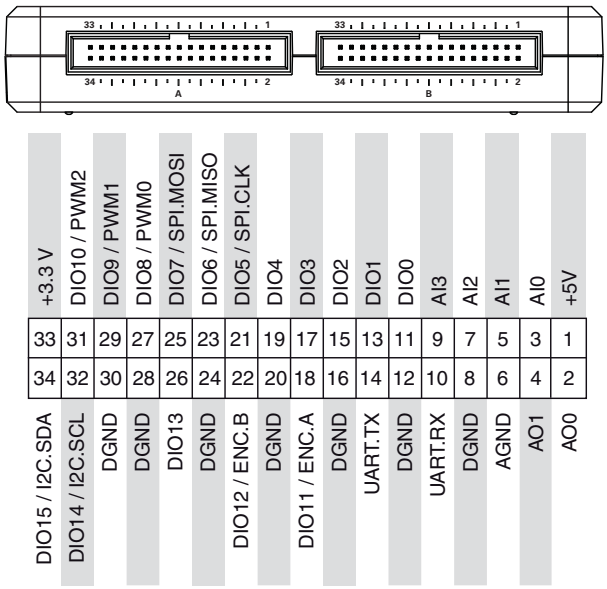

Figure B.1: Primary/Secondary signals on MXP Connectors A and B

Signal Name	Reference	Direction	Description
+5V	DGND	Output	+5 V power output.
AI <0..3>	AGND	Input	0-5 V, referenced, single-ended analog input channels. Refer to the *Analog Input Channels* section for more information.
AO <0..1>	AGND	Output	0-5 V referenced, single-ended analog output. Refer to the *Analog Output Channels* section for more information.
AGND	N/A	N/A	Reference for analog input and output.
+3.3V	DGND	Output	+3.3 V power output.
DIO <0..15>	DGND	Input or Output	General-purpose digital lines with 3.3 V output, 3.3 V/5 V-compatible input. Refer to the *DIO Lines* section for more information.
UART.RX	DGND	Input	UART receive input. UART lines are electrically identical to DIO lines.
UART.TX	DGND	Output	UART transmit output. UART lines are electrically identical to DIO lines.
DGND	N/A	N/A	Reference for digital signals, +5 V, and +3.3 V.

Figure B.2: Description of signals on MXP Connectors A and B

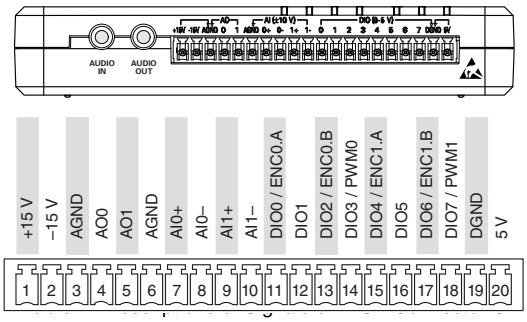

Signal Name	Reference	Direction	Description
+15V/-15V	AGND	Output	+15 V/-15 V power output.
AI0+/AI0-; AI1+/AI1-	AGND	Input	±10 V, differential analog input channels. Refer to the *Analog Input Channels* section for more information.
AO <0..1>	AGND	Output	±10 V referenced, single-ended analog output channels. Refer to the *Analog Output Channels* section for more information.
AGND	N/A	N/A	Reference for analog input and output and +15 V/-15 V power output.
+5V	DGND	Output	+5 V power output.
DIO <0..7>	DGND	Input or Output	General-purpose digital lines with 3.3 V output, 3.3 V/5 V-compatible input. Refer to the *DIO Lines* section for more information.
DGND	N/A	N/A	Reference for digital lines and +5 V power output.

Figure B.3: Description of signals on MSP Connector C

B.5.2 Analog Input

Aggregate sample rate: 500 kS/s,
Resolution:12 bits,
Overvoltage protection:±16 V,
MXP connectors:
Configuration: Four single-ended channels per connector,
Input impedance: >500 kΩ acquiring at 500 kS/s;1 MΩ powered on and idle;4.7 kΩ powered off,
Recommended source impedance:3 kΩ or less,
Nominal range: 0 V to +5 V,
Absolute accuracy: ±50 mV,
Bandwidth: >300 kHz,
MSP connector:
Configuration:Two differential channels Input impedance: Up to 100 nA leakage powered on; 4.7 kΩ powered off,
Nominal range: ±10 V,

Working voltage (signal + common mode): ±10 V of AGND,
Absolute accuracy: ±200 mV,
Bandwidth: 20 kHz minimum, ¿50 kHz typical.

B.5.3 Analog Output

Aggregate maximum update rates
All AO channels on MXP connectors:45 kS/s,
All AO channels on MSP connector and audio output channels:345 kS/s,
Resolution:12 bits,
Overload protection ±16 V,
Startup voltage : 0 V after FPGA initialization,
MXP connectors:
Configuration: Two single-ended channels per connector,
Range: 0 V to +5 V,
Absolute accuracy: 50 mV,
Current drive: 3 mA,
Slew rate : 0.3 V/μs,
MSP connector:
Configuration : Two single-ended channels,
Range: ±10 V,
Absolute accuracy: ±200 mV,
Current drive: 2 mA,
Slew rate: 2 V/μs.

Bibliography

[1] Jia-Jun Wang. Simulation studies of inverted pendulum based on pid controllers. *Simulation Modelling Practice and Theory 19*, na:440–449, 2011. (document), 1.2, 1.3

[2] Yong Xin Bo Xu Hui Xin Jian Xu and Lingyan Hu. The computer simulation and real-time control for the inverted pendulum system based on pid. *Communication Systems and Information Technology, LNEE 100*, na:729–736, 2011. (document), 1.2, 1.4

[3] T Rakesh Krishnan. On stabilization of cart-inverted pendulum system: An experimental study. Master's thesis, National Institute of Technology, Rourkela, 2012. 1

[4] Arthur D. Kuo. The six determinants of gait and the inverted pendulum analogy: A dynamic walking perspective. *Human Movement Science*, 26(4):617 – 656, 2007. European Workshop on Movement Science 2007. 1

[5] Bram Vanderborght, Bjrn Verrelst, Ronald Van Ham, Michal Van Damme, and Dirk Lefeber. Objective locomotion parameters based inverted pendulum trajectory generator. *Robotics and Autonomous Systems*, 56(9):738 – 750, 2008. 1

[6] F. Grasser, A. D'Arrigo, S. Colombi, and A. C. Rufer. Joe: a mobile, inverted pendulum. *IEEE Transactions on Industrial Electronics*, 49(1):107–114, Feb 2002. 1, 1.2

[7] N. M. A. Ghani, D. Ju, H. Z. Othman, and M. A. Ahmad. Two wheels mobile robot using optimal regulator control. In *2010 10th International Conference on Intelligent Systems Design and Applications*, pages 1066–1070, Nov 2010. 1, 1.2

[8] H. W. Kim and S. Jung. Control of a two-wheel robotic vehicle for personal transportation. *Robotica*, 34(5):11861208, 2016. 1

[9] M. Hehn and R. D'Andrea. A flying inverted pendulum. In *2011 IEEE International Conference on Robotics and Automation*, pages 763–770, May 2011. 1

[10] Anh N D. Vibration control of an inverted pendulum type structure by passive mass spring pendulum dynamic vibration absorber. *Journal of Sound and Vibration*, Volume 307(1):187–201, 2007. 1

[11] N. Shiroma, O. Matsumoto, S. Kajita, and K. Tani. Cooperative behavior of a wheeled inverted pendulum for object transportation. In *Intelligent Robots and Systems '96, IROS 96, Proceedings of the 1996 IEEE/RSJ International Conference on*, volume 2, pages 396–401 vol.2, Nov 1996. 1.2

[12] R. Nakajima, T. Tsubouchi, S. Yuta, and E. Koyanagi. A development of a new mechanism of an autonomous unicycle. In *Intelligent Robots and Systems, 1997. IROS '97., Proceedings of the 1997 IEEE/RSJ International Conference on*, volume 2, pages 906–912 vol.2, Sep 1997. 1.2

[13] M. Shivakumar M. Stafford, M. Basavanna. Two wheeled balancing autonomous robot. *Int. J. of Advanced Research in Computer and Comm. Eng.*, 4(11):119–122. 1.2

[14] Nivedita Rajak. Stabilization of cart-inverted pendulum using pole-placement method. page na. 1.2, 1.2

[15] Katsuhiko Ogata. *Modern Control Engineering*. Prentice Hall, 2010, 2010. 1.2

[16] Kai Cheng Wende Li, Hui Ding. An investigation on the design and performance assessment of double -pid and lqr controllers for the inverted pendulum. In *UKACC Internation Conference on Control 2012*, na, pages 190–196, na, 2012. na. 1.2

[17] Lal Bahadur Prasad Barjeev Tyagi Hari Om Gupta. Optimal control of nonlinear inverted pendulum system using pid controller and lqr: Performance analysis without and with disturbance input. *International Journal of Automation and Computing 11(6)*, na:661–670, 2014. 1.2

[18] Wanying Zhang Junfeng Wu and Shengda Wang. A two-wheeled self-balancing robot with the fuzzy pd control method. *Mathematical Problems in Engineering*, 2012. 1.2

[19] N. Yubazaki J. Yi. Stabilization fuzzy control of inverted pendulum systems. *Articial Intelligence in Engineering 14*, na:153–163, 2000. 1.2

[20] JOSKO PETRIC and ZELJKO SITUM. Inverted pendulum driven by pneumatics. *Int. J. Engng Ed.*, 19:597–602, 2003. 1.2

[21] DAVOR Zorc Tihomir Zilic, Danijel Pavkovic. Modeling and control of a pneumatically actuated inverted pendulum. *ISA Transaction 48*, na:327–335, 2009. 1.2

[22] A. Neumaier. *Applied Optimization*. Kluwer, 2004. 2.1

[23] Prof. Dawn Tilbury Prof. Bill Messner. Control tutorials for matlab & simulink, 2017. 2.1.1, 2.1.4

[24] Dvorak. Model of the pneumatic double actuating cylinder. 2009. 2.1.2

[25] Edmond Richer and Yildirim Hurmuzlu. A high performance pneumatic force actuator system, 2001. 2.1.2

[26] Laura Gastaldi Guiseppe Quaglia, massimo Sorli. Static and dynamic non linear identification and modelling of pneumatic valves. 2004. 2.1.2.2

[27] Jian Sun. *Pulse-Width Modulation*. Springer, 2012. 2.1.5

[28] Harold S Black. *Modulation theory*. Van Nostrand Reinhold, 1953. 2.1.5

[29] Fluidon Gmbh. `https://www.fluidon.com/en/`. 2.2.1

[30] S. Lehnho C. Steinbrink. Simulation-based validation of smart grids status - quo and future research trends. 4